

**Fundamentals of spatial vision in the barn owl  
(*Tyto alba pratincola*):**

Ocular aberrations, grating acuity,  
contrast sensitivity, and vernier acuity

Von der Fakultät für Mathematik, Informatik und Naturwissenschaften  
der Rheinisch-Westfälischen Technischen Hochschule Aachen  
zur Erlangung des akademischen Grades  
eines Doktors der Naturwissenschaften  
genehmigte Dissertation

vorgelegt von

Diplom-Biologe  
Wolf Maximilian Harmening  
aus Köln

Berichter :   Universitätsprofessor Dr. Hermann Wagner  
                  Universitätsprofessor Dr. Frank Schaeffel

Tag der mündlichen Prüfung: 25. März 2008



*für Noah*



# Contents

<b>1</b>	<b>Introduction</b>	<b>1</b>
1.1	Optical properties of vision . . . . .	2
1.2	Limits of spatial vision . . . . .	3
1.3	Hyperacuity phenomena . . . . .	4
1.4	Barn owl vision . . . . .	7
1.5	Organization of the thesis . . . . .	12
<b>2</b>	<b>Materials and Methods</b>	<b>15</b>
2.1	Animal subjects . . . . .	15
2.2	Procedures in wavefront aberration experiments . . . . .	16
2.3	Procedures in behavioral experiments . . . . .	18
2.3.1	Experimental setup . . . . .	18
2.3.2	Visual stimulation and viewing conditions . . . . .	20
2.3.3	Initial behavioral conditioning . . . . .	21
2.3.4	Transfer experiments . . . . .	22
2.3.5	Task design and reward strategy . . . . .	23
2.3.6	Psychophysical threshold estimation . . . . .	25
<b>3</b>	<b>Ocular aberrations</b>	<b>27</b>
3.1	Introduction . . . . .	28
3.2	Materials and Methods . . . . .	29
3.2.1	Subjects . . . . .	29
3.2.2	Measurement protocol and aberrometer . . . . .	29
3.2.3	Data analysis . . . . .	30
3.3	Results . . . . .	33
3.3.1	Wavefront raw data . . . . .	33
3.3.2	Second-order aberrations . . . . .	36
3.3.3	Higher order aberrations . . . . .	36
3.3.4	PSFs, retinal image quality and MTFs . . . . .	36
3.4	Discussion . . . . .	38

3.4.1	Methods . . . . .	38
3.4.2	Implications of the results . . . . .	40
<b>4</b>	<b>Spatial contrast sensitivity</b>	<b>45</b>
4.1	Introduction . . . . .	46
4.2	Materials and Methods . . . . .	47
4.2.1	Subjects . . . . .	47
4.2.2	Experimental setup and stimuli . . . . .	48
4.2.3	Psychophysical procedures . . . . .	50
4.2.4	Data analysis and grating acuity . . . . .	51
4.3	Results . . . . .	53
4.3.1	Training, control experiments, and response bias . . . . .	53
4.3.2	Contrast threshold estimation . . . . .	54
4.3.3	Contrast sensitivity function . . . . .	56
4.3.4	Grating acuity . . . . .	57
4.4	Discussion . . . . .	59
4.4.1	Methodological considerations . . . . .	59
4.4.2	Implications of the results . . . . .	59
4.4.3	CSF and grating acuity . . . . .	60
<b>5</b>	<b>Vernier acuity</b>	<b>65</b>
5.1	Introduction . . . . .	66
5.2	Materials and Methods . . . . .	67
5.2.1	Subjects . . . . .	67
5.2.2	Experimental setup and general procedure . . . . .	67
5.2.3	Visual stimuli and data acquisition . . . . .	68
5.3	Results . . . . .	69
5.3.1	Staircase procedure and response bias . . . . .	69
5.3.2	Vernier thresholds . . . . .	69
5.3.3	Bar versus grating stimuli . . . . .	73
5.3.4	Monocular versus binocular viewing conditions . . . . .	74
5.4	Discussion . . . . .	74
5.4.1	Method . . . . .	74
5.4.2	Is it hyperacuity? . . . . .	75
5.4.3	Stimulus configuration and viewing condition . . . . .	75
<b>6</b>	<b>General discussion</b>	<b>79</b>
6.1	The eye . . . . .	80

6.2	Visual acuity . . . . .	82
6.3	Contrast sensitivity . . . . .	84
6.4	Specialities of avian vision . . . . .	86
<b>7</b>	<b>Summary</b>	<b>91</b>
	<b>References</b>	<b>93</b>
	<b>Danksagung</b>	<b>109</b>
	<b>Curriculum vitae</b>	<b>111</b>





# List of Figures

1.1	Visual resolution and hyperacuity . . . . .	6
1.2	Barn owl eyes . . . . .	10
2.1	Tscherning aberrometry . . . . .	16
2.2	Dummy aberrometer . . . . .	17
2.3	Experimental setup in behavioral tests . . . . .	19
2.4	Barn owl spectacle frame . . . . .	21
2.5	Stimulus transition . . . . .	24
3.1	Wavefront setup . . . . .	31
3.2	Wavefront maps and Zernike terms A . . . . .	34
3.3	Wavefront maps and Zernike terms B . . . . .	35
3.4	Defocus, astigmatism and HOA . . . . .	37
3.5	Retinal image quality . . . . .	39
3.6	Modulation transfer function . . . . .	40
4.1	Experimental setup for CSF and grating acuity experiments . .	49
4.2	Example for behavioral data pooling . . . . .	52
4.3	Psychometric functions at 11 spatial frequencies . . . . .	55
4.4	Barn owl contrast sensitivity function . . . . .	57
4.5	Grating acuity results . . . . .	58
4.6	Barn owl CSF comparison . . . . .	61
5.1	Exemplary staircase experiment . . . . .	70
5.2	Biased response behavior . . . . .	70
5.3	Vernier acuity thresholds . . . . .	71
5.4	Influence of stimulus configuration and viewing conditions . .	73



# 1 Introduction

How does the world look like through the eyes of an animal?

Intriguing as the question may sound at first sight, it might be an impossible task to give a satisfyingly comprehensive answer. Nevertheless, within the field of neuroscience, more effort has gone into studying the visual system than any other sensory modality, in humans as well as in animals. The key objective of visual neuroscience is to explain how the brain transforms retinal images into the coherent visual world we experience everyday. This might be undertaken at the very microscopic scale, finding out about how the physical energy of light is transformed into physiological signals, and how those are further processed — or on a more holistic scale, precisely describing how observers react to visual stimulation, ultimately preparing the ground to understand the perceptual high-level process of seeing.

The aim of this thesis was to elaborate some of the most fundamental functional aspects of spatial vision in an animal that is by nature a truly specialized animal: the barn owl. This was done both at the very first stages of vision, as well as at later perceptual stages, involving the animals to participate in behavioral experiments. Specifically, the objectives of the thesis were:

- to study the optical properties of barn owl eyes with the help of state-of-the-art aberrometry techniques,
- to address the neural portion of spatial vision in this bird by psychophysical measurements of its contrast sensitivity function and grating acuity threshold, and finally
- to describe neural enhancements of the owl's visual experience, allowing it to detect tiny spatial details beyond the limit set by the resolution of their eyes, studied in a series of hyperacuity experiments.

## 1.1 Optical properties of vision

When light enters the eye it is refracted due to its different velocities of propagation in the different ocular media, and an inverted image of the visual scene is formed at the nervous back of the eye, the retina. The accuracy of this process, and, ultimately, the quality of the retinal image, is dependent on several physical constraints.

Foremost, the refractive surfaces of the eye, the cornea and the ocular lens, have the largest impact on image formation. The shape of the cornea and lens will cause light rays to refract to a distinct degree. In all eyes that have been tested so far, the shape of the refracting surfaces show tiny irregularities, causing the incident light to refract in a slightly irregular manner. As a result of these ocular aberrations, the retinal image will be blurred. Furthermore, the lens of most vertebrates has accommodative properties, being able to change its refractive power to bring objects of different distances into focus. If the accommodative capabilities are insufficient to meet the optical requirements given by the eye's geometry (i.e. the observer is ametropic), retinal image quality will be degraded. Other optical side effects, like scatter-light and stray-light, can degrade image quality to unfeasible degrees as well.

Another origin of retinal image degradation is diffraction. Diffraction is the breaking up of a beam of light when it passes a sharp edge of an opaque object. In the vertebrate lens-eye, diffraction is present due to the pupil, a small opening of variable size that allows control of the total amount of light passed onto the retina. If light originating from a point light source passes the pupil, it is diffracted. The spread light will produce a series of dark and light bands that interfere with each other to form the so called Airy-disc, an expanded area of variable brightness. This image degradation is also experienced as retinal blur. The amount of blur due to diffraction depends on the size of the pupil, with large pupils producing less diffraction (Campbell and Gubisch, 1966).

A state-of-the-art technique that is well suited to measure the influence of the afore mentioned physical properties on the image forming process, is wavefront aberrometry. This objective measuring technique, described in detail in **chapter 3** (starting on page 27), was applied to assess the optical quality of the barn owl eye. The eye's point-spread function (PSF), its modulation transfer function (MTF), and theoretical retinal image quality were calculated from wavefront maps that were measured in eight barn owl eyes.

## 1.2 Limits of spatial vision

After the formation of an image on the retina, may it be perfectly crisp or desperately blurry, the largest part of the process of vision is yet to take place, and the question of what the observer actually sees is far from being resolved. One of the common approaches to gain insights into the visual world an observer experiences, is to specify the limits of the observer's visual capabilities, or, expressed in more psychophysical terms, to measure the observer's perceptual threshold for a given visual task. With long standing tradition, a sensible first step is to measure the observers visual acuity.

### Visual acuity

The term visual acuity refers to the ability of an observer to resolve fine spatial details in a visual scene. It is bequeathed that, in ancient times, resolving power of human observers was measured by the ability to separate nearby double stars or clusters, like *Mizar* and *Alcor* in the handle of the *Big Dipper* (Morgan, 1991), those being 12 arcmin apart. Given the fixed distance between those objects, the estimate of resolving power was coarse. Nowadays, the observer's acuity can be estimated precisely using a typical eye chart in an optometrist's office (figure 1.1 a). Alternatively, it can be measured by determining the observer's discrimination threshold in a simple visual task similar to those shown in figure 1.1 (b–c).

In all those tasks typical thresholds are in the range of 30–60 arcsec (Campbell and Green, 1965b), resembling the average distance between adjacent photoreceptors in the most sensitive part of the retina, the fovea (Curcio et al., 1990). As positional information in the photoreceptor-layer is passed to the ganglion-cell layer and from there further up the optical nerve to higher brain areas, visual acuity largely depends on the particular way this connection is established. Positional information is preserved best, it seems, if single ganglion cells receive input from single photoreceptors, and hence their receptive field is as small as possible (Merigan and Katz, 1990).

In this thesis, visual acuity of the barn owl was measured with adaptive psychophysical techniques. Three barn owls were trained to discriminate gratings of different orientation. In the course of the experiments, the spatial frequency of the grating was increased until the owl's discrimination threshold was determined. Grating acuity results from one animal are presented in **chapter 4** (starting on page 45).

## Contrast sensitivity

A next step in characterizing an observer's visual experience, is to describe visual processing for objects that are larger than the resolution limit. One key feature that makes objects distinguishable is the amount of luminance that is reflected relative to the background or relative to other objects. This relative luminance difference is referred to as luminance-contrast, or simply contrast.

The so-called spatial contrast sensitivity function (CSF) relates the ability of an observer to visually detect spatial gratings of different spatial frequencies to the amount of contrast present in the grating. If measured behaviorally, the CSF incorporates visual functions of both physical (i.e. the visual transfer function of the eye) and, to a greater extent, physiological nature (i.e. visual processing in the nervous system). The CSF may, therefore, be regarded as one of the fundamental functional descriptions of a visual system.

In human observers and virtually any animal that has been tested so far, the CSF renders a band-limited inverted U-shaped function, with a typical high- and low-frequency attenuation. The high frequency roll-off in humans is regarded as a combined consequence of physical constraints leading to optical degradation (such as the diffraction limit and ocular aberrations), and receptor cell spacing on retina level (Campbell and Green, 1965a; Cornsweet, 1970). The low frequency attenuation can be explained solely by neural factors, such as extent of lateral inhibition (Cornsweet, 1970), antagonistic surround mechanisms (Westheimer, 1972), or relative insensitivity of low spatial frequency filters (Graham, 1972).

Spatial contrast sensitivity was determined in the barn owl in a series of behavioral experiments, similar to the ones described in the preceding section. The owls had to discriminate the orientation of gratings for eleven different spatial frequencies. With the appliance of an adaptive staircase procedure, contrast was lowered until discrimination performance reached threshold level. The inverse of threshold was defined as contrast sensitivity and composed the progression of the contrast sensitivity function. These results are also presented in **chapter 4**.

## 1.3 Hyperacuity phenomena

As demonstrated in the previous section, the ability of humans to resolve fine spatial details is limited by the physical nature of light, the optical properties

of the eye and the neural components creating vision. Typically, normal acuity values of human observers are in the range of 30–60 arcsec (test yourself in figure 1.1 c).

Surprisingly, there are tasks such as the vernier, where threshold may be as low as 2–5 arcsec. This corresponds to perceiving spatial details of about 0.02 mm in size at a distance of 1 m, or the size of a 2 €-coin at a distance of 10 km. One can better appreciate the astonishing precision of this performance by re-considering the optical properties of the eye. In the spatially most sensitive region of the human retina, the fovea, receptive field size of ganglion-cells is in the range of 30 arcsec. Thus, humans can resolve detail with an accuracy of better than at least one fifth of the distance of the most sensitive photoreceptors. Westheimer called these highly sensitive spatial judgments hyperacuities, to distinguish them from measures of visual acuity that assess resolution capability (Westheimer, 1975). Almost any type of target configuration can be used to measure hyperacuity, as long as a positional difference in the target is the distinguishable entity. In figure 1.1 (d–g) the most common varieties of hyperacuity targets are shown.

Visual hyperacuity has now been studied for over a hundred years, the first report of vernier hyperacuity dating back to the end of the nineteenth century (Wülfing, 1892). By now, it is still of ongoing interest to describe and explain these peculiarities of spatial vision. One of the interesting points about hyperacuity is that it should not come as a surprise, if considered in the context of the computational power of the visual system. Due to the point spread function (PSF) of the eye's optics, a very small dot of light projected onto the retina will expand to the so-called Airy disk, and, hence, activate many different photoreceptors (figure 1.1 h and i). Thus, there is no reason to expect a simple relation between the acuity exhibited by the system and the spacing of adjacent photoreceptors. It could be shown, that in a physiological plausible model of human foveal ganglion cell responses, hyperacute performance can be mediated by the magnocellular pathway (Wachtler et al., 1996). On the other hand, responses of visual mechanisms tuned for size and orientation were shown to explain the performance in a variety of hyperacuity tasks (Wilson, 1986).

There is a vast set of demonstrations of hyperacuity in the human visual system at hand, but there are only a few studies describing similar observations in animal subjects. Specifically, monocular hyperacuity reports are limited to monkeys (Kiorpes et al., 1993), cats (Murphy and Mitchell, 1991) and rats (Seymour and Juraska, 1997), all reporting hyperacute performance in the applied tasks. Finally, in the scope of the present thesis, the question arises: Do

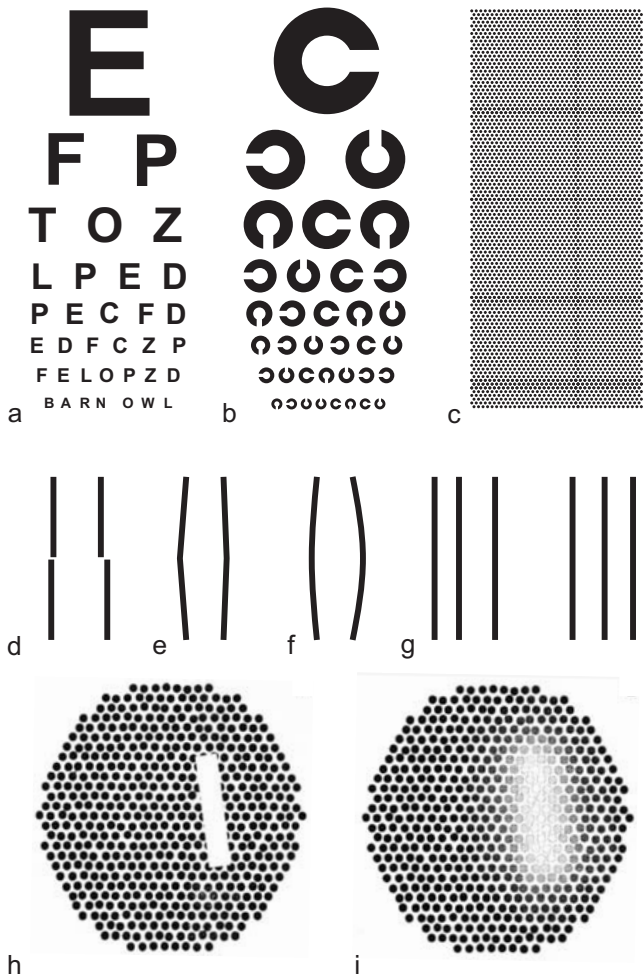


Figure 1.1: (a) An optometrist’s letter chart. The observer’s task is to correctly identify letters. (b) Landolt-C’s, the position of the ring opening has to be named. In humans, the optotypes in (a) and (b) yield thresholds of about 30–60 arcsec, which is generally referred to as two-point acuity or *minimum separable*. (c) An area comprised of tiny dots, demonstrating two-point resolution if viewed at about arm’s length distance. (d–g) Optotypes that will yield hyperacute thresholds. (d) Vernier: report the direction of the offset. (e) Chevron: report the shift direction of the midpoint. (f) Curvature: is the line bend left or rightwards? (g) Bisection: is the center bar displaced left or right of center? (h) Simulation of human cone layer with superimposed bar stimulus. (i) Excitation of cones caused by this stimulus. Blur is induced by the PSF of they eye and could explain retinal hyperacuity coding (h,i modified after Wachtler et al. (1996)).



birds have hyperacute vision? In **chapter 5** of this thesis (starting on page 65), this issue is addressed in a series of psychophysical experiments, measuring the discrimination threshold for typical vernier stimuli in the barn owl visual system. Additionally, to account for possible task difficulty differences, two different vernier stimuli were used as targets, each presented under monocular and binocular viewing conditions.

## 1.4 Barn owl vision

### Early vision: the barn owl eye and retina

In general, birds are highly visual animals. The avian globe, in relation to the size of the skull, is very large, advantageous to allow a larger image to be projected onto the retina, and thus to contribute vastly to visual acuity (Güntürkün, 2000). In birds, approximately 50% or more of the cranial volume of the skull is occupied by the eye, whereas in humans, the eye occupies less than 5% of the skulls volume (Waldvogel, 1990).

The eyes of the barn owl, with an axial length of about 17.5 mm, are clearly smaller than those of humans (24.5 mm) (Hughes, 1977; Schaeffel and Wagner, 1996), but according to a study by Howland, barn owl eyes are almost twice as long as allometry based on body weight would suggest (Howland et al., 2004). Typical for all avian eyes, the nearly hemispheric posterior region of the globe is disproportionately larger than the anterior segment (Kern, 1991, 1997). The anterior and posterior segments of the globe are united by an intermediate region based on the scleral ossicles (Murphy and Dubelzieg, 1993). The overall shape of the barn owl eye is tubular (figure 1.2 c) – typical for owls –, in which a concave intermediate segment is elongated anteroposteriorly, forming a tube before joining the posterior segment at a sharp angle (King and McLelland, 1984; Waldvogel, 1990; Kern, 1991, 1997; Güntürkün, 2000). This special eye design is believed to improve visual acuity at low light levels due to the larger retinal image with a constrained focal length (Martin, 1982). The ratio between focal length and maximal entrance pupil diameter, the f-number, is comparably low in the barn owl (1.3, versus 2.1 in humans). This ultimately results in a brighter retinal image, and might be another example for an adaptation to a nocturnal lifestyle (Schaeffel and Wagner, 1996).

As a result of the largeness of the globe and its fit within the orbit, any torsional movement of the globe is strongly limited, although all six extraocular

eye muscles are present (Williams, 1994). In the barn owl, specifically, there were only minor eye movements reported, with a maximum amplitude of about  $2^\circ$  (Steinbach and Money, 1973; Dulac and Knudsen, 1990). However, due to a long and flexible neck, barn owls can turn their head quickly to extreme angles, probably to compensate the limitations set by their eyes' immobility (Knudsen and Konishi, 1979; Knudsen and Knudsen, 1985; Dulac and Knudsen, 1990; Masino and Knudsen, 1993).

As part of the typical lens-eye of vertebrates, barn owl eyes have a transparent, avascular lens, that, together with the cornea, serves to refract incoming light, and to focus it on the retina to create an acute image. The lens can accommodate, but, in contrast to mammals, the avian lens has an annular pad around its central core, that might serve as a hydrostatic mechanism for transmitting pressure from the ciliary muscle to the central core to facilitate accommodation (Evans and Martin, 1993). A direct relationship exists between the size of the annular pad and the degree of accommodative ability (Samuelson, 1991). Compared to other owls, the accommodative abilities in barn owls are large, amounting to about 6–12 D (Howland et al., 1991; Schaeffel and Wagner, 1992). Barn owls also use accommodation as a distance cue for short distances (Wagner and Schaeffel, 1991). They are not able to accommodate independently in both eyes (coupled accommodation) (Schaeffel and Wagner, 1992), which might indicate that binocular vision is of elevated importance for these animals (see also next section on page 9).

The retina of birds is comprised of the typical cell-layers found in other vertebrates. However, there are differences regarding vascularization, morphology, and areas of visual acuity that are worth mentioning. First, the vascularization of the retina of birds is reduced, and it receives nourishment by the pecten oculi. The pecten extends from the optic nerve into the vitreous chamber (figure 1.2 d), and by saccadic oscillations of the pecten during eye and head movements, nourishment is performed via diffusion through the vitreous body (Pettigrew et al., 1990). The pecten also provides an oxygen gradient to the retina (Wingstrand and Munk, 1965), subserves acid-base balance (Brach, 1977), and maintains a constant intraocular temperature (Murphy and Dubelzieg, 1993).

Second, the bird retinae contain, as in humans, cones and rods, the former functioning in daylight vision and sharp visual acuity, the latter being devoted to low-light vision and the detection of shapes and motion. While the retinae of diurnal birds are dominated by a special double-cone cell type (Meyer, 1977a), nocturnal owls, as the barn owl, have rod-dominated retinae, with a

mean rod:cone ratio of about 30:3 (Oehme, 1961; Braekevelt, 1993; Braekevelt et al., 1996).

Third, and more important for visual acuity, many birds have specialized regions within the retina capable of producing visual acuity greater than outside those regions (termed visual streak or area centralis). This is achieved by a larger density of photoreceptors and ganglion cells within these regions. In primate mammals and some birds, these areas display a typical physical depression, named fovea. Most raptorial birds are bifovent, having a fovea located in the temporal retina in addition to the more common centrally located fovea (Meyer, 1977b; Inzunza et al., 1991). Owls have only temporal foveae, and, uniquely to them, those foveae contain primarily rods (Fite, 1973; Fite and Rosenfield-Wessels, 1975).

In the barn owl retina, only a scarcely distinct temporal fovea is present (figure 1.2 e after Oehme (1961)). The position of the barn owl fovea coincides with a retinal area of elevated ganglion cell density (figure 1.2 d after Wathey and Pettigrew (1989)), and determines the visual axes of both eyes to be almost parallel (figure 1.2 b). Also, a visual streak with higher ganglion cell density, proceeding from the temporal area centralis to nasal regions could be identified (Wathey and Pettigrew, 1989). Assuming that ganglion cells in area centralis are involved in spatial acuity tasks, it is possible to calculate a theoretical value for visual acuity. It turned out that, with about 8 cyc/deg, theoretical grating acuity is comparably poor in the barn owl. Confirming this theorized value, a pattern electro-retinogram (PERG) study estimated grating acuity to be 6.9 cyc/deg (Ghim and Hodos, 2006). Among other raptors and birds, these results put the barn owl, and owls in general, at the very low end of the acuity spectrum (6–7.5 cyc/deg in the Great horned owl (Fite, 1973), 8 cyc/deg in the tawny owl (Martin, 1984), and 6 cyc/deg in the little owl (Porciatti et al., 1989)). As an outstanding example for high resolution capabilities, acuity values of around 140 cyc/deg have been reported for the wedge-tailed eagle (*Aquila audax*) (Reymond, 1985).

## Later stages: neural components of vision

In the barn owl, as in many other owls, one of the prominent features of vision are the frontally oriented eyes. Being confronted with the owl's face, one gets the impression as if their eyes look straight ahead (figure 1.2 a). Regarding what the owl might look upon, this notion is probably not far from reality, as we have just seen from the position of area centralis described in the previ-

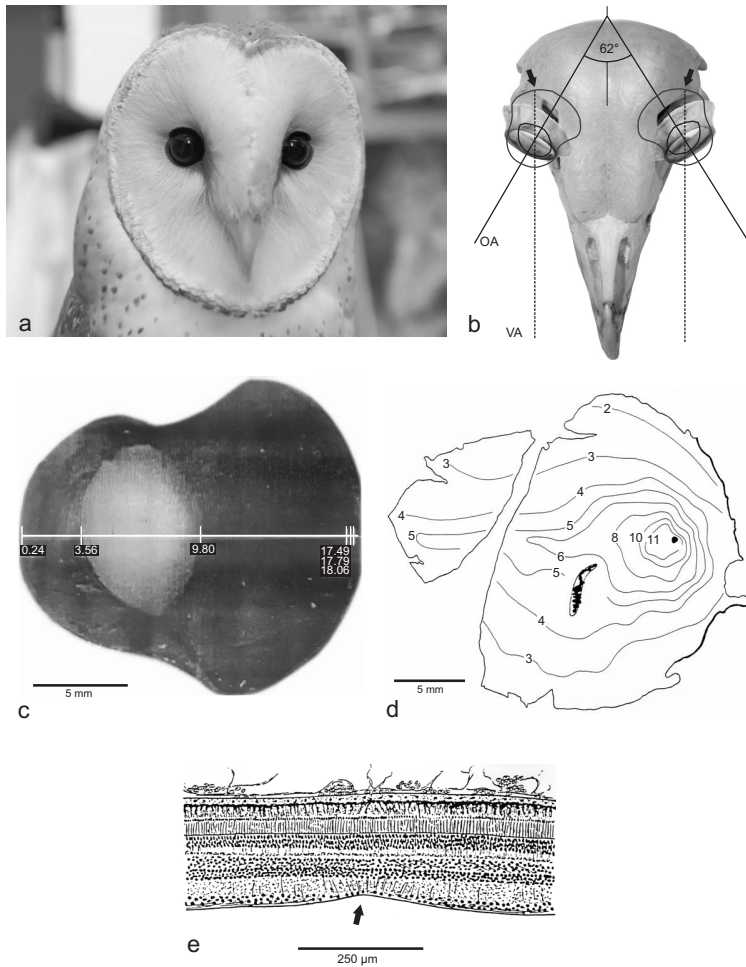


Figure 1.2: (a) A photograph of a barn owl's head. The prominent eyes are oriented frontally, while the feather ruff probably coincides with the border of each monocular field of view. (b) A sketch of the position of the eyes, superimposed on a photograph of the barn owl's skull and the scleral ossicles. Note that their optical axes (OA) diverge by about  $62^\circ$ , while the visual axes (VA) are almost parallel (after Martin (1984) and Pettigrew (1986)). (c) An ultrasonographic scan of an owl eye. Numbers are positional data, given in mm (modified after Schaeffel and Wagner (1996)). (d) Ganglion cell density across the whole mounted retina. Numbers are thousands of cells per  $mm^2$ . The dark patch marks the pecten's foramen (modified after Wathey and Pettigrew (1989)). (e) Retinal cross section at foveal region, marked by the arrow (modified after Oehme (1961)).

ous section. Still, the optical axes in barn owl eyes diverge by approximately  $62^\circ$  (Martin, 1984). The geometrical setup of the eyes in the owl skull can be reviewed in figure 1.2 b. In another nocturnal owl, the tawny owl (*Strix aluco*), the optical axes diverge to a similar degree, and it has been shown that the monocular field of view of the two eyes overlap to form an unusual large binocular field of view (Martin, 1984).

Though the actual field of view of the barn owl was never measured directly, several other findings revealed that the barn owl indeed has binocular vision. Being stated alone, this fact has no implications further than that objects in the binocular field of view can be viewed with both eyes at the same time. It was a matter of investigation to find out if the owl uses this geometrical setting to draw further information out of a visual scene: information that can be used to extract spatial relations, such as depth and distance. This visual capability is called stereopsis. To the largest extent, stereopsis relies on the neural comparison of the images falling on the retinae in both eyes. Due to the different vantage points of the eyes, retinal images differ slightly. These differences are called disparities, and form the physical foundation from which a calculation of spatial depth relation is made possible.

It has been shown that the visual Wulst, a part of the avian forebrain which is largely dedicated to visual information processing, show analogies to the primary visual cortex (V1) of mammals as described by Hubel and Wiesel (1962). It turned out that, in the barn owl, the visual Wulst is enlarged and displays selectivity for orientation and motion direction (Pettigrew and Konishi, 1976; Liu and Pettigrew, 2003). More interestingly, the visual Wulst exhibits a high degree of binocular interaction and selectivity for binocular disparity (Pettigrew, 1979; Wagner and Frost, 1993; Nieder and Wagner, 2000). In addition, in a series of seminal psychophysical experiments, it was demonstrated that barn owls indeed use stereopsis as a depth cue. Moreover, the barn owls tested could discriminate random dot stereograms with hyperacute performance (van der Willigen et al., 1998, 2002), a feat that is also present in human and primate observers (Hadani et al., 1980).

A recent study involving a miniature camera placed on the owl's forehead shed light on the attentional mechanisms of vision in this bird. The results revealed that during an active search task, owls repeatedly and consistently direct their gaze in a way that brings objects of interest to a specific retinal location. Additionally, it was suggested a top-down modulation of gaze control when owls view natural targets. (Ohayon et al., 2008). The barn owl's ability to visually extract higher level features was further demonstrated in another

behavioral study. Here, it was shown that these animals, as humans, are prone to perceive illusionary contours (Nieder and Wagner, 1999).

## 1.5 Organization of the thesis

In this **first chapter** of the thesis, a short introduction to the first stages of spatial vision was presented. Additionally, the topic of hyperacuity phenomena was briefly introduced. To a larger extent, the visual system of the barn owl was reviewed. The **second chapter** covers the methodological approach I chose to elaborate these fields in the barn owl visual system. General psychophysical procedures as well as a description of the technical equipment used throughout all experiments are given. The main part of the thesis is laid down in chapters three to five. Here, the results of three different studies are presented. Specifically, these were, (a) objective measurements of the optical properties of barn owl eyes by wavefront aberrometry (**Chapter 3**), (b) psychophysical measurements of the spatial contrast sensitivity function and grating acuity with an orientation discrimination task (**Chapter 4**), and (c) the description of a hyperacute phenomenon in the barn owl visual system, measured behaviorally in monocular and binocular vernier acuity experiments (**Chapter 5**). The **sixth chapter** of the thesis concludes with a general discussion of the presented results. It reviews the main findings and their implications, and relates to observations made in other animals. Here, the final conclusions are drawn, addressing the question how the world might look through the eyes of a barn owl. The **last chapter** provides a one-page summary of the thesis.







## 2 Materials and Methods

### 2.1 Animal subjects

In total, 6 adult American barn owls (*Tyto alba pratincola*) were used as experimental animals. Eight eyes of four animals were studied in the wavefront aberration experiments, three animals were tested in the vernier acuity experiments and one animals' contrast sensitivity and grating acuity was measured. Taken from the institute's breeding stock, all owls were hand-raised and tame. They could be easily carried between their aviaries and the experimental room while tied to a wooden perch. No attempt was made to reverse the owls' nocturnal cycle. Experiments took place on 5–6 days a week. The owls' diet consisted of dead 1-day old domestic chicks and mice. To avoid deficiency symptoms, the owls received an additional vitamin supplement once in two weeks. To ensure motivation in behavioral tests, the owls' weight was maintained at about 90 % of their free feeding weight. They were rewarded with small pieces of chick muscle-tissue, approximately 2 grams in weight. Water was always given *ad libitum*. All of the subjects carried an aluminium head-post, which was implanted onto the forehead of their skull under anaesthesia earlier during life. For a detailed description of the surgical procedure and the used drugs refer to Nieder and Wagner (1999). In the vernier acuity experiments, the head-post was used to fix a small custom build spectacle frame to the owls head.

Care and treatment of the subjects was carried out in accordance with the guidelines for animal experimentation as approved by the "Landespräsidium für Natur, Umwelt und Verbraucherschutz Nordrhein Westfalen", Recklinghausen, Germany, and complied with the "NIH Guide for the use and care of laboratory animals".

## 2.2 Procedures in wavefront aberration experiments

Ocular wave aberrations of eight eyes of four barn owls were measured at the Institute of Ophthalmology in Aachen. The aberrometer used in the experiments was a Tscherning-type measuring system (ORK aberrometer, Schwind Eye Tech Solutions, Kleinostheim, Germany) with a 660 nm laser-diode illumination beam and 168 measuring spots. The Tscherning measuring principle can be reviewed in figure 2.1. Briefly, a laser dot pattern is projected onto the retina and its reflection is recorded via indirect ophthalmoscopy by a low-light camera. The retinal image is further processed to calculate the center of gravity for each of the illumination spots. The deviation of the retinal spot position from the orthogonal grid pattern that produced the retinal image is the numerical basis for the calculation of the ocular wavefront. The wavefront is expressed as a weighted sum of Zernike terms up to the 6<sup>th</sup> order.

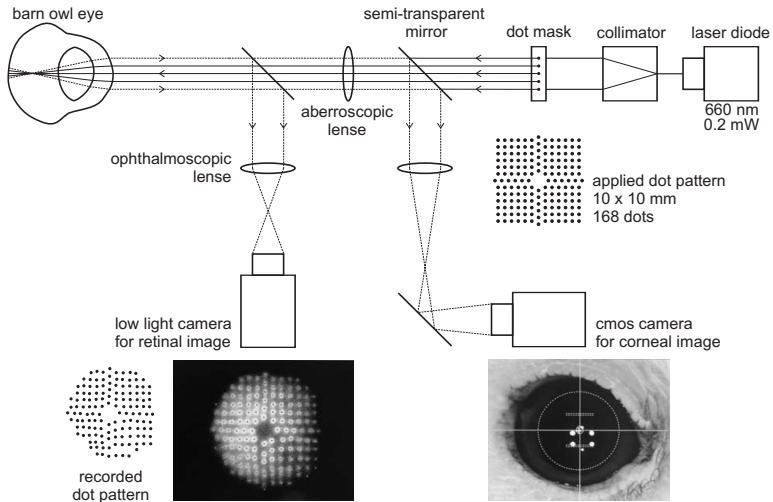


Figure 2.1: Basic principle of Tscherning aberrometry. A dot pattern of known configuration, produced by a laser illumination source, is projected onto the retina of the eye under test. Its retinal reflection is recorded by a low-light camera by indirect ophthalmoscopy. In the bottom part of this figure an exemplary recording comprised of the corneal and retinal image of a barn owl eye is shown as well. Notice the difference between applied and recorded dot pattern.

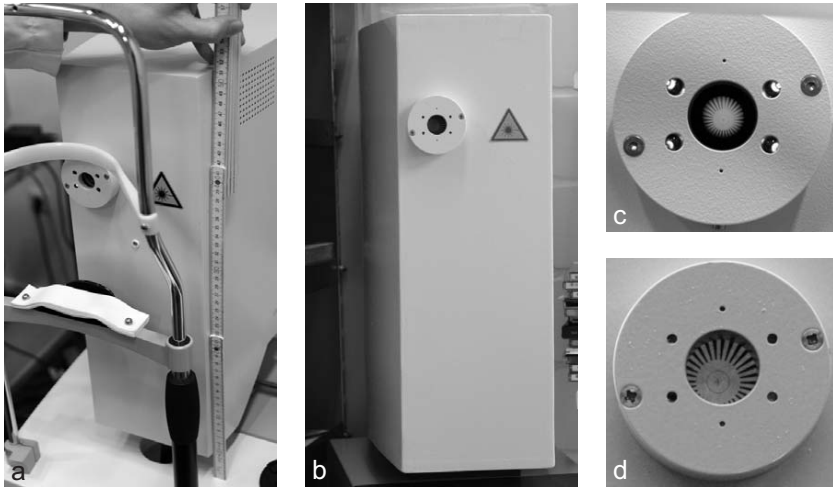


Figure 2.2: Photographs of the original aberrometer (a) and the dummy aberrometer (b). The latter was used to habituate the owls to sit calmly in front of the aperture. A close-up view on the corresponding aperture is shown in (c), original, and (d), dummy. The small target cross inside the aperture was lit from behind in both the original and dummy aberrometer.

Before the owls were taken to the measuring site, all animals were habituated to sit calmly in front of a dummy-aberrrometer (figure 2.2). The dummy was built from ply wood, had the exact dimensions of the original aberrometer, a similar color and surface finish, and was also equipped with an inside-mounted light bulb, that illuminated a target cross resembling the condition in the original aberrometer. The owls got used to the procedure quickly and showed good cooperation.

During measurements the owls were handled by one of the two experimenters. The lights in the experimental room were dimmed, producing about  $5 \text{ cd/m}^2$  on the walls or the experimental table. The owl, sitting on a wooden perch, was placed in front of the aberrometer by fixing its perch to a metal stand, that was rigidly attached to the experimental table. One experimenter held the head of the tame owl in its hands, making it steadily facing the aperture of the aberrometer. The other experimenter controlled the correct positioning and focus of the aberrometer by observing the corneal image of the owl eye, and also triggered single measurements. There were no drugs given to lubri-

cate the eye, block accommodation or influence pupil size. The owls blinked normally during the experiments. Each owl was tested in one experimental session which took about 2 hours. Each session comprised several individual measurements (6–20) for both eyes.

## 2.3 Procedures in behavioral experiments

### 2.3.1 Experimental setup

All behavioral experiments were performed in a custom build sound and light attenuated chamber (outer dimensions: 1.5 x 2 x 1.5 m). The inside walls of the chamber were covered with sound-absorbing foam and a black mat garden foil to minimize unwanted reflections originating from the stimulus display. A small air fan, invisibly mounted into the ceiling wall, drew fresh air into the chamber, and, additionally, produced a continuous low background noise level. A rigid metal stand placed in easy reach of the chamber opening was used to fix the owl's sitting perch in front of the response and feeding apparatus. The automated feeder with the response keys, the stimulus display and an infrared observation camera were mounted onto an adjustable aluminium rack that was rigidly attached to the inner walls of the chamber. An additional infrared camera was placed along side the stand of the owl perch. A detailed photograph of the chamber interior is shown in figure 2.3.

The response apparatus consisted of two large custom build response keys. Their front plate could be depressed by a light touch of the owls beak. A micro-switch similar as is used in electronic computer mice, produced an audible click when the key was pushed correctly. The micro-switches in each of the two keys were connected to an USB input interface of the workstation via wiring to the circuit controlling the two main buttons of a standard computer mouse. In this way, automatic response recording was possible with easy-to-implement devices and algorithms. The carousel feeder, covered with a top plate leaving reach to the reward food items through a small opening (feeding hole), was driven by a step motor that advanced a rotating acrylic feeding dish (36 single feeding cups per dish). The step motor was controlled via TTL-pulses produced by an USB input/output device (BMC Messsysteme GmbH, Maisach, Germany). This device also automatically triggered a white-light LED that was mounted below the feeding hole. The LED was switched on whenever the feeding dish rotated in feeding position, making the feeding cup

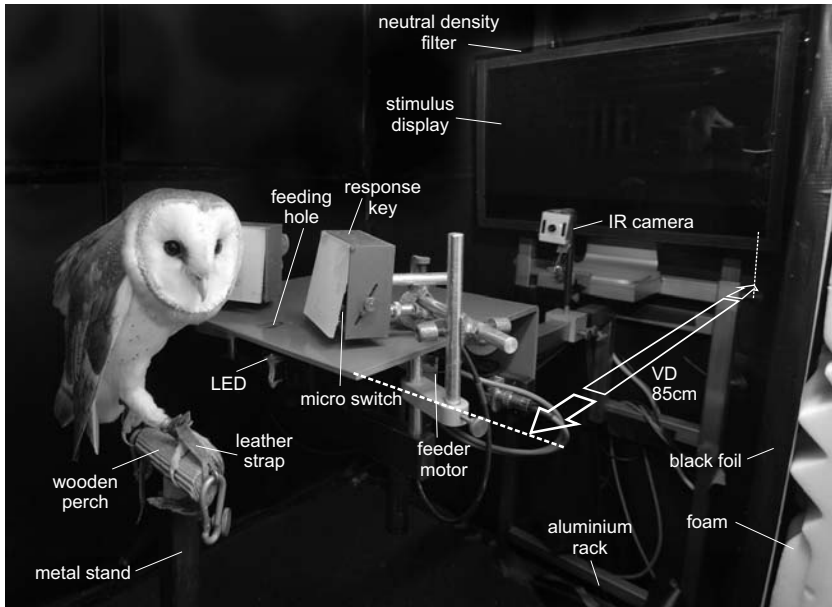


Figure 2.3: A photograph of the behavioral setup viewed through the chamber opening. On the right side parts of the inner wall lining are visible (white sound-absorbing foam, black mat garden foil). The view on the feeding dish is obstructed by the feeder cover. In this picture the 23" wide-screen TFT is shown. Note that under experimental conditions the room was completely dark.

and food item visible to the owl. The light switched off after 1.5 seconds. Other than the stimulus display itself, no additional light source was used.

The computer workstation (G5 PowerMac, Apple Inc., Cupertino, USA), positioned outside of the chamber, delivered the visual stimuli, controlled the feeding logic, and recorded behavioral responses. Custom software was written in ANSI-C programming language with the aid of a popular, GPU supported graphics library (OpenGL, GLUT). The use of these libraries had the advantage of relatively easy implementation of geometrical described visual stimuli and built-in anti-aliasing algorithms. The latter were applied to present sub-pixel shifts in the vernier target stimulus.

### 2.3.2 Visual stimulation and viewing conditions

All visual stimuli were presented via a computer display. The stimulus display was either a 17"-TFT panel (Hansol LCD, Seoul, South Korea) or a wide-screen 23"-TFT panel (Apple Inc.). Both displays were operated at their native resolution (1280 x 1024 pixels and 1920 x 1680 pixels, respectively), digitally controlled by an 8-bit graphics board (Nvidia GeForce 6800 GPU, Santa Clara, USA). Because the chamber was completely dark, at stimulus onset in CSF experiments, substantial light intensity changes could occur. To keep glare and unwanted adaptation effects in those cases as low as possible, an additional large sheet of neutral density filter was placed in front of the stimulus display (LEE Filters, Andover, UK). The filter lowered overall luminance by 0.92 log units, with a linear relationship between absolute luminance and luminance reduction.

Stimulus presentation was monitored constantly during experimenting via an additional computer display that was connected to the second, cloned output of the graphics board. This display panel was placed at the experimenter's table outside of the chamber. Here, barn owl's gaze and general behavior could be monitored by observation of two small CRTs connected to the infrared cameras inside the chamber. Viewing distance was held constant at 85 cm in all behavioral experiments, but was not measured during experiments. A careful observation of the owls' behavior revealed that, while watching the display, the owls remained in a frozen posture. During fixation, the owls repeatedly held their head directly above the feeding hole, midway between the two response keys. In this way, viewing distance could be estimated accurately. At viewing distance, one pixel subtended 1.052 and 1.044 arcmin, respectively, depending on the stimulus display (see above).

In the contrast sensitivity measurements, accurate contrast defined stimuli had to be applied. Stimulus contrast was carefully determined by measuring the luminance of the brightest and darkest parts of the stimulus at the center of the display at viewing distance. Some calibration procedures were written to measure luminance quickly for each gray value used in the CSF experiments. All luminance measurements were conducted with the Minolta LS-100 luminance-meter (Konica Minolta Medical and Graphic Imaging Europe GmbH, München, Germany). To produce a linear relationship between gray values set in the display system and actually measured luminance values,  $\gamma$ -correction was applied.

In order to deliver monocular stimuli in the vernier acuity experiments, a

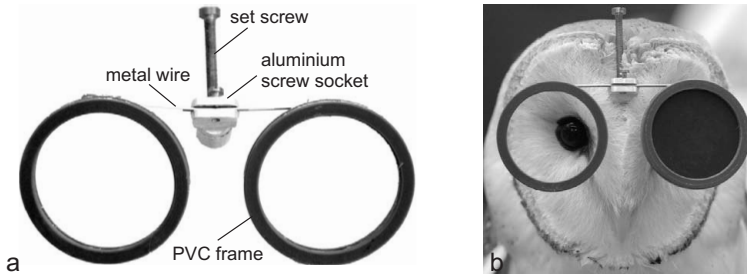


Figure 2.4: (a) Photograph of the barn owl spectacle. Its weight was 7 g. The PVC-frames could carry pieces of cardboard to occlude one eye (b). Generally, the owls were not bothered by wearing the spectacle alone. With the occluder equipped, however, performance and cooperation of two out of three owls was largely deteriorated.

custom built spectacle frame was used (figure 2.4). The spectacle was made of two PVC frames connected by a thin metal wire. A screw-socket, made of aluminum and placed midway between the two frames, was shaped to fit firmly onto the head-post the owl carried on its forehead. Total weight of the spectacle was 7 g. In the monocular viewing conditions the owls wore the spectacle with a small piece of black cardboard fitted to one of the frames, occluding either the left or right eye's view. In order to keep conditions as constant as possible, the owls also wore the spectacle during binocular presentation. In those cases, of course, the occluding cardboard was omitted.

### 2.3.3 Initial behavioral conditioning

All animal subjects were hand raised, tame and habituated to daily human contact. Therefore, handling and day-to-day experimenting could be carried out without putting the owls under considerable strain, and, as a result, the owls displayed good cooperation in all experiments. Nevertheless, the subjects had to be motivated appropriately to perform in psychophysical experiments on a constant and accurate level, since individual measurement sessions lasted 20 to 30 minutes, and sometimes included stimuli that were, presumably, difficult to detect.

The general procedure to shape the animals performance in the different tasks was operant conditioning with a positive reinforcement allocation. The animals weight was maintained at about 90 percent of their free-feeding weight.

Reinforcement was given by small pieces of chick muscle tissue, delivered by a carousel feeder with 36 feeding cups per dish. Usually, two dishes could be fed per day. In this way, owls could be reinforced for the desired behavior about seventy times per day. Behavioral shaping was accomplished stepwise. First, the animals had to learn to sit calmly inside the experimental chamber and to receive rewards from the feeder. In a next step, rewards were only given after one of the two response buttons was depressed by a touch of the owl's beak in a pecking-like manoeuver. The animals got used to this concept very fast and usually needed less than two weeks to show successful key pecking.

The next stage was the more difficult part of owl training. The owls were to peck one of the two keys *after* they fixated the stimulus display for some seconds. To draw the owl's attention towards the screen and have them orientated correctly towards it, a small bright observation stimulus was presented on the screen. It had a diamond shape, and changed its brightness constantly in a loop, giving it an overall pulsating appearance. After owls performed well on this task, the last step was carried out, where task complexity processed to the final level. The owls had to fixate the observation stimulus for a random amount of seconds (1–5 s), and were presented afterwards a target stimulus upon which the response keys were released to be pushed. The target stimulus was drawn randomly from a set of two different stimulus configurations which corresponded each to one of the two response keys. That is, if the owl was given target stimulus A, a push of the right response key was rewarded, while a push of the left response key ended the trial without reward, and returned the screen in observation mode again. Consequently, a given target stimulus B reversed this relation. It took about six to nine months of intensive training to finally have three naive animals to perform reliably in this task. On the other hand, two other owls used in the studies were already used to visual discrimination paradigms and did not have to undergo the above-mentioned training steps. These owls could start in transfer training sessions right away.

### 2.3.4 Transfer experiments

Transfer training sessions were carried out after the owls mastered in the initial basic discrimination paradigm, as was introduced above. In transfer sessions, the configuration of training stimuli A and B were altered successively until their appearance arrived at the final configuration A' and B', that was actually used in the experimental sessions. That is, after the transition from the initial easy-to-discriminate targets A and B to the final version, A' and B' had only



one single distinguishable feature left. In the vernier acuity experiments this feature was a horizontal offset in a pair of abutting bars and gratings, and in the CSF experiments this feature was the orientation of the sinusoid of a Gabor patch. The transition steps and the final stimulus configuration as were used in the two different behavioral studies can be reviewed in figure 2.5.

### 2.3.5 Task design and reward strategy

A prerequisite for perceptual sensitivity measures, such as the discrimination sensitivity for displaced lines in a grating stimulus (vernier acuity), or discrimination sensitivity for the orientation of contrast defined Gabor patches (contrast sensitivity), is the successful perceptual discrimination of the two respective stimulus configurations. That is, the barn owls had to learn to memorize each of the two configurations and, on stimulus onset, compare its memory to the presented stimulus and push the corresponding response key. This approach can be regarded as an one-interval, two alternative forced choice discrimination task, similar as it is widely used in psychophysical studies. In every experimental condition, the time course of stimulus presentation was self-paced. The birds were, therefore, allowed to examine the stimuli as exact as needed.

As soon as the owls displayed successful discrimination of the training stimuli, the experimental phase began. We defined the discrimination success as being accomplished if the owls performed significantly better than a binomial chance process would govern. As an example, if 100 trials were presented, a 99% percent confidence interval would assign that more than 63 trials had to be correct responses to meet this requirement. Because stimulus alternation followed a pseudo-randomized order, allowing no more than three consecutive presentation of one of the two alternatives, we raised the significance limit by additional 10 percent. Given the example above, the owls had to be correct in 73 percent of the trials. Generally, when no experiments took place, the owls' performance was sustained with in-between training sessions. If the owls displayed unreliable performance at high stimulus intensities during an experimental session, the session was aborted and a normal training session filled the gap.

As in the training sessions, correct responses in experimental sessions were rewarded by food items. Reward contingencies were always 100 percent, giving the animal perfect feedback about the correctness of its choice. This had the advantage of less frustration due to unrewarded correct responses, but also had the disadvantage such that perceptual learning processes were not neces-

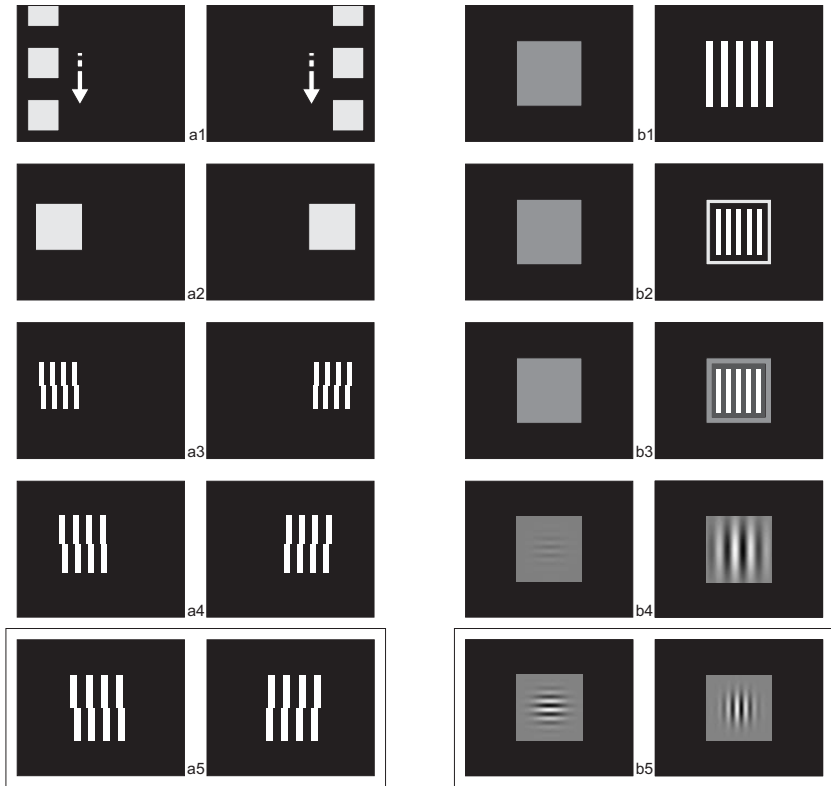


Figure 2.5: In the left panel the training transition steps used in the vernier acuity study are shown (a). Each row represents the stimulus configuration pair that corresponded to 'right' and 'left' responses. Panel a1 shows the first training stimulus pair, panel a5 the final stimulus configuration. The initial stimuli (a1) consisted of a bright large surface that repeatedly moved across the display from top to bottom during presentation, either in the left or right half of the screen. The blocks were presented statically in the second step (a2), changed to a vernier grating (a3), that consecutively moved to the screen center (a4), to finally arrive at the vernier grating stimulus that was used in the experiment (a5). In the right panel, (b), the transitions for the CSF stimuli are shown. Throughout the transition, the 'left' configuration was altered stepwise from a uniform gray surface (b1) to a gabor patch with horizontal sinusoid (b5) by adjusting its contrast. The 'right' configuration started with a square wave grating (b1), for which contrast was decreased (b2, b3) until a gabor patch with high standard deviation of the Gaussian was shown (b4). Finally, standard deviation was set to 0.48 and matched the configuration in the experiments (b5).

sarily to be excluded as an additional factor influencing threshold performance. To minimize this influence, experimental variables, such as stimulus configuration in vernier experiments, or spatial frequencies in CSF experiments, were always applied in roving alternations. If perceptual learning, though, had taken place, its effect would have influenced the results equally across experimental conditions, and, as a result, would have ruled out systematic impact.

### 2.3.6 Psychophysical threshold estimation

In both behavioral studies (vernier acuity and contrast sensitivity experiments) an adaptive staircase was applied to place stimulus intensities adequately for a subsequent estimate of the underlying perceptual threshold. However, threshold estimation procedures differed in both studies.

In contrast sensitivity and grating acuity experiments the staircase procedure was modified according to the two-down, one-up rule. That is, stimulus intensities were increased after two consecutive correct responses, and decreased on every false response. Stimulus intensities, then, converged to levels at which the subject responded 70.7% of the time correctly (Treutwein, 1995). Hereafter, the ratio of correct responses at each intensity level was calculated and plotted as a function of stimulus intensity. The data was then fitted by a two-parameter logistic function with a bootstrap method described in greater detail by Wichmann and Hill (2001a,b). Threshold performance was set half-way between chance level and high-intensity level, accounting for lapses the owl displayed at high stimulus intensities. The data of two such psychometric functions recorded on consecutive days were pooled in order to balance out fluctuating performance. For a more detailed description of the procedure review section 4.2.4 on page 51.

In vernier acuity experiments, the discrimination threshold was derived directly from a variable number of reversal points of simple up-down staircase tracks. Two tracks were applied in a randomly interleaved manner and their overall threshold was expressed as the arithmetic mean of the thresholds for the individual tracks. All tracks that were biased according to two different criteria were omitted from further analysis. For a more detailed description of the procedure review section 5.2.3 on page 68.



### 3 Ocular aberrations



#### **Abstract**

Optical quality in barn owl eyes is presented in terms of measuring the ocular wavefront aberrations with a standard Tscherning-type wavefront aberrometer under natural viewing conditions. While accommodative state was uncontrolled, all eyes were focused within 0.4 D with respect to the plane of the aberrometer. Total RMS wavefront error was between 0.06 and 0.15  $\mu\text{m}$  (mean: 0.10  $\mu\text{m}$ , STD: 0.03  $\mu\text{m}$ , defocus canceled) for a 6 mm pupil. The results suggest that image quality in barn owl eyes is excellent.

## 3.1 Introduction

The barn owl is an excellent candidate for studies of orientation behavior both in the auditory and visual domain, because it displays several functional, anatomical and physiological specializations. The most prominent feature of vision in these birds are the frontally oriented eyes, which create a large binocular field of view, an indicator for increased ethological importance of the use of stereo vision (Martin, 1984; Martin and Katzir, 1999; Wagner and Luksch, 1998). Consistently, behavioral studies showed that barn owls possess global stereopsis and use disparity as a depth cue with hyperacute precision (van der Willigen et al., 1998, 2002, 2003). Electrophysiological studies revealed that the visual Wulst of barn owls shows a high degree of binocular interactions and contains disparity sensitive cells that are tuned to characteristic disparities (Pettigrew and Konishi, 1976; Wagner and Frost, 1993, 1994; Nieder and Wagner, 2000). A more recent study found that barn owls also can discriminate non-aligned features in visual stimuli on a hyperacute level when viewed monocularly, a phenomenon known as vernier acuity in human visual research (refer to chapter 5 of this thesis, starting on page 65). This study also pointed to a similar computation of vernier targets in humans and owls, because the results in owls displayed a typical crowding/masking effect and a threshold improvement by a similar ratio which is typical for binocular summation in vernier experiments conducted with human subjects (Banton and Levi, 1991; Malania et al., 2007).

Objective measurements of the metrics of the barn owl eye implicated that these eyes are designed to maximize image quality while maintaining an increased level of retinal information convergence, advantageous especially under low light conditions (Martin, 1982; Schaeffel and Wagner, 1996). With an axial length of about 17.5 mm, the barn owl eye is relatively large (Schaeffel and Wagner, 1996), being almost twice as long as allometry based on body weight would suggest (Howland et al., 2004). Generally, a larger eye results in a larger retinal image, and thus, in an improved resolving power. On the other hand, indirect measurements of normal visual acuity (i.e. grating acuity estimation by ganglion cell counts and by pattern electro-retinogram) showed that visual acuity in these birds is comparably poor (Ghim and Hodos, 2006; Wathey and Pettigrew, 1989). Here, we wanted to find out to what degree vision in the owl is limited by the optical properties of their eyes. For that purpose we studied optical quality in means of an objective measurement of the ocular wavefront aberrations with a standard Tscherning-type aberrometer in

the awake barn owl under natural viewing conditions.

Wavefront aberrometry for the assessment of optical quality in human eyes has been widely used and can also be often found in clinical applications directly linked to eye surgery (Marcos, 2006; Thibos, 2000; Thibos et al., 2002c). Besides human eye studies, the measurement of wave aberrations was also applied in animal eye studies. So far, these include wavefront-error reports in eyes of mice (de la Cera et al., 2006a), cats (Huxlin et al., 2004), chicken (Thibos et al., 2002b), tree shrews (Ramamirtham et al., 2003) and monkeys (Coletta et al., 2003; Ramamirtham et al., 2005, 2006).

## 3.2 Materials and Methods

### 3.2.1 Subjects

Experimental animals were four adult American barn owls (*Tyto alba prat-incola*, three males, one female). Subject ages were between one and three years. All owls were taken from the institute's breeding stock and were hand-raised. They were kept in aviaries throughout their lives. All owls carried a "head-holder", a small aluminium stick, that was implanted onto the skull of their forehead under anaesthesia at an earlier time during life (for details of the procedure see Nieder and Wagner (1999)). Animals were kept at about ninety percent of their free feeding weight, because they participated in other behavioral experiments in which food deprivation was essential. A single measurement session was conducted with each owl and lasted no longer than three hours. Care and treatment of the owls were carried out in accordance with the guidelines for animal experimentation as approved by the "Landespräsidium fr Natur, Umwelt und Verbraucherschutz Nordrhein Westfalen", Recklinghausen, Germany, and complied with the "NIH Guide for the use and care of laboratory animals".

### 3.2.2 Measurement protocol and aberrometer

All measurements were conducted at the Department of Ophthalmology in Aachen. The experimental room was lit dimly by tungsten light, producing a luminance between 2 and 7 cd/m at the walls, the experimental table and the aberrometer, which matched the luminance of the fixation target inside the aberrometer. Barn owls were sitting on a wooden perch that was attached to

the experimental table directly in front of the aberrometer (see Figure 3.1). After a short period of adaptation to the lightning conditions the experiment was started. One of the experimenters held the tame owl and its head in a natural viewing position. Since barn owls lack any eye movements, relative eye position could be controlled by adjusting the head position. The correct alignment of the head and, thus, the eye in front of the aberrometer was achieved by constantly monitoring pupil size and shape. After a few attempts the animals were used to this procedure and showed good cooperation. No drugs were given to lubricate the eye, enlarge pupils or block accommodation. The owls blinked normally during the imaging session (i.e. about 6 times/minute).

The aberrometer was a Tscherning-type system (Schwind Eye Tech Solutions, Kleinostheim, Germany), with a 660 nm laser-diode illumination source and 168 measuring spots. Measuring acuity and reproducibility of this machine was tested with artificial and natural eyes of known error before measurements were conducted, and lay in the normal range ( $\pm 0.08$  D for defocus and cylinder,  $0.02 \mu\text{m}$  for higher order aberrations (Mrochen et al., 2000)). A schematic sketch of the aberrometer's general components can be found in Figure 3.1b. The pupil was illuminated by six infrared (IR) diodes that were circularly arranged around the aperture of the aberrometer. The corneal image together with a set of superimposed aiding lines was constantly monitored by a CMOS camera and, thus, provided reliable centering and focusing of the pupil. Purkinje reflexes of the IR diodes were always held well within the inner part of the pupil (compare Figure 3.1c). The whole system was mounted on a moving stage which was quickly adjustable in all three spatial dimensions to align the aberrometer aperture with the subject's pupil and to adjust focus. A single measurement took less than 50 msec. During this time an array of parallel laser beams of known spatial configuration was projected onto the retina of the measured eye and its retinal reflection was recorded by indirect ophthalmoscopy with a CMOS low-light camera. Typical images consisted of about 140 reflection spots (exemplary retinal image in Figure 3.1d). The measuring procedure was repeated in the same way for each eye several times (6 to 26 repetitions). Image analysis was carried out off-line after each measurement session.

#### 3.2.3 Data analysis

In total, eight eyes of four owls were studied in four measurement sessions. In each session 6 to 26 retinal images for each eye were recorded. With the application of a centroiding algorithm fitting the intensity profiles of each illumina-



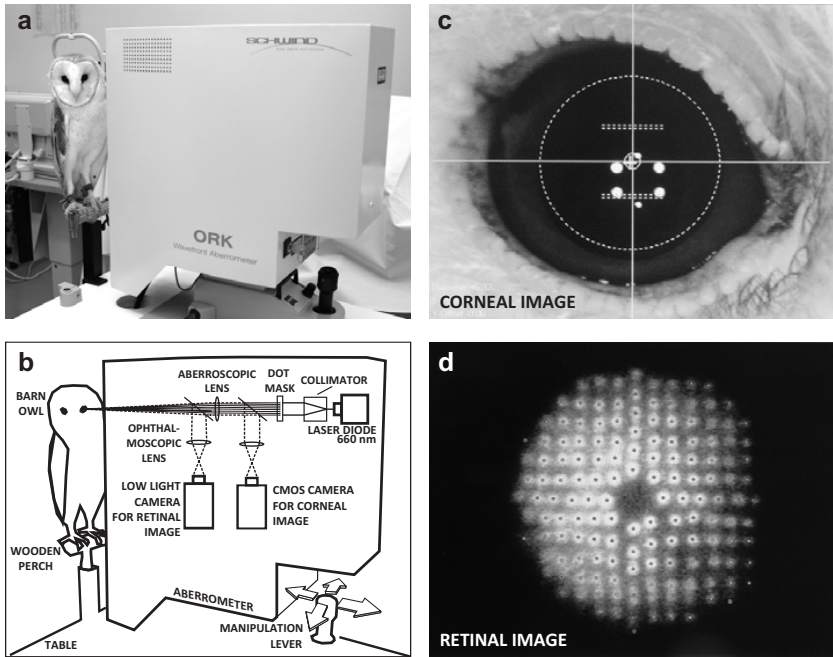


Figure 3.1: Materials and methods. (a) Owl PT in front of the aberrometer. During measurements owls were gently restrained manually by one of the experimenters to provide accurate positioning and centering of the eye in front of the aberrometer. (b) Schematic sketch of the setup and the Tscherning-system (Schwind ORK Wavefront Aberrometer). The whole system was mounted on a moving stage which was easily adjustable along all three axes in space via a manipulation lever. (c) Corneal image with superimposed aiding lines as seen online during measurements. The bright spots are first Purkinje reflexes of six IR-diodes that were circularly arranged around the aperture of the aberrometer. The dotted circular outline marks the pupil (in this image 6.32 mm diameter). (d) Typical retinal image from which the wavefront was calculated. The small dark markers within the bright illumination spots denote calculated centers of gravity for each spot.

tion spot to a Gaussian function in the retinal image, relative spot displacement was recorded. From these displacements the underlying wavefront was calculated and expressed in terms of the Zernike polynomial expansion up to the 6th order. Individual Zernike coefficients and the orthonormal set of Zernike polynomials, as recommended for describing wave aberration functions (Thibos et al., 2000), are presented in this study. The orthonormal set of Zernike terms and orders are also called the root-mean-square (RMS) wavefront error contribution of that term or orders. Ordering convention of single Zernike terms followed the OSA standards for reporting the optical aberrations of eyes (Thibos et al., 2002a). The RMS of a single Zernike term was calculated according to (3.1).

$$RMS(Z_n^m) = c_n^m \sqrt{\frac{2(n+1)}{1+i}} \quad (3.1)$$

where  $i = 0$  if  $m=0$ , and  $i = 1$  if  $m \neq 0$  (with  $c$ : Zernike coefficient in  $\mu\text{m}$ ;  $n$ : polynomial order;  $m$ : meridional frequency). The defocus term ( $Z_2^0$ , #4 in single indexing scheme) was converted to equivalent diopters ( $D$ ) by (3.2).

$$D = -4\sqrt{3} \frac{RMS(Z_2^0)}{r^2} \quad (3.2)$$

(with  $r$ : pupil radius in mm (Thibos et al., 2002a)). Due to the fact that accommodative state was uncontrolled in our setup, the true refractive state of the birds was not measured. Instead, the here presented defocus is the defocus relative to the plane of the aberrometer. Consistently, the defocus term was canceled for any further data analysis throughout this study, unless it is stated otherwise. Astigmatism, expressed in terms of equivalent diopters of the crossed cylinder ( $C$ ), was calculated from Zernike terms  $Z_2^2$  and  $Z_2^{-2}$  by (3.3).

$$C = \sqrt{J_0^2 + J_{45}^2} \quad (3.3)$$

with  $J_0 = -2\sqrt{6} \frac{RMS(Z_2^2)}{r^2}$  and  $J_{45} = -2\sqrt{6} \frac{RMS(Z_2^{-2})}{r^2}$

These transformations are derived from Thibos et al. (2002a). Because measured values of pupil size were between 6.3 and 7 mm, we chose to perform our measurements with a 6 mm aperture, concentrically placed at the actual pupil. For further data analysis calculating the point spread function (PSF), the modulation transfer function (MTF), and calculating convoluted images, the

best centered shots in each eye were chosen and averaged (6-10 for each eye) for all subjects separately. Convolution of a computationally designed image (vector graphic of an eye chart) was computed as follows: The original image was transformed to a grayscale bitmap and scaled in size to match the angular size of the PSF diameter calculated from the wavefront data of the according eye. The PSF was then taken as the kernel for a point-wise multiplication with the pixel neighborhood in the original image. The calculation was performed via a two dimensional convolution in the spatial frequency domain with the Matlab function `conv2`. Convoluted images were then re-scaled, cropped to original size, and adjusted in intensity by normalization to display a saturated image.

## 3.3 Results

### 3.3.1 Raw data: Retinal illumination spot image, wavefront and single Zernike terms

During measurements pupil diameter of all eyes varied between 6.3 mm and 7.1 mm, which could differ for both eyes because barn owls can control pupil size in both eyes independently (Schaeffel and Wagner, 1992). Given this pupil size, the 6 mm measurement aperture could always be used, and thus, around 150 illumination spots in each retinal image were used for the calculation of the underlying wavefront. Typical image quality at the retina and arrangement of the illumination spots can be seen in Figure 3.1d. Compared to studies performed with Hartmann-Shack aberrometry in humans (Liang and Williams, 1997), monkeys (Ramamirtham et al., 2005), chicken (de la Cera et al., 2006b), cats (Huxlin et al., 2004) and mice (de la Cera et al., 2006a), illumination spot quality observed in our study was slightly degraded with respect to visual spot edge determination, but of comparable quality regarding spot size and numbers.

Wavefront images for 3rd and higher order aberrations over the 6mm pupil were extremely flat, with low amounts of higher order aberrations, and revealed a mirror-symmetry between left and right eye only in subject OL and PT (see Figure 3.2, first column). Single Zernike terms, shown in the second column of Figure 3.2, are ordered following the OSA conventions (Thibos et al., 2000). Figure 3.2 also shows higher order terms in a magnified inset. Zernike term #4 (defocus) was the largest in all eyes. The mean absolute defocus term across

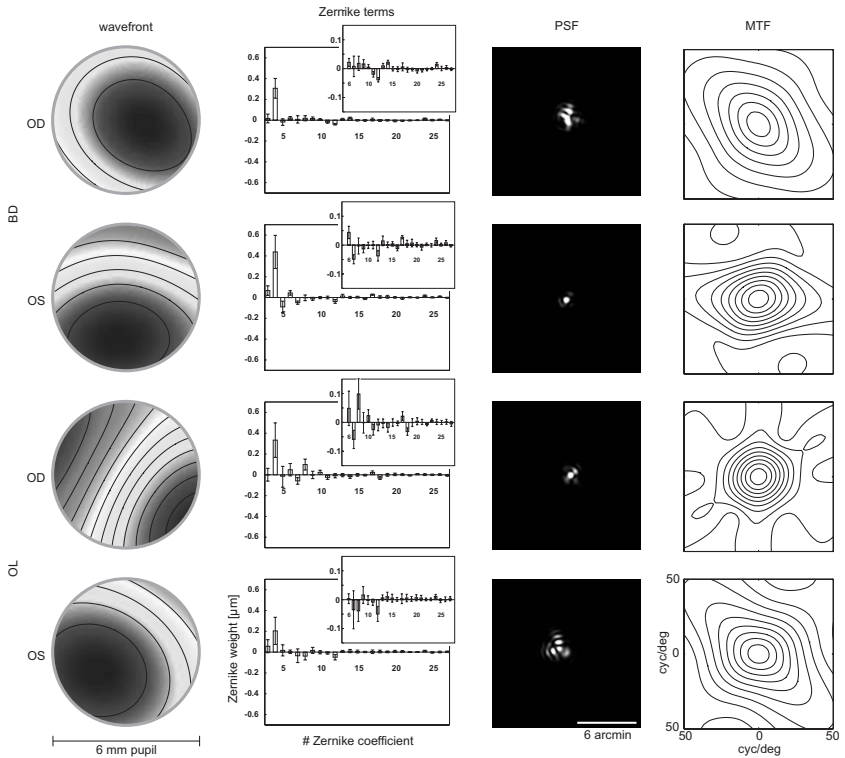


Figure 3.2: Summarizing results. See also figure on the following page. First column are wavefront maps calculated from Zernike  $3^{rd}$  order aberrations and higher order aberrations. Note that lines are only  $0.05 \mu\text{m}$  apart. Zernike coefficients, shown in the second column, are ordered in single indexing scheme following OSA convention, error bars are standard deviations. Zernike coefficients 0 to 2 are not shown. Small inset in the upper right corner are  $3^{rd}$  to  $6^{th}$  Zernike orders. Point-spread functions (PSF) with canceled defocus term ( $Z_2^0$  set to zero) are shown in the third column. They were normalized in intensity to display saturated images. In modulation transfer function (MTF) plots the lines are in steps of 0.1 modulation transfer units. Defocus was canceled. All data are calculated for 6 mm pupils and a 660 nm illumination.

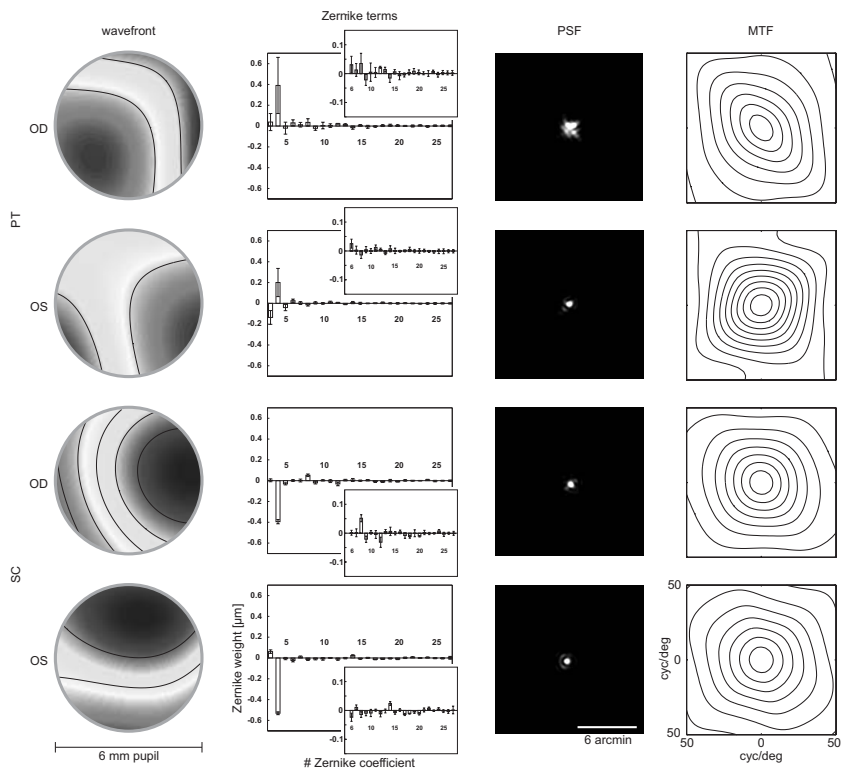


Figure 3.3: Wavefront results for owl subjects PT and SC. For explanation refer to caption of figure 3.2 on the preceding page.

all subjects was  $0.35 \mu\text{m}$  (STD:  $0.11 \mu\text{m}$ ), while the mean of absolute higher order terms was  $0.012 \mu\text{m}$  (STD:  $0.017 \mu\text{m}$ ) across all subjects. Expressed in this way, the defocus term accounted for 96.6 % of all aberrations (2nd to 6th order) across all subjects. Aberrations up to the 6th order were present but contributed only in a minor fashion to total wavefront error.

#### 3.3.2 Second-order aberrations

With reference to the plane of the aberrometer, the eyes of three owls displayed negative defocus. Mean spherical equivalent for defocus (Zernike term #4) was between  $-0.12$  and  $-0.40$  D for subjects BD, OL and PT (see Figure 3.4a). Interocular variability was similar to inter-individual variability. Mean standard deviation in these subjects was  $0.12$  D. On the other hand, subject SC showed similar defocus magnitude, but with opposite sign (OS:  $+0.40$  D, OD:  $+0.30$  D). Mean standard deviation was comparably small ( $0.013$  D). Astigmatism was calculated for all eyes from Zernike terms #3 and #5 according to equation 3, and combined to a spherical equivalent of the crossed cylinder between  $0.014$  D and  $0.065$  D (mean:  $0.033$  D, STD:  $0.020$  D). Across all subjects, no clear astigmatism axis was observable.

#### 3.3.3 Higher order aberrations

Generally, higher order aberrations (HOA) measured in this study were very low. To compare the impact of astigmatism and higher order aberrations on total wavefront error, the root mean square wavefront error (RMS) for the two second order terms (crossed cylinder astigmatism) are plotted together with the RMS of 3rd to 6th order terms (referred to as the HOA) in Figure 3.4b. 2nd order RMS was between  $0.018 \mu\text{m}$  (OD in OL) and  $0.140 \mu\text{m}$  (OS in SC). Mean 2nd order RMS was  $0.061 \mu\text{m}$ , with a standard deviation of  $0.044 \mu\text{m}$ . The HOA RMS was between  $0.04 \mu\text{m}$  (OD in PT) and  $0.15 \mu\text{m}$  (OS in BD), with a mean of  $0.088 \mu\text{m}$  and a standard deviation of  $0.033 \mu\text{m}$ . Zernike term #12 (spherical aberration term) was positive in 6 eyes and negative in the others, with a mean of  $0.025 \mu\text{m}$  (STD:  $0.016 \mu\text{m}$ ).

#### 3.3.4 PSFs, retinal image quality and MTFs

We calculated the point-spread function (PSF) for each eye separately from the averaged Zernike terms of the best centered shots available (6–10 each). PSF

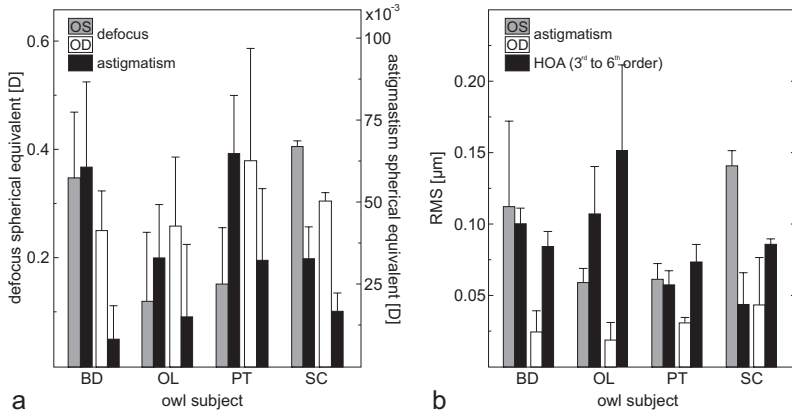


Figure 3.4: (a) Defocus and astigmatism. Spherical error derived from Zernike term  $Z_2^0$  (defocus) and terms  $Z_2^2$  and  $Z_2^{-2}$  (astigmatism, crossed cylinder) expressed in units of spherical equivalent in all subjects and eyes. Error bars denote standard deviations across measurements. Note the two different ordinates for defocus and astigmatism. (b) Lower and higher order aberrations. The 2<sup>nd</sup> order RMS (without defocus) is plotted together with 3<sup>rd</sup> to 6<sup>th</sup> order RMS (HOA) for each eye in all animals. Error bars denote standard deviations across measurements.

plots for each subject are shown in column 3 of Figure 3.2. The PSFs were calculated with canceled defocus (Zernike term #4 computationally set to 0  $\mu\text{m}$ ). The PSFs after focus correction were extremely centered and resembled the diffraction limited PSF in four eyes, while in the other four eyes slight decentering and typical astigmatism effects were observed (compare OS in subject OL). In Figure 3.5 a more direct comparison between owl (OS in subject BD), human, and the diffraction limited PSF is shown. Again, PSF plots are the 'best focus' PSFs. The influence of astigmatism and higher order aberrations on retinal image quality can also be observed in a set of computationally derived images. Figure 3.5 (bottom right) shows a vector graphic resembling a Snellen acuity chart often used in human visual acuity tests. The gaps between the smallest letters reading the words 'BARN OWL' subtend 1 arcmin, making them the 20/20 acuity benchmark. The other charts in this figure are derived from a two-dimensional convolution of the original image with the PSF kernel presented at the top. To better identify differences between the two versions (owl vs. human), a cut-out magnification is shown as well. As a conclusion based solely on retinal image quality, both human and owl should be able to

identify the smallest letters presented in this chart.

The complete two-dimensional modulation transfer functions (MTFs) for the 6 mm pupil of all eyes are plotted in the rightmost column of Figure 3.2 (2nd to 6th orders, defocus term canceled). Two radial cross-sections (x and y direction of Figure 3.2) of the MTF for all eyes are averaged and plotted in Figure 3.6 (thin dashed lines). The diffraction limited 6 mm pupil is plotted for reference as well. For comparison, the mean MTF of all owl eyes are plotted together with the mean MTF of two human subjects which participated in this study as well (pupil size was scaled to 6 mm with a re-converted Taylor polynomial). Again, only the defocus-corrected condition is shown. Note that the two human subjects had 20/20 vision. Both human and owl mean modulation transfers (MTs) are almost identical across all spatial frequencies. The owl MT exceeds human MT slightly below 20 cyc/deg and falls short of human MT above 30 cyc/deg.

## 3.4 Discussion

### 3.4.1 Methods

To our best knowledge, the here presented data is the first animal eye wavefront-error study carried out with a Tscherning-type wavefront sensor (TTWS). In recent publications of wavefront measurements in different animals the Hartmann-Shack sensor (HSS) is used most frequently (de la Cera et al., 2006a,b; Huxlin et al., 2004; Ramamirtham et al., 2005, 2003; Thibos et al., 2002b). Nonetheless, results from TTWSs are of comparable acuity and reproducibility (Mrochen et al., 2000), especially when larger pupils are measured, because the typical lower spatial resolution in TTWS becomes negligible with larger pupil area. Throughout the literature several examples for the use of TTWS can be found (Jahnke et al., 2006; Kaemmerer et al., 2000; Krueger et al., 2001; Mierdel et al., 1997, 2001; Mrochen et al., 2000, 2003; Prieto et al., 2000). Generally, benefits from the use of TTWSs are that the ingoing light path is used for measurement and that the illumination light source lies in the visible part of the spectrum. HSSs are more frequently used in state-of-the-art wavefront measurement applications, because they are less sensitive to scattering, and usually perform at higher resolution.

One of the key requirements in wavefront analysis is the alignment of the subjects visual axis with the optical axis of the measurement system (Thibos



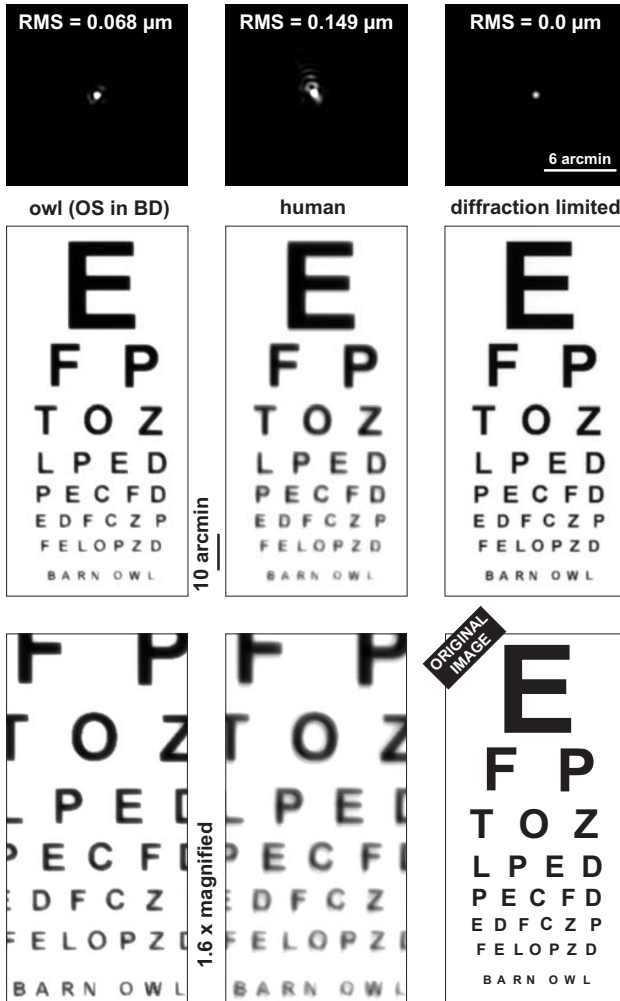


Figure 3.5: Comparing PSFs and retinal image quality. Top row: exemplary PSF in owl BD (OS), PSF of a human subject, and for the diffraction limited pupil. PSFs were calculated for the best focus condition (Zernike term #4 set to zero), and for a 6 mm pupil. The total RMS ( $2^{nd}$  to  $6^{th}$  orders without defocus) is shown. Middle row: A theoretical representation of retinal image quality derived from the convolution of the original image (bottom left) for the best focus condition in the owl (left), the human eye (middle), and the diffraction limited eye (right) is shown. The 'BARN OWL'-line corresponds to a 20/20 vision eye chart character size. In the bottom row (left and middle) a cut-out magnification (x 1.6) is shown.

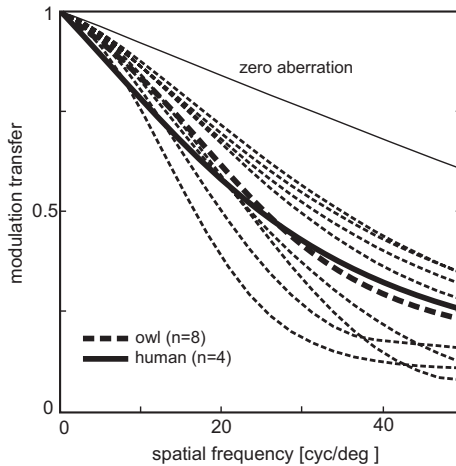


Figure 3.6: MTFs in owls and humans. The cross-sectional averaged MTFs of all eyes measured in this study are presented for  $2^{nd}$  to  $6^{th}$  Zernike orders (thin dashed lines). The averaged MTF of all owl eyes is given (thick dashed line) together with the mean of four human MTFs (thick solid line). All MTFs are calculated for a 6 mm pupil with cancelled defocus. The diffraction limited eye is shown for reference. Note that the two human subjects had 20/20 vision.

et al., 2002a). We achieved this with control of head position and orientation while constantly monitoring pupil size and shape. A misalignment in x-y-position would have resulted in a non-centered pupil, a misalignment about any of the two torsional eye axes in yaw and pitch direction would have resulted in an ellipsoid pupil shape. This procedure of correct eye positioning is possible in the barn owl, because this animal has an extremely limited potential in moving its eyes relative to its head (Dulac and Knudsen, 1990; Knudsen and Konishi, 1979; Knudsen and Knudsen, 1985; Masino and Knudsen, 1993; Steinbach and Money, 1973).

### 3.4.2 Implications of the results

Although a small fixation cross was shown to the eye under test during the experiments, it remains unclear, whether the animals accommodated correctly with reference to the plane of the aberrometer. Due to the fact that accommodative state was not measured independently, and the barn owl generally displays a relatively high accommodative range of about 6–12 D (Howland

et al., 1991; Schaeffel and Wagner, 1992), the here measured relative defocus was omitted from further analysis. Without drawing conclusions about normal defocus from our data, results from an earlier developmental study in barn owls showed, that refractive errors larger than 1 D disappeared during the first two weeks of juvenile development in this animal (Schaeffel and Wagner, 1996).

Despite the uncertainty of the true amount and sign of defocus in barn owl eyes, all animals show little amounts of astigmatism and very little higher order aberrations. Typical values of HOA in humans are about 3.3 times larger than HOA reported here (Howland, 2002; Porter et al., 2001). Also, HOA in eyes of another nocturnal species, the cat, are about 3.7 times larger than those of the owl (Huxlin et al., 2004). While HOA are lower in the barn owl compared to those in human eyes in an absolute sense, this difference might become even more prominent when put into relation with absolute eye size. Axial length of barn owl eyes is about 3/4 of that of human eyes (17.5 vs. 24.5 mm, (Hughes, 1977; Schaeffel and Wagner, 1996)), and following an observation by Howland, with the same set of optics and pupil size, the wave aberrations in the smaller eye should be larger than in the bigger one (Howland, 2005). We also showed typical PSFs of the owl eye and compared it to that derived from one human subject. Convolved images revealed that theoretical retinal image quality is comparable in man and owl (compare also Artal (1990)). Mean modulation transfer of all tested owl eyes almost exactly matched modulation transfer in the two human subjects we included in this study. Taken together, the data presented here show that averaged retinal image quality in the eyes of barn owls is excellent.

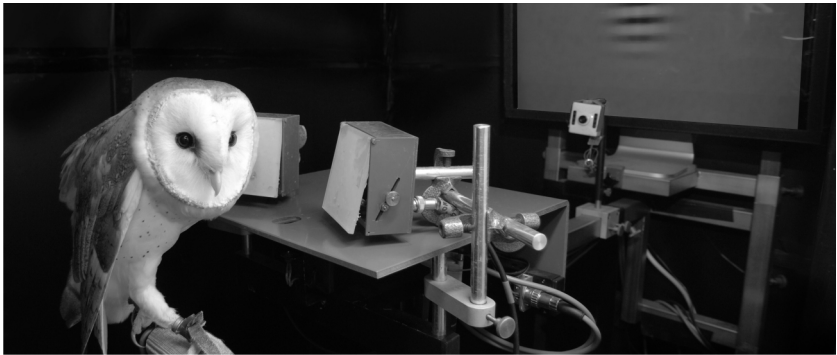
Nevertheless, based on retinal ganglion cell counts, barn owls show only poor grating acuity of about 7.8 cyc/deg (Oehme, 1961; Wathey and Pettigrew, 1989). This finding is supported by a pattern electro-retinogram study which calculates grating acuity to be 6.98 cyc/deg in the barn owl (Ghim and Hodos, 2006). The question arising from these findings is why the optics of the owl's eye would have evolved in a fashion allowing the formation of a retinal image with a quality that is far beyond a visual acuity given by the neural components creating vision in this bird. A similar question has been discussed in a recent study measuring the optical quality in cat eyes (Huxlin et al., 2004). The authors propose that given the nocturnal lifestyle of the cat combined with an almost three times larger pupil area in cats compared to humans at the same light levels, cats should experience significantly more optical interference than humans at the same light level. The authors conclude that the cat's optics are relatively good because otherwise additional aberrations would degrade vision

to levels of unsustainability (Huxlin et al., 2004). Given the relatively low high-frequency visual acuity in the barn owl (below 10 cyc/deg), this argument might not stand up to a quantitative analysis. On the other hand, being equipped with excellent optics that raise the MTF over all spatial frequencies, the owl might take advantage from an elevated contrast sensitivity for low spatial frequencies close to its neural sample pattern (compare Figure 3.6). Thus, while flying in the dark, owls might better manoeuvre through and avoid hitting low spatial frequency objects like e.g. limbs of a tree, and better visually identify items of prey. As an example, a mouse (6 cm) viewed from typical striking distance (5 m) would subtend about 0.7 cyc/deg, which matches the owl's contrast sensitivity function peak quite well (Ghim and Hodos, 2006).





## 4 Spatial contrast sensitivity



### Abstract

In this study a psychophysical approach measuring the spatial contrast sensitivity function (CSF) in the visual system of the barn owl (*Tyto alba pratincola*) is presented. Contrast sensitivity was measured in a two-alternative forced choice orientation discrimination task. Gaussian filtered sinusoidal gratings were used as stimuli. During a single experimental session, spatial frequency was held constant while contrast was varied, following a two-down one-up staircase procedure. The CSF found here renders the typical band-limited, inverted u-shaped function reported for a set of species in other studies. Maximal sensitivity was found at a spatial frequency of 1.01 cyc/deg. At this spatial frequency, contrast discrimination threshold was about 0.06, or, in terms of contrast sensitivity, about 18. Grating acuity was estimated from the CSF high frequency cut-off and yielded 3.8 cyc/deg. In a second experiment in which contrast was held constant and spatial frequency was varied, grating acuity was measured directly (3.6 cyc/deg). Compared to electrophysiological results, maximal contrast sensitivity found in the present study was increased by a factor of two. Compared to anatomical and electrophysiological estimates, grating acuity values were, on the other hand, reduced by the same factor.

## 4.1 Introduction

Successful interaction with the environment requires knowledge about it. In vision, information is largely mediated by light that is reflected from the surfaces of objects that form the environment. One feature that makes objects distinguishable is the amount of luminance that is reflected relative to the background or other objects. This relative luminance difference is referred to as luminance-contrast. Contrast is one of the important visual feature that make observers recognize their surroundings.

The spatial contrast sensitivity function (CSF) is, therefore, one of the fundamental functional descriptions of a visual system. It relates the ability of an observer to visually detect spatial gratings of different spatial frequencies to the amount of luminance-contrast present. If measured behaviorally, the CSF incorporates visual functions of both physical (i.e. the visual transfer function of the eye) and, to a greater extent, physiological nature (i.e. visual processing in the nervous system of the observer). The CSF may, therefore, be regarded as a direct measure of the perceptual high-level process of seeing.

Campbell and Green (1965b) were the first to measure the CSF in the human visual system, emphasizing the importance of visual processing for objects larger than the resolution limit. Apart from humans, the CSF has been measured in animals of different taxa with various psychophysical techniques. Among those are macaques (de Valois et al., 1974), squirrel monkeys (Merigan, 1976), owl monkeys (Jacobs, 1977), bush babies (Langston et al., 1986), cats (Blake et al., 1974; Bisti and Maffei, 1974), rats (Birch and Jacobs, 1979), ground squirrels (Jacobs et al., 1980), tree shrews (Petry et al., 1984), wallabies (Hemmi and Mark, 1998), goldfish (Northmore and Dvorak, 1979), pigeons (Nye, 1968), eagles (Reymond, 1985), and kestrels (Hirsch, 1982). In virtually all animals tested so far, the CSF renders, as in humans, a band-limited, inverted u-shaped function (Uhlrich et al., 1981). Sensitivity is best at intermediate spatial frequencies and is reduced at both higher and lower spatial frequencies. The high frequency roll-off in humans is regarded as a combined consequence of physical constraints leading to optical degradation (such as the diffraction limit and wave aberrations), and receptor cell spacing on retina level (Campbell and Green, 1965a; Cornsweet, 1970). The low frequency attenuation can be explained solely by neural factors, such as extent of lateral inhibition (Cornsweet, 1970), antagonistic surround mechanisms (Westheimer, 1972), or relative insensitivity of low spatial frequency filters (Graham, 1972).



Here, we present a psychophysical measure of spatial contrast sensitivity in the visual system of the barn owl. The barn owl is a highly specialized animal. Their visual capabilities have been demonstrated in several behavioral, physiological, and anatomical studies. Its prominent large eyes, being almost twice as long as allometry based on body weight would suggest (Howland et al., 2004), are oriented frontally, and, thus, create an unusual large binocular field of view (Martin, 1984). These eyes have excellent optical quality (Schaeffel and Wagner, 1996), showing only one third the amount of higher order aberrations found in human eyes (refer to chapter 3 vs. Howland (2002)). Barn owls can discriminate random dot stereograms with hyperacute precision (van der Willigen et al., 1998, 2002), a finding accompanied by several physiological studies demonstrating a high degree of binocular interaction and selectivity in the visual Wulst of these birds (Pettigrew and Konishi, 1976; Wagner and Frost, 1993, 1994). Barn owls, similar to humans, can discriminate vernier targets on a hyperacute level when viewing with one eye alone (chapter 5). Barn owls are distracted by crowded stimuli similar as humans are (Barrett et al., 1999; Malania et al., 2007), and show binocular summation ratios of similar magnitude (Banton and Levi, 1991). Barn owls also do perceive illusory contours (Nieder and Wagner, 1999). A recent study shed light on the attentional mechanisms of vision in this bird (Ohayon et al., 2008), and suggested a top-down modulation of gaze control when owls view natural targets.

Yet having this set of interesting and diverse approaches to barn owl vision at hand, there are only two studies dealing with the underlying basic properties of spatial vision in this bird. Barn owl visual acuity has been estimated by ganglion-cell density (Wathey and Pettigrew, 1989), and contrast sensitivity was recorded in a pattern electro-retinogram (PERG) study (Ghim and Hodos, 2006). To be able to relate the above mentioned results to the basic features of the barn owl's visual system more directly, we measured the barn owl's contrast sensitivity function and its grating acuity in a set of behavioral experiments.

## 4.2 Materials and Methods

### 4.2.1 Subjects

The experimental animal was one male adult barn owl (*Tyto alba pratincola*, subject SL), taken from the institute's breeding stock. The owl was hand-raised and tame. Its body weight was maintained at about 90% of its free feeding

weight. Water was given ad libitum. It was given food (chick meat) only in the experimental booth via a food dispenser or as a reward directly after the experiment inside the lab. Training and experiments took place on 5 days per week. When no experiment was carried out the owl was fed in its aviary. Care and treatment of the subject was carried out in accordance with the guidelines for animal experimentation as approved by the "Landespräsidium für Natur, Umwelt und Verbraucherschutz Nordrhein Westfalen", Recklinghausen, Germany, and complied with the "NIH Guide for the use and care of laboratory animals".

### 4.2.2 Experimental setup and stimuli

All experiments were conducted in a sound and light proof chamber, with no additional light source other than the stimulus display. The owl was sitting on a wooden perch in front of two response keys that were symmetrically placed left and right to an automated food dispenser. Its head was unrestrained and, upon the onset of a trial, oriented fronto-parallel relative to the stimulus display. Viewing distance was 85 cm, making one pixel subtend 1.044 arcmin of visual angle (figure 4.1).

The stimuli were gaussian filtered sinusoidal gratings (Gabor patch) of two discrete axes of orientation. The sinusoidal function propagated either in 0° or 90° direction relative to the coordinate system of the display (horizontal or vertical orientation, respectively, see figure 4.1). The standard deviation of the Gaussian was held constant at 0.48 while the phase of the sinusoid was altered trial-by-trial randomly in a 180° interval (not in training sessions). The Gabor patch, 12.2 degree of visual angle in diameter, was shown centered on the screen when a trial was initiated. The rest of the display was filled with an uniform gray surface. The whole screen was covered with a large sheet of linear neutral density filter (Lee Filter) that lowered overall luminance by approximately one log unit, producing a mean luminance of  $2.741 \text{ cd/m}^2$ , equally distributed at the whole Gabor patch area. Stimulus contrast was controlled by modification of the amplitude of the sinusoid and measured at viewing distance in a pre-experimental calibration sequence with the Minolta LS-100. Our display system was able to produce stimulus contrasts ranging from 0.991 to 0.0092 reliably. Contrast is defined throughout this study according to the Michelson-formula:  $\text{contrast} = (lum_{max} - lum_{min}) / (lum_{max} + lum_{min})$ . The choice of spatial frequencies used in the training sessions and experiments was according to results from pilot testing and earlier studies with the same animal

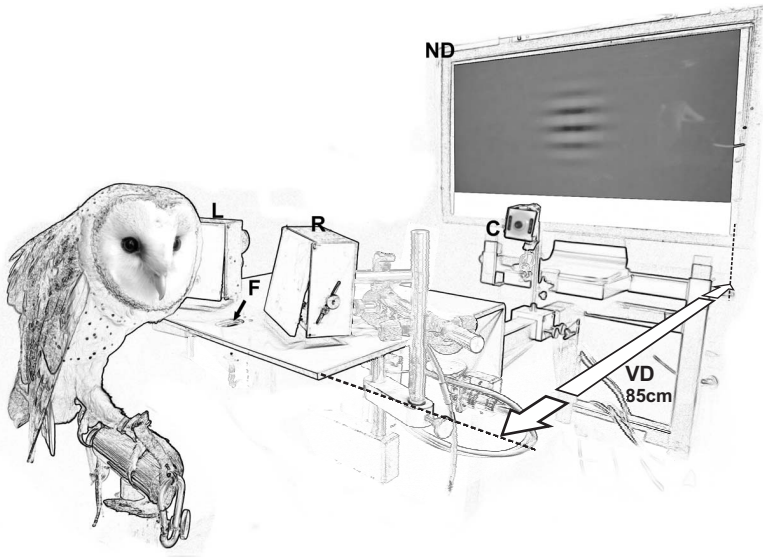


Figure 4.1: A sketch of an inside view of the experimental booth, showing the relevant parts of the experimental setup. The barn owl was sitting on a wooden perch fixed in front of an automated feeder, which delivered small pieces of meat upon correct responses (F). The two response keys, corresponding to the two stimulus configurations, were in easy reach of the owls beak (L,R). Viewing distance (VD) was 85 cm. The computer display was covered with a linear neutral density filter to reduce glare (ND). This picture shows the situation when the horizontal oriented Gabor patch was shown. A small IR-camera monitored the owls gaze, which in case of a fronto-parallel orientation triggered trial progress (C). Note that under experimental conditions the room was completely dark.

subject and setup (chapter 5).

Visual stimulus generation was controlled by custom written software (ANSI-C with the Open-GL utility kit GLUT), running on an Apple G5 workstation with a 8-bit graphics board (NVidia Geforce 6800 GPU), and digitally output on a 23" Apple Cinema Display. Owl responses were recorded via a custom built USB-interface, hooked up to the standard computer mouse input. The feeder was controlled by TTL-pulses produced by a USB input/output device (BMCM, Germany).

### 4.2.3 Psychophysical procedures

A small, flashing fixation target was shown in the center of the display between trials to attract the owl's gaze and to support correct orientation. When the subject oriented its gaze toward the screen, a trial was initiated and the stimulus was shown. After stimulus onset the owl had to peck one of two response keys, with the left key corresponding to a horizontal oriented grating and the right key to the vertical orientation. Horizontal or vertical gratings were presented in a pseudo-random order. That is, no more than three repetitions of one of the two alternatives were presented consecutively. The owl was rewarded after every correct response, false responses were not punished. The time course was self-paced to allow the owl an exact observation of the stimulus. Whenever the owl made large head movements and stopped fixating the display, the trial was aborted.

The owl was extensively trained to discriminate the two different gabor patches correctly before experiments began. During this training phase the stimulus contrast, its spatial frequency, and the phase position of the sinusoid was held constant (contrast: 0.991, spatial frequency: 0.61 cyc/deg, phase: 90°). We termed the performance level in the training task as being significant and moved on to the experimental phase, when the owl's performance lay above the 99 % confidence interval of a binomial process performing at chance level. As an example, in an experiment consisting 100 trials, significant performance was given if at least 63 correct responses were observed.

After the training phase and prior to contrast sensitivity experiments, several control experiments were conducted. First, we altered the pseudo-random design of the trial sequence to allow up to 7 repetitions of one alternative consecutively. This control intended to rule out strategy learning in the subject, making him, at low stimulus intensities, guessing better than chance level. Secondly, we wanted to find out whether the owl had incorporated a perceptual stable concept of the visual feature that had to be discriminated, and responded according to orientation only. Therefore, we presented Gabor patches with (a) sinusoids of random phase, (b) three spatial frequencies not shown during training (at fixed ratios 1.5, 0.75, and 0.5 fold the training wavelength), and (c) random spatial frequencies drawn from an even larger interval.

Typically, a single experimental session consisted of about 70 to 100 trials. Every experimental session was conducted at a single spatial frequency. Stimulus intensity choice within a session followed a simple up-down transformed rule. That is, stimulus intensity (i.e. contrast) was decreased after two consec-

utive correct responses and was increased after every false response. In this way, converging to stimulus intensities at which the animal responded 70.7 % of the time correctly, the choice of stimulus intensities presented to the animal lay near the threshold. To prevent a quick fatigue and frustration of the owl, bonus trials at high stimulus intensities were given from time to time. The eleven spatial frequencies used in our experiments ranged from 0.38 to 2.17 cyc/deg, and, thus, covered about 2.5 octaves of the spectrum. The different spatial frequencies were applied in an iterative order. That is, we started with a high spatial frequency, moved on to a low spatial frequency, followed by an intermediate spatial frequency and so on.

For further analysis, the results of two consecutive experimental sessions at each spatial frequency were combined to build the basis of psychophysical raw data (see figure 4.2 for an example). This was done by re-calculating the performance level at each stimulus intensity from the pooled data of both runs. This procedure balanced out inconsistencies in performance that occurred on different testing days. Note that it did not necessarily produce an average threshold of both runs.

#### 4.2.4 Data analysis and grating acuity

For all eleven spatial frequencies, the behavioral performance, i.e. the percentage of correct responses, was plotted as a function of stimulus intensity. With a popular bootstrap method described by Wichmann and Hill (2001a) used in the Matlab function *psfit*, a logistic function  $\Psi(x)$  (4.1) was fitted to the data points, generating a complete psychometric function.

$$\Psi(x) = \gamma + (1 - \gamma - \lambda) * \frac{1}{1 + e^{\frac{\alpha - x}{\beta}}} \quad (4.1)$$

where  $\Psi(x)$  is behavioral performance at stimulus intensity  $x$ ,  $\alpha$  and  $\beta$  are the fit parameters. Contrast threshold was defined as the stimulus intensity on the psychometric function half-way between lower ( $\gamma$ ) and upper ( $\lambda$ ) asymptote. The lower asymptote was set to 0.5, the upper asymptote was corrected to account for lapses the owl sometimes showed at high stimulus intensities. With a statistical re-sampling of the data points ( $n=1000$ ), the 95 % confidence intervals at threshold level were calculated (Wichmann and Hill, 2001b). The contrast sensitivity and its confidence interval was calculated as the inverse of the contrast threshold.

## 4 Spatial contrast sensitivity

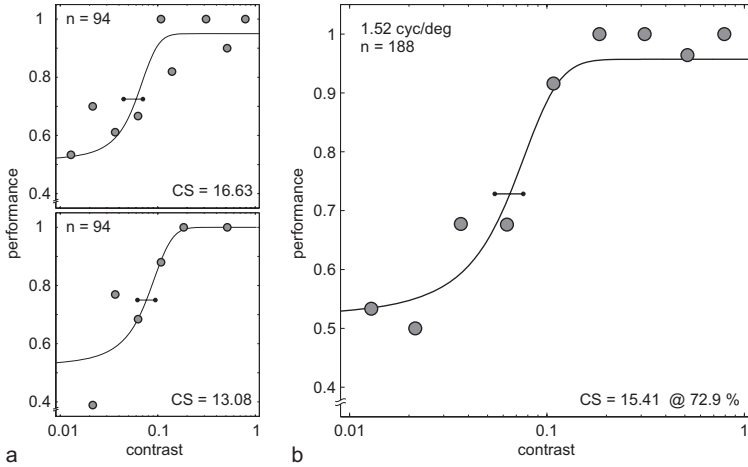


Figure 4.2: An example for the combination process used throughout this study. In (a) two psychometric functions of subsequent experimental sessions are shown. The ratio of correct responses were defined as behavioral performance and denoted on the y-axis. In this example, spatial frequency was 1.52 cyc/deg. Both sessions were comprised of 94 trials each. Contrast threshold and, inversely, contrast sensitivity (CS) were calculated from fitting a logistic psychometric function to the data, and were defined at the inflection point of that function. The horizontal bar is the 95% confidence interval at threshold level. Note that trial numbers in each session are not equally distributed over contrast intensities due to the applied staircase rule (see section 4.2.3 for explanation). In (b) the two sessions are combined by re-calculating the performance at each contrast level for the pooled data from (a). Note that the logistic function fits the data better as in (a), as is also reflected by the smaller confidence interval of the threshold.

The CSF was described by a double exponential function, that was fitted to contrast sensitivity data by a method of least squares (Uhrich et al., 1981). Grating acuity was, then, derived computationally from an extrapolation of the CSF beyond the high frequencies tested. Additionally, grating acuity was measured directly in a way similar to the method described above: at two different fixed contrast levels (0.991 and 0.779) spatial frequency was altered according to the transformed up-down rule. A psychometrical function was then fitted to the behavioral discrimination performance at the different levels of spatial frequency. The grating acuity threshold was defined as the spatial frequency at the inflection point of the corresponding psychometrical function. Confidence intervals were calculated as stated above.

## 4.3 Results

### 4.3.1 Training, control experiments, and response bias

The owl reached significant behavioral performance after only 13 sessions. Mean training performance was  $81.96 \pm 7.78$  % correct responses in the first 15 training sessions after reaching the criterion, and  $89.53 \pm 6.35$  % correct in all training (or bonus) trials recorded. In 6 control sessions the phase of the Gabor patch was applied randomly. In all of these sessions the owl responded more than 90 % correctly (mean:  $95.0 \pm 1.8$  %). All other control sessions were conducted twice and fell well within the range of normal training performance. In particular, these were two times 92.1 % correct for random wavelength, 79.6 % and 94.6 % correct for up to 7 repetitions (see section 4.2.3), 87.8 % and 94.8 % correct for 0.5 fold training wavelength, 93.6 % and 89.6 % correct for 0.75, and 87.8 % and 91.5 % correct for 1.5 fold training wavelength.

In total, 1189 training and bonus trials, 684 control trials, and 2642 experimental trials were recorded. 2017 trials made up the contrast sensitivity experiments, the remaining 625 trials were used for grating acuity experiments. Bias was calculated for the experimental sessions as follows: by applying the binomial distribution (with  $n$ : total number of trials,  $p$ : percentage of horizontal stimuli actually shown to the owl) a 95 and 99 % confidence interval (abbreviated as CI, hereafter) was calculated for each experimental condition (spatial frequency, or contrast level in the grating acuity experiments). The interval, therefore, reflected the number of 'horizontal' responses (abbreviated as HR, hereafter) the owl could give without displaying a statistically significant bias. This bias analysis was applied over the whole range of stimulus intensities (global bias), and for two intervals on the intensity scale separately (split bias). One interval, defined as near threshold, was comprised of stimulus intensities lower than threshold and one intensity above threshold. The remaining stimulus intensities made up the 'above threshold' interval.

For both contrast sensitivity and grating acuity experiments, no statistical significant bias was observed when a 99 % confidence interval was applied. However, on the 95 % CI level, in some cases a bias was present. In the contrast sensitivity experiments the owl displayed a global response bias in 6 out of 11 cases (at 2.17, 1.01, 0.87, 0.76, 0.61, 0.38 cyc/deg), but with no consistent direction of bias. That is, in 4 cases he preferred horizontal over vertical responses, while in the other two this relation was reversed. The owl never displayed bias in trials that lay above threshold, but only in the near threshold

trials. There was only one case in which a global bias was present in the absence of bias in the split condition (0.38 cyc/deg). In one case (2.03 cyc/deg), only split bias in near threshold trials was present.

In the grating acuity experiments the owl showed a response bias, generally preferring vertical over horizontal responses. Interestingly, this bias was differently distributed over the stimulus intensities for the two contrast levels tested. At maximum contrast (0.991) the owl showed no significant bias at low stimulus intensities near the threshold (spatial frequency  $\leq 3.0$  cyc/deg). Here, the CI ranged from 60 to 81 HR, while the owl chose 63 HR ( $n=136$ ). At larger stimulus intensities ( $n=207$ ), the owl chose 85 HR, with a CI ranging from 92 to 119 HR. At the second contrast level (0.779) this relation was reversed. There was no significant bias at high stimulus intensities (HR: 49, CI: 39–56), and again a bias towards 'vertical' responses at lower intensities (HR: 79, CI: 87–112).

### 4.3.2 Contrast threshold estimation

In total, 11 different spatial frequencies, spanning about 2.5 octaves of the spectrum, were tested. We started with a high spatial frequency, moved on to a low spatial frequency, followed by an intermediate spatial frequency and so on. For each of the eleven wavelengths, two single experimental sessions were conducted. The results of the two runs were combined to calculate a single psychometric function (see figure 4.2 for an example). Contrast sensitivity at the given spatial frequency was derived from the inflection point of that function. Mean trial number per spatial frequency was  $183.4 \pm 35.3$  (refer to table 4.1). In all combined sessions, 7 to 10 stimulus intensities were tested. Except in one case (2.0 cyc/deg) there were always at least 3 intensity steps above or below threshold. Mean trial numbers near the threshold (4 intensity steps centered around threshold) were  $106.3 \pm 22.1$ . Threshold levels lay between 72.5 and 75 % correct responses. Deviances from the theoretical midpoint in the psychometrical function (75 % correct responses) appeared due to lapse correction at high stimulus intensities in 6 out of 11 cases (see figure 4.3 for an overview of all eleven psychometric functions).

A maximum sensitivity of 18.87 (CI: 17.24–22.73) was found at a wavelength of 60 pixels (1.01 cyc/deg). This value corresponds to a Michelson contrast of 0.053. With longer wavelengths, contrast sensitivity decreased monotonically. At the longest wavelength (160 pixels, 0.38 cyc/deg), contrast sensitivity dropped to 2.632 (CI: 2.320–3.367), corresponding to a contrast of 0.38.



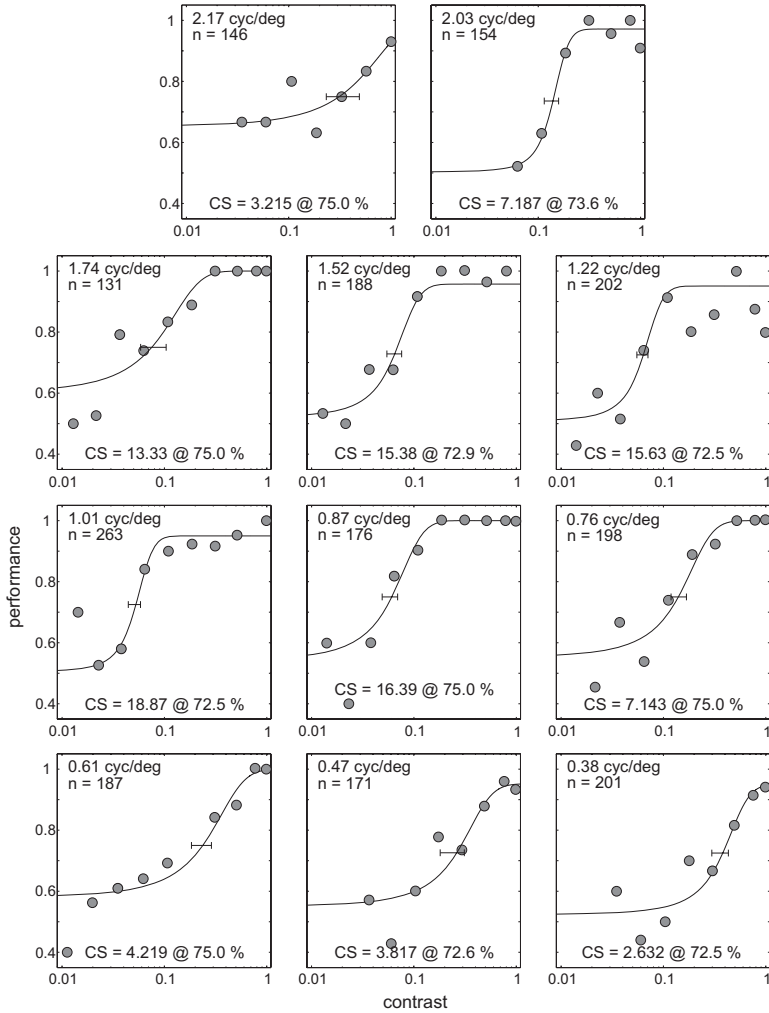


Figure 4.3: Combined psychometric functions at all spatial frequencies tested (see figure 4.2 for an example of the combination process). Behavioral performance, i.e. the ratio of correct responses, is plotted as a function of contrast level.  $\lambda$  is the wavelength of the sinusoid,  $n$  the number of trials, CS is contrast sensitivity at the denoted level of performance. Note that the number of trials were not applied equally over the whole range of contrasts, but that trials near the threshold appeared more often due to the staircase procedure (see text for explanation). The solid line is the logistic fit to the data. The horizontal line denotes the 95% confidence interval derived from bootstrapping the original data. Note also that threshold level was defined depending on the upper asymptote, which could differ due to lapses at high contrast levels.

Table 4.1: Contrast sensitivity (CS) values at all spatial frequencies (SF). The 95 % confidence interval borders (CI), number of trials, and the performance level at which threshold was defined are given as well.

SF[cyc/deg]	CS	CI	trials	performance level [%]
2.17	3.215	2.040 - 4.291	146	75.0
2.03	7.187	6.329 - 8.772	154	73.6
1.74	13.33	9.615 - 16.95	131	75.0
1.52	15.38	13.16 - 18.52	188	72.9
1.22	15.63	14.08 - 18.18	202	72.5
1.01	18.87	17.24 - 22.73	263	72.5
0.87	16.39	14.49 - 20.41	176	75.0
0.76	7.143	5.952 - 8.403	198	75.0
0.61	4.219	3.472 - 5.435	187	75.0
0.47	3.817	3.215 - 5.525	171	72.6
0.38	2.632	2.320 - 3.367	201	72.5

Contrast sensitivity at wavelengths shorter than 60 pixels decreased monotonically, reaching the minimal sensitivity of 3.215 (CI: 2.040–4.291) at 28 pixels. Here, threshold contrast was 0.31.

### 4.3.3 Contrast sensitivity function

Contrast sensitivity values derived from the combined experimental sessions were plotted against spatial frequency on a double logarithmic scale (see figure 4.4). Sensitivity values increased strictly monotonic from low spatial frequencies up to intermediate spatial frequencies, where sensitivity was maximal (18.87 at 1.01 cyc/deg). Consistently, going further to higher spatial frequencies, sensitivity decreased strictly monotonic. A double exponential function (4.2) was fitted to the normalized data by a method of least squares. This four-parameter function was found to provide a good fit to the CSF of several species (Uhlrich et al., 1981).

$$S(\gamma) = 100(K_1 e^{-2\pi\alpha\gamma} - K_2 e^{-2\pi\beta\gamma}) \quad (4.2)$$

where  $S(\gamma)$  is contrast sensitivity at spatial frequency  $\gamma$ . Our best fit was found for the following parameters:  $K_1 = 1.536$ ,  $K_2 = 1.562$ ,  $\alpha = 0.2489$ ,  $\beta = 0.2556$ . Peak sensitivity derived from this function was 13.91 at a spatial frequency of 0.963 cyc/deg. The width of the CSF was measured in octaves as

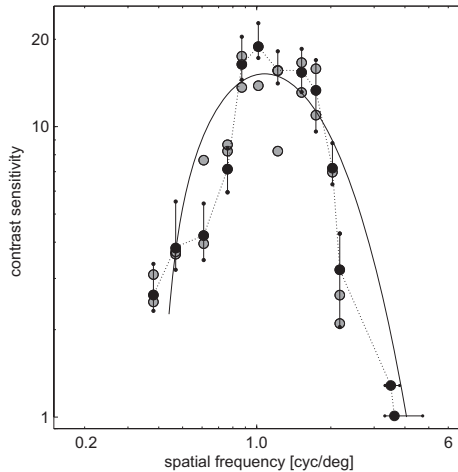


Figure 4.4: The contrast sensitivity function in the barn owl visual system. Contrast sensitivity was defined as the inverse of contrast thresholds and was plotted against spatial frequency. The dark circles are the sensitivity values derived from combination of two consecutive experimental sessions. The thresholds resulting from the single sessions are plotted in gray. The vertical bars are the 95 % confidence intervals calculated from the combined psychometric functions (see figure 4.3). The sensitivity values were fitted to a double exponential function by a method of least-squares (solid line). The two thresholds found in the grating acuity experiments are drawn for reference as well (bottom right). The dotted line connects contrast sensitivity thresholds and is drawn for pictorial purposes only.

the distance between the spatial frequency on either side of the peak frequency at which sensitivity declined by a factor of two. That is, width at half amplitude was 2.69 octaves (0.45–2.90 cyc/deg). The high frequency cut-off ( $S(\gamma) = 1$ ) was 3.81 cyc/deg.

#### 4.3.4 Grating acuity

Grating acuity was measured at two contrast levels (0.991 and 0.779) with a method similar to the one used in the contrast sensitivity experiments and with identical stimulus configuration. In total, 343 trials in 4 experimental sessions were recorded at maximum contrast. Grating acuity, expressed as the wavelength of the sinusoid at which discrimination performance was at threshold, was at both contrast levels similar: at 0.991 contrast level, grating

## 4 Spatial contrast sensitivity

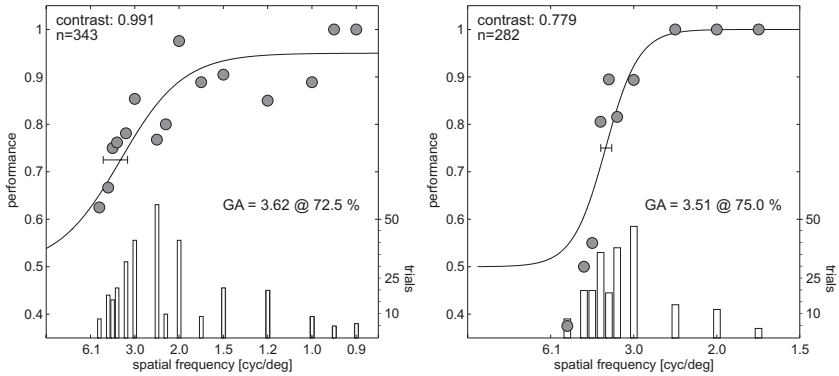


Figure 4.5: Grating acuity was measured at two contrast levels. The left panel shows the results at the highest contrast level possible with our display system (0.991). The circles denote discrimination performance at a given wavelength of the Gabor patch presented. The solid line is the logistic fit to the data, the small horizontal bar is the 95 % confidence interval at threshold (Wichmann and Hill, 2001a,b). At maximum contrast, 343 trials were recorded, with the majority lying around threshold level (see bar plot at the bottom of each panel, denoting trial numbers per stimulus intensity). Grating acuity threshold was found at a wavelength of 16.78 pixels, equalling a spatial frequency of 3.62 cyc/deg. Due to lapses at high stimulus intensities, the upper asymptote of the psychometric function was corrected. In the right panel, the results for the 0.779 contrast level are shown. In total, 282 trials were recorded, grating acuity was at 17.36 pixels, equalling 3.51 cyc/deg. Note that in the condition shown in the right panel, additional spatial frequencies (1.0, 0.7, 0.6 cyc/deg) were tested and lead to 100% correct responses. For figural purposes, these are not shown here.

acuity was 16.78 pixels (CI: 12.86–18.36 pixels). This value equals a spatial frequency of 3.62 cyc/deg. Here, performance level at threshold was 72.5 % correct responses, due to lapses at high stimulus intensities. Out of the 343 trials, the 7 smallest intensity steps (12, 14, 15, 16, 18, 20, 25 pixel) made up about 60 percent of all trials. This was due to the staircase rule applied to stimulus intensity choice (compare figure 4.5).

In the lower contrast condition (0.779) grating acuity was 17.36 pixels (CI: 15.98–18.30 pixels), or 3.51 cyc/deg, defined at 75.0 % correct response level. Here, out of 282 trials recorded in 3 sessions, 202 trials (71.6 %) were recorded near threshold level (12, 14, 15, 16, 17, 18, 20 pixels).

## 4.4 Discussion

### 4.4.1 Methodological considerations

Presenting acute contrast defined stimuli on a LCD computer display is theoretically limited in at least two ways: First, the minimal luminance-contrast possible to be displayed might be not suited for extreme low-contrast stimuli. We measured the actual contrast at every amplitude-step used in the experiments with the Minolta LS-100 luminance meter in a calibration sequence. The system was able to present contrasts below 0.01 reliably, and since all discrimination thresholds found in the experiments were at contrasts above 0.05, the display was suited for our purposes. Second, due to only 256 grayscale levels possible to be output by the graphics-card, at low contrasts and/or low spatial frequencies, the system might introduce unwanted high frequency borders in the intended sinusoidal signal. The stimulus, then, would appear "jagged" and not smooth. We tested this psychophysically with a human observer, reporting the jaggedness of the stimulus. Again, aliasing artifacts appeared only at contrasts below 0.01, lying clearly beyond the range of contrasts actually tested in the experiments. We concluded from this, that our display system, while inappropriate for human observers, was suitable for contrast thresholding in the comparably limited range given by the visual system of the barn owl. This notion was also reflected by the low-frequency roll-off displayed in the actually measured contrast sensitivity function.

### 4.4.2 Implications of the results

Based on the results of the control experiments, we conclude that the owl was able to incorporate a concept of the task, making a decision based on the orientation of the grating in the Gabor patch alone, a prerequisite for the use of the orientation discrimination paradigm. In trials with gratings of spatial frequencies that were never used in the training sessions before, the owl showed similar performance as in the training sessions. This was also true when the grating was presented with random phase configuration. Moreover, the responses to the stimulus showed robustness against a change in inter-trial alternative choice to a quite large extent. While in training trials no more than three repetitions of one alternative occurred consecutively, this was changed to a maximum of 7 possible consecutive repetitions in the control sessions. Again, performance did not drop significantly, though this change might have increased fatigue and

frustration in the owl. We conclude from this, that the applied psychophysical method and stimuli produced a stable behavioral response in the animal.

On the other hand, in some experimental sessions (6 out of 11), the owl showed a significant response bias towards one of the alternatives. This bias was not consistent (4 sessions in which horizontal responses were preferred, 2 times reversed order), and disappeared completely at a lower level of statistical first-order error. That is, with a 99 % confidence interval, bias was no longer present. Interestingly, there was only one case in which the animal showed a global bias without the presence of bias in near threshold trials. In all other cases, a significant bias occurred only in near threshold trials. The preferred bias that appeared in the grating acuity experiments supports the idea, that in this special case it could have been a biased detection process, making the task to detect vertical gratings 'easier' than horizontal gratings. This type of bias is also present and well described in human and primate observers and termed orientation anisotropy (Campbell et al., 1966; Mansfield and Ronner, 1978). However, in almost half of the biased sessions in our contrast sensitivity experiments, the vertical-horizontal preference was reversed, and, moreover, in almost half of all sessions no bias was visible at all. Therefore, there is no clear evidence for an orientation anisotropy in our data.

### 4.4.3 Comparative approach to barn owl contrast sensitivity and grating acuity

The data presented here are the first measure of the behavioral spatial contrast sensitivity function in the visual system of the barn owl. A maximum contrast sensitivity of around 18 was found at a spatial frequency of around 1 cyc/deg. Sensitivity declined rapidly for spatial frequencies smaller than 0.8 cyc/deg. Grating acuity was derived from the high-frequency cut-off of the CSF to be 3.8 cyc/deg. Furthermore, grating acuity was reported independently at two high contrast levels in a second behavioral experiment. Here, grating acuity was found to be on the order of 3.6 cyc/deg.

For validation, these results can be compared to at least two studies, in which contrast sensitivity and grating acuity was measured and computed electrophysiologically and anatomically, respectively (figure 4.6). In an anatomical study, retinal ganglion cell density was used as the basis for a grating acuity estimation. A maximum ganglion cell density of 11000–12500 per  $mm^2$  was reported at the area centralis, and, thus, a grating acuity of 7.9–8.4 cyc/deg was calculated by application of the Shannon sampling theorem and an as-

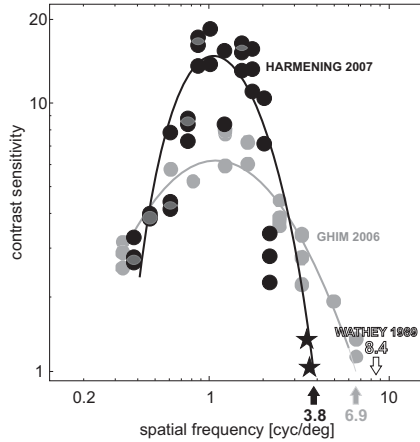


Figure 4.6: Comparative view on contrast sensitivity and grating acuity in the barn owl. The black dots and black solid line are the contrast sensitivity values and CSF found in the present study. The light gray dots and solid line are a re-plot of the CSF found by Ghim with the pattern electroretinogram (Ghim and Hodos, 2006). The arrows at the lower right indicate the different results for grating acuity in the different studies. Specifically, these are an estimate according to the CSF from our study (black), from an extrapolation of Ghim (light gray), and from an estimate based on ganglion-cell count by Wathey (outlined) (Wathey and Pettigrew, 1989). The behavioral measures of grating acuity from the present study are marked ★.

sumed retinal magnification factor of  $0.15 \text{ mm/deg}$  (Wathey and Pettigrew, 1989). While the geometry of the barn owl eye is described in detail (Schaffel and Wagner, 1996), it remains unclear how many of the ganglion cells in area centralis are involved in spatial acuity tasks. Moreover, considering the topography of ganglion cell density in the retina of barn owls, displaying a horizontal streak of high cell density (5000–8000 per  $\text{mm}^2$ ), behavioral acuity values lower than the theorized 8 cyc/deg become reasonable (Wathey and Pettigrew, 1989).

In the electrophysiological study, the authors measured contrast sensitivity in 4 barn owls with the pattern electro-retinogram (Ghim and Hodos, 2006). Combined peak sensitivity of about 6 was found at a spatial frequency of 1.1 cyc/deg (figure 4.6). In this study, grating acuity (6.98 cyc/deg) was computed based on extrapolation of the CSF beyond the measured high spatial frequencies, similar as in the present study. While the spatial frequency at which sensitivity peaks is in good accordance with our results, deviations appear in

maximum sensitivity values and high frequency cut-off. These might be due to the different methodological approach: the PERG method is known to produce about 40 % lower values of peak sensitivity when compared to behavioral data in the same subject (Hodos et al., 2002; Peachey and Seiple, 1987). When individual results of subjects in their study are compared to ours (contrast sensitivity of 9 versus 16), this rule finds a relatively good quantitative accordance. Grating acuity deviances might be due to different luminance values used for visual stimulation. In their study, mean luminance of the display was  $94 \text{ cd/m}^2$ . Our experiments were conducted at intermediate light levels ( $2.7 \text{ cd/m}^2$ ), being a more than 30 fold reduction of mean luminance. In human, primate, and cat subjects it has been shown that a reduction of stimulus luminance affects the CSF, and, therefore, grating acuity estimates to a large extent (Patel, 1966; de Valois et al., 1974; Jacobs, 1977; Bisti and Maffei, 1974; Blake et al., 1974).

With a grating acuity of 3.6–8.4 cyc/deg, the barn owl is in good company with other owls. Specifically, acuity values have been obtained in the little owl (6 cyc/deg) (Porciatti et al., 1989), the great horned owl (6–7.5cyc/deg) (Fite, 1973), and the tawny owl (8 cyc/deg) (Martin, 1984). Compared to other raptorial birds, owls lie on the lower end of the acuity spectrum. Known behavioral acuity values span from extraordinary high values in the wedge tailed eagle (140 cyc/deg) (Reymond, 1985; Schlaer, 1972), to manlike values of around 70 cyc/deg in the Australian brown falcon (73 cyc/deg) (Reymond, 1987) or in the American kestrel (about 50 cyc/deg) (Hirsch, 1982). Superb acuities of 160 cyc/deg in the American kestrel (Fox et al., 1976) have been questioned due to a about 3 fold lower anatomical resolution (46 cyc/deg) (Dvorak et al., 1983), and were re-tested in another study (39.7–71.4 cyc/deg) (Gaffney and Hodos, 2003). Grating acuity of some other non-raptorial birds have been measured, either electrophysiologically or behaviorally, and the results place them somewhere between owls and eagles on the acuity scale. Among those are for example the quail (6.8 cyc/deg) (Hodos et al., 1991), the domestic chick (7.7–8.6 cyc/deg) (Schmid and Wildsoet, 1998), the Blue Jay (15–19 cyc/deg) (Fite and Rosenfield-Wessels, 1975), the pigeon (18 cyc/deg) (Porciatti et al., 1991), the rook (30 cyc/deg) (Dabrowska, 1975), and the magpie (30–33 cyc/deg) (Dabrowska, 1975).

The grating acuity of the barn owl reported here is of comparable magnitude of results found in the cat (3.5–7.0 cyc/deg) (Berkley, 1976) and the galago (2.6–4.3 cyc/deg) (Langston et al., 1986), a prosimian primate. This observation across animal species of such divergent phylogenetic origins supports the speculation that their common nocturnal lifestyle is the important ecological



factor setting the limits to spatial vision (refer to sections 3.4.2 and 6.2).



## 5 Vernier acuity



### **Abstract**

Vernier acuity thresholds were obtained psychophysically in three adult barn owls with vertical bars and sinusoidal gratings. A minimal displacement threshold of 0.58 arcmin was observed with the bar stimulus under binocular viewing conditions. The mean binocular bar threshold was 2.51 arcmin. Bar thresholds were lower than grating thresholds. Monocular thresholds, obtained in one bird only, were typically higher than binocular thresholds. With grating acuity being about 3.75 arcmin in this bird, we conclude that the findings reported here indicate that vernier acuity is hyperacute in the barn owl. The data presented here are the first demonstration of vernier acuity thresholds in birds.

## 5.1 Introduction

The ability of humans to detect tiny spatial offsets in paired lines, dots, or objects is known as vernier acuity. Psychophysical measures of vernier thresholds yield values down to 1–5 seconds of arc (Westheimer and McKee, 1977; Sullivan et al., 1972; Levi and Klein, 1982). Compared to thresholds derived from tasks that are physically limited by foveal cone spacing, such as two-point or grating acuity, vernier acuity thresholds are about 6–30 fold lower (Edelman and Weiss, 1995; McKee, 1991; Curcio et al., 1990). Thus, humans can determine the relative positional difference of spatially non-aligned features with a precision that corresponds to only a fraction of the eye's resolving power. This makes vernier acuity a 'hyperacuity' phenomenon (Westheimer, 1975). So far vernier thresholds have been obtained with humans (Wülfing, 1892), monkeys (Kiorpes et al., 1993), cats (Murphy and Mitchell, 1991) and rats (Seymour and Juraska, 1997), but not in birds.

The barn owl is a highly specialized nocturnal predator with exceptional preying skills. In particular, barn owls are renowned for their superior sound-localization capabilities (Wagner et al., 2005). However, also the visual system in this bird shows anatomical, functional and physiological specializations. The barn owl has frontally oriented eyes with high-quality optics (Schaeffel and Wagner, 1996) that create an unusual large binocular field of view compared to other birds (Martin, 1984). The barn owl has coupled accommodation in both eyes (Schaeffel and Wagner, 1992), and an enlarged visual Wulst with a high degree of binocular interaction and selectivity for binocular disparity (Pettigrew, 1979; Wagner and Frost, 1993; Nieder and Wagner, 2000). It has been shown that owls possess stereopsis and use disparity as a depth cue with hyperacute precision (van der Willigen et al., 1998, 2002). Furthermore, barn owls are also able to perceive illusory contours (Nieder and Wagner, 1999). Spatial visual acuity (i.e., minimum separable) in barn owl has been indirectly reported as an anatomical measure of ganglion cell density (Wathey and Pettigrew, 1989) and electrophysiologically in a pattern electro-retinogram (PERG) study (Ghim and Hodos, 2006). These studies found a theoretical grating acuity of 8.4 cyc/deg and 6.9 cyc/deg, respectively. The question asked here is whether the barn owl displays hyperacuity in a vernier task. This was tested behaviorally with two kinds of stimuli under binocular and monocular viewing conditions.

## 5.2 Materials and Methods

### 5.2.1 Subjects

Experimental animals were three male adult barn owls (*Tyto alba pratincola*, Subjects SL, OL, PT) taken from the institute's breeding stock. Earlier during life a small aluminium stick was fixed to the owls' skull with dental cement under anaesthesia (for details see Nieder and Wagner (1999)). This stick was used to fix a custom made spectacle frame to the owls' head with which one eye could be occluded. Training and experiments took place on 6 days per week. Owls were given food (chick meat) only in the experimental booth via a food dispenser or as a reward directly after the experiment inside the lab. When no experiment took place owls were fed in their aviary. Care and treatment of the owls were in accordance with the guidelines for animal experimentation as approved by the Regierungspräsidium Köln, Germany, and complied to the "NIH Guide for the care and use of laboratory animals".

### 5.2.2 Experimental setup and general procedure

The birds were trained extensively with the largest vernier shift which was used in the experiments until they reached significant performance, i.e. 68% correct in the discrimination task. After this training phase, the experimental phase started. All experiments were performed inside a sound-attenuated and darkened booth. Birds were sitting on a perch 85 cm in front of a 17" TFT panel (ran at its native resolution: 1280 x 1024 pixels). Whenever the owl oriented its gaze toward the screen, a trial was initiated and a fixation target was shown in the center of the screen. The fixation target consisted of a small flashing diamond-shaped bright surface (30 arcmin in square, 2 Hz, 180  $cd/m^2$ ). After a variable time delay (2–5 s), the fixation target disappeared and the vernier stimulus appeared. The birds had to peck one of two response bars, corresponding to a left or right vernier shift in the stimulus. The response bars were symmetrically placed to the left and right of a remotely operated food dispenser that delivered, only on correct responses, small pieces of chick meat. False responses were neither rewarded nor punished. The time course was self-paced to allow owls an accurate examination of the stimulus. A trial was interrupted whenever the birds made large head movements and stopped fixation of the screen. Head movements and fixation were controlled by observing the gaze and eyes under infrared illumination on a TV monitor. Behavioral performance

was controlled and monitored by custom-written software (ANSI-C application using the OpenGL Utility Kit/GLUT) running on a Silicon Graphics workstation that also delivered the visual stimuli.

### 5.2.3 Visual stimuli and data acquisition

Two different vernier stimuli were used in the experiments. The first stimulus ('grating') was a vertical sine wave grating presented on dark background ( $180 \text{ cd/m}^2$  peak luminance,  $0.43$  minimum luminance,  $70$  degree in square). Michelson contrast was calculated from the measured values to be  $0.995$ . Spatial frequency was constant and set to a non critical large value ( $0.6 \text{ cyc/deg}$ ). The vernier shift was introduced as a horizontal phase shift of the lower part of the grating relative to its upper part. The second stimulus ('bar') can be regarded as a cut-out of one cycle from the grating stimulus (compare inset in Figure 3. Note that, for illustrative purposes the stimuli here are drawn as square wave gratings). Grating or bar stimuli and monocular or binocular viewing conditions were applied in a random order.

A typical experiment consisted of about 120 trials of stimulus presentation and owl responses. Since we presented either left or right vernier shifts, owls could response left or right exclusively (2-AFC). Two staircases were recorded in parallel in a randomly interleaved manner. On every correct response the vernier shift in the stimulus decreased by one step, false responses lead to a shift increment (1-up 1-down). The initial value was set to a 20 pixel vernier shift. Following steps were 17, 14, 12, 10, 9, 8, 7, 6, 5, 4, 3, 2, 1, 0.75, 0.5, 0.25 pixel. At the 0.85m viewing distance one pixel equalled 1.0526 minutes of arc. In order to present sub-pixel shifts we used anti-aliasing procedures which come along as built-in functions with the OpenGL Utility Kit (GLUT).

At least 8 reversal points in each staircase pair were taken to calculate the arithmetic mean for each left and right track. After statistical check for equality, reversal points for both tracks were pooled and the threshold was expressed as their overall mean. Thus, single threshold values presented here are the mean values of at least 16 reversal points. In order to present a precise estimation of true absolute thresholds we omitted all staircases from the estimation which were biased according to two bias criteria. First we calculated the binomial distribution for every case and rejected all results in which owls answered significantly unbalanced (5.1).

$$P(k) = \binom{n}{k} p^k (1-p)^{n-k} \leq 0.05 \quad (5.1)$$

(With  $P(k)$ : probability for  $k$  left responses,  $k$ : number of left responses,  $p$ : probability for left stimulus,  $n$ : trials). Secondly we did a statistical comparison between thresholds for left and right stimulus configuration after averaging reversal points. If differences were significant ( $p \leq 0.05$ ) according to the Mann-Whitney U-test we rejected the staircase.

## 5.3 Results

### 5.3.1 Staircase procedure and response bias

Due to our criteria to account for bias, we first categorized our results into valid, invalid and unusable cases. Out of a total of 98 staircases we used 44 staircases for threshold estimation (valid case, Figure 5.1). We define a valid case as a staircase in which the reversal points for left and right tracks converged to values that were statistically equal (U-test,  $p < 0.05$ ).

The other 54 staircases were excluded from the estimation due to a statistical difference for left and right threshold values (27 invalid, compare Figure 5.2 a) and unbalanced responding (27 unusable, compare Figure 5.2 b). In total, we could record 10 valid staircases for subject SL, 22 for subject PT, and 12 for subject OL. Due to a strong response bias in subject OL and SL under monocular conditions (i.e. wearing the spectacle frame and occluding one eye), all but one monocular thresholds were obtained in subject PT. The number of trials needed to reach the first reversal point below threshold value in each staircase was counted. On average owl PT needed 58.9 trials to reach threshold level, owl OL needed 60.7 trials, and owl SL needed 45.8 trials, which is significantly earlier than the two others (U-test,  $p < 0.01$ ). No significant difference between conditions in single subjects was observed. Table 1 gives a detailed view on numbers of valid, invalid and unusable staircases for each subject, stimulus configuration and viewing condition. This table demonstrates that all three owls were reliable in binocular tests, with the least number of unusable cases occurring for binocular bar stimuli. Monocular tests were impossible in owl SL and resulted in many unusable cases in owl OL.

### 5.3.2 Vernier thresholds

We could estimate vernier thresholds for all animals and conditions. However, monocular thresholds were mainly based on data from one animal. The thresh-

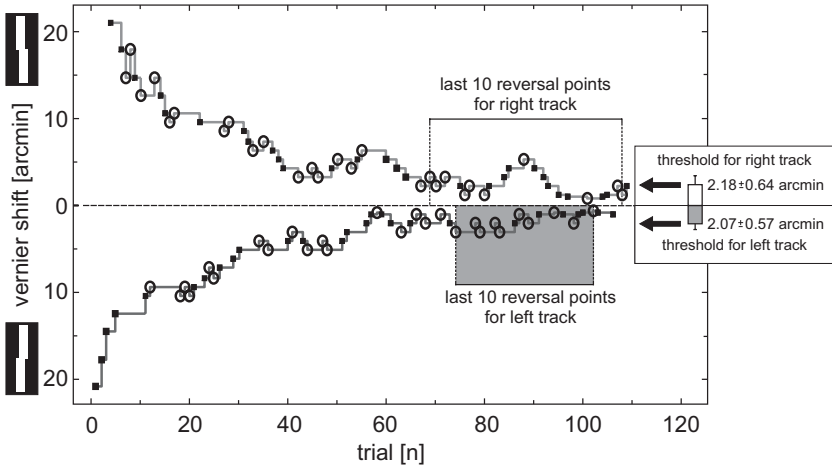


Figure 5.1: Staircase procedure. Exemplary result for subject PT under binocular viewing conditions with bar stimulus. Two randomly interleaved staircases were presented at the same time. Ordinate values indicate trial number, abscissa indicates vernier shift in minutes of arc for right and left shifts, respectively. Squares are trials, circles mark reversal points in the staircase. For illustrative purposes trials are connected by a gray line. In this case, the last 10 reversal points were averaged for threshold estimation. Dotted line corresponds to zero shift. Black arrows together with bar plot mark calculated thresholds for left and right track. Error bars are standard deviations.

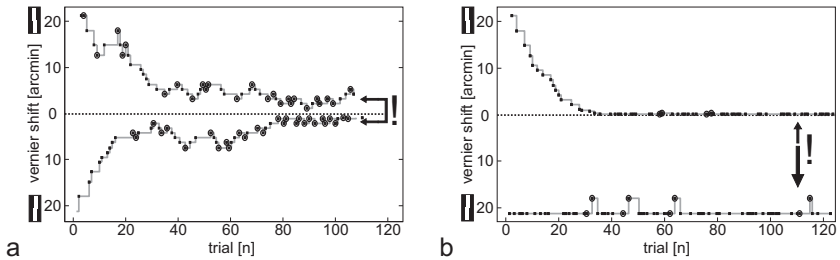


Figure 5.2: Biased response behavior. (a) Exemplary staircase result of owl PT under monocular viewing conditions with the bar stimulus. After averaging the last 10 reversal points, thresholds for left and right track are unequal according to the U-test. (b) Exemplary result of a strong bias in subject OL (monocular, grating), preferring RIGHT over LEFT responses, regardless of the presented stimulus. OL pushed in almost 80% of the cases the right response key. These staircase curves were excluded from the threshold estimation. See method part for further explanation of exclusion criteria.



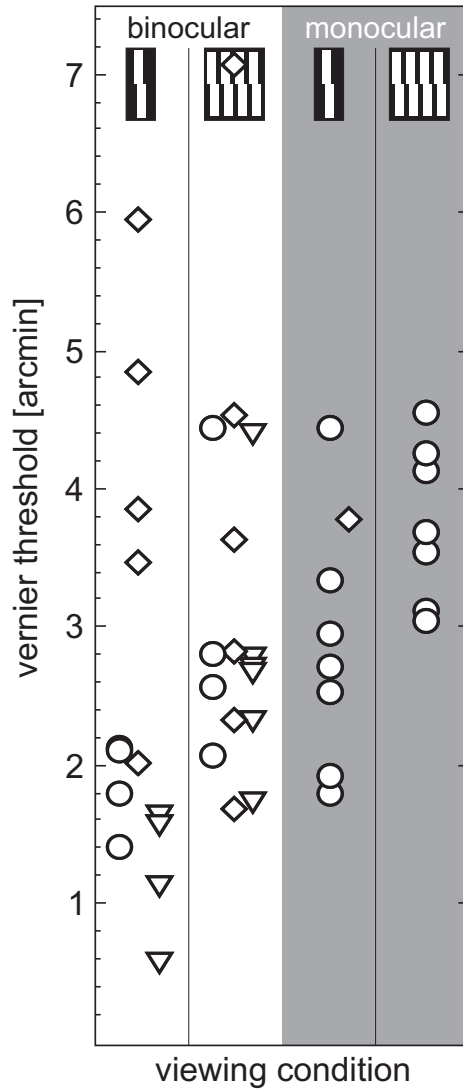


Figure 5.3: Summary of threshold values for all subjects and conditions. Marker differences indicate the three owl subjects (circle: PT, diamond: OL, triangle: SL). Insets at the bottom show stimulus configuration (grating vs. bar). Thresholds for subject OL show the largest scatter. The lowest thresholds are clearly lower than the anatomical resolution.

## 5 Vernier acuity

Table 5.1: Staircase experiments for all owl subjects and all conditions. Bold numbers are total number of experiments for each condition. Numbers in brackets are valid/invalid/unusable cases.

Owl subject	Number of thresholds		
	SL	PT	OL
Bar binocular	8(4/4/-)	6(4/2/-)	7(6/1/-)
Grating binocular	15(6/4/5)	9(4/5/-)	13(5/4/4)
Bar monocular	-(-/-)	12(7/4/1)	9(-/1/8)
Grating monocular	-(-/-)	9(7/2/-)	10(1/-/9)
Total	23(10/8/5)	36(22/13/1)	39(12/6/21)

Table 5.2: Minimal and mean vernier thresholds for all subjects and conditions

Owl subject	Vernier thresholds (arcmin)					
	SL		PT		OL	
	Min	Mean	Min	Mean	Min	Mean
Bar binocular	0.58	1.21	1.41	1.86	2.02	4.02
Grating binocular	1.73	2.77	2.08	2.97	1.69	3.67
Bar monocular	-	-	1.80	2.81	3.78	3.78
Grating monocular	-	-	3.04	3.75	-	-

olds differed from animal to animal, and they differed in the four test conditions. Owl SL had significantly lower minimal and mean thresholds, compared to the other owls (U-test,  $p < 0.05$ ). Owl OL had the highest thresholds, except for minimal binocular grating threshold. The lowest absolute threshold value ( $0.58 \text{ arcmin} \pm 0.23 \text{ SD}$ ) was found in subject SL under binocular viewing conditions with the bar stimulus. The highest threshold ( $7.07 \pm 1.27 \text{ arcmin}$ ) was derived from measures with subject OL under binocular viewing conditions with the grating stimulus. Except for owl OL, minimal and mean thresholds for the bar stimulus measured under binocular viewing conditions yielded lowest values across all animals (see Table 5.2). Highest thresholds were found for the bar stimulus under monocular viewing conditions in owl OL. Except for owl OL, all thresholds measured with the bar stimulus yielded lower minimal and mean thresholds than those measured with the grating stimulus. Threshold scatter between animals differed. While subjects SL and PT had a mean standard deviation of about 0.6 arcmin across all thresholds, subject OL's standard deviation was about 3 fold higher (mean SD: 1.70 arcmin, compare Figure 5.3).

### 5.3.3 Bar versus grating stimuli

Results from all subjects were used to compare the influence of stimulus configuration on performance. A total of  $n=21$  thresholds were derived with the bar stimulus under test and  $n=23$  with the grating stimulus (both binocular and monocular). In two out of three subjects (PT and SL) a significant difference between the two stimulus configurations was observed (see Figure 5.4). In subject PT mean threshold for bar stimulus was 2.46 arcmin (SEM=0.26) while grating thresholds averaged to 3.47 arcmin (SEM=0.25). U-test was significant ( $p < 0.025$ ). Even more significant was the difference found in owl SL ( $p < 0.01$ ). Here, mean bar threshold was 1.21 arcmin (SEM = 0.24) and grating threshold was 2.77 arcmin (SEM=0.36). Thresholds for bar and grating stimuli in subject OL were on average almost identical (3.98 arcmin for bar and 3.67 arcmin for grating). Thresholds of owl OL were the highest in an absolute sense and showed the highest standard deviations ( $SD_{BAR} = 1.47$ arcmin,  $SD_{GRATING} = 1.94$ arcmin) as well.

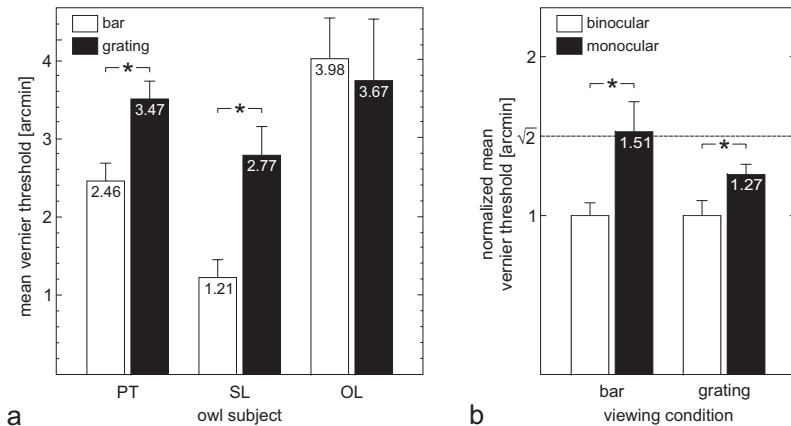


Figure 5.4: Comparing the effect of stimulus configuration in subjects. According to the U-test, grating vernier acuity yielded significant higher thresholds than bar vernier acuity in subjects PT ( $n = 22$ ,  $p < 0.025$ ) and SL ( $n = 11$ ,  $p < 0.01$ ). For subject OL no differences were found. Note that subject OL not only had the highest mean thresholds for both stimulus configurations, but also highest standard deviations. Numbers are arithmetical means of thresholds, error bars are standard error of means (SEM), and asterisks denote significantly different means.

### 5.3.4 Monocular versus binocular viewing conditions

For this comparison data from subject PT were used. In total  $n=8$  staircases were recorded under binocular conditions and  $n=14$  under monocular conditions (both with bar and grating stimuli). We recorded monocular thresholds with right ( $n=7$ ) and left eye ( $n=7$ ) occluded, respectively. Thresholds for the two eyes were not significantly different (U-test,  $p > 0.2$ ). Therefore, the data were pooled. The arithmetic mean of binocular bar measurements yielded 1.86 arcmin (SEM=0.09), while monocular bar thresholds averaged to 2.81 arcmin (SEM=0.18). The 1.86 arcmin were used as a normalization factor, and, thus, monocular thresholds were about 1.5 times higher than the binocular thresholds (Figure 5.4). The U-test did reveal a significant difference between the two conditions ( $p < 0.001$ ). The arithmetic mean of binocular grating measurements yielded 2.97 arcmin (SEM=0.17), while monocular grating thresholds averaged to 3.76 arcmin (SEM=0.07). Normalization demonstrated that monocular thresholds were about 1.3 times higher than the binocular thresholds. Again, the U-test showed a significant difference ( $p < 0.005$ ).

## 5.4 Discussion

By using the simple one-up one-down staircase method, we demonstrated that barn owls can discriminate vernier offsets in computer generated visual stimuli. It is discussed whether this finding is evidence that in this bird, as in the human visual system, vernier acuity is a hyperacuity phenomenon. Furthermore, our results showed that discrimination performance in the vernier task is affected by two conditions, i.e. binocular vs. monocular viewing conditions and bar vs. grating stimulus configuration.

### 5.4.1 Method

Reproducibility of threshold values indicates that the staircase method is a feasible tool for testing barn owls on difficult visual tasks. Earlier attempts were conducted using the method of constant stimuli and calculating the complete psychometrical function. Since data points in such functions consisted of records made on several days, this method suffered from reproducibility (compare (de Weerd et al., 1990)). On the other hand, staircase experiments yielded valid results in about 45% of the cases.

### 5.4.2 Is vernier acuity a hyperacuity phenomenon in the barn owl?

The data presented here are the first behavioral report of vernier acuity thresholds in an avian visual system. We showed that barn owls can discriminate tiny spatial offsets in vertical bars and gratings. In order to benchmark this finding our thresholds needed to be compared with conventional spatial visual acuity thresholds. Spatial visual acuity, i.e. two-point acuity or grating acuity, has been determined in the barn owl only indirectly in an anatomical study (Wathey and Pettigrew, 1989) and by PERG (Ghim and Hodos, 2006). The results estimate spatial visual acuity to be 8.4 and 6.8 cyc/deg, respectively. In our results lowest values for vernier acuity were on the order of 0.6 arcmin. In our stimulus situation, using bars as a stimulus, an argument put forward by Harris and Fahle (1995) might hold, and, thus, the measured values have to be doubled to obtain the true vernier thresholds. Thus, we arrive at 1.2 arcmin. If half of a cycle in a grating is regarded as the separable visual entity, 1.2 arcmin equals 25 cyc/deg. This is a 3 fold better threshold value than the grating acuities reported (Wathey and Pettigrew, 1989; Ghim and Hodos, 2006).  $7/44 = 16\%$  of the threshold values were in the hyperacute range, even after the above mentioned correction. This was observed in each of the three animals. Therefore, we conclude that barn owls can determine the relative positional difference of spatially non-aligned features with a precision that corresponds to only a fraction of their eye's resolving power. Following terminology in human visual research, vernier acuity is a hyperacuity phenomenon in barn owls.

### 5.4.3 Influence of stimulus configuration and viewing conditions

In two out of three animals bar thresholds were significantly lower than thresholds measured with the grating stimulus. The reason why this effect was not observed in the third owl is unclear. Earlier studies of human vernier acuity reported that a competing stimulus placed adjacent to a vernier offset results in a reduction of vernier thresholds (Westheimer and Hauske, 1975). In the context of vernier acuity this effect may be produced by either lines that flank a single line vernier stimulus, or by increasing the number of periods of a vernier-grating stimulus (Levi and Klein, 1985; Barrett et al., 1999), a situation comparable to our grating stimulus. This interference of spatially adjacent stimuli in the human visual system is often referred to as crowding, or mask-

ing effect (Pelli et al., 2004). Its presence in the barn owl visual system could indicate that common mechanisms may underlie vernier acuity in these two species.

Furthermore, the results presented here showed that binocular vernier acuity outperformed monocular vernier acuity by some 30–50%, depending on the stimulus configuration (grating vs. bar). An improvement in performance by  $\sqrt{2}$  (41%) would indicate that binocular summation plays a role, which is due to the doubling of receptors (i.e. eyes) solving the task (Campbell and Green, 1965a). Earlier studies with human subjects reported that vernier discrimination is better with two eyes than with one, showing summation ratios around 40–60% (Banton and Levi, 1991; Frisen and Lindblom, 1988; Lindblom and Westheimer, 1989). This binocular advantage is similar to that found for contrast-detection thresholds in humans, and the amount of summation is dependent on the stimulus contrast. Therefore, a direct comparison of the here found summation ratios and the human summation ratios will be accomplished satisfyingly only if data of the contrast sensitivity function in the barn owl are available.

The current data show that barn owls can discriminate vernier stimuli below 1 arcmin displacement angle. Based on grating acuity estimation our findings indicate that vernier acuity is a hyperacute percept in this species. The lowest threshold (0.58 arcmin) is 3 fold lower (better) than the assumed grating acuity. Statistical analysis of different viewing conditions indicates that binocular viewing outperforms monocular viewing by some 30–50%. Thus binocular summation seems to play a role in vernier discrimination by owls. Performance is similarly affected as in humans by the choice of stimulus configuration. Bar stimuli yielded lower values than grating stimuli, an effect referred to as crowding in human subjects.







## 6 General discussion

The visual system of the barn owl has yet been studied in an ample variety of neuroscientific approaches. To name only a few, these range from anatomical-histological studies of retinal circuitry (Oehme, 1961), to electrophysiological characterizations of brain areas that are largely devoted to vision (Nieder and Wagner, 2000), from behavioral descriptions of perceptual performances in stereo-acuity tasks (van der Willigen et al., 1998), to video-based gaze analysis revealing attentional mechanisms in barn owl vision (Ohayon et al., 2008). — An impressive aggregation that demonstrate the scientific importance conceded to the studies of animal vision.

Nevertheless, what was surprisingly lacking from barn owl literature up to now, was the description of the very basal visual capabilities of this animal. These are, specifically, measures of the behavioral visual acuity and sensitivity, both generally constituting the very limits of spatial vision in an animal. I regard those as the functional foundations of a visual system, and any further analysis of the system should take them into account.

With this thesis, I undertook some quantitative analysis of three basic visual capabilities in the barn owl. Optical quality of the owl eye was assessed with objective measurements of wavefront aberrations. In a set of psychophysical experiments, the ability to distinguish gratings of different orientation was used to measure the bird's absolute resolving power. Contrast sensitivity was measured with the same technique along another dimension. Here, luminance contrast at several spatial frequencies was varied in an adaptive procedure until the discrimination threshold, and hence, contrast sensitivity was obtained.

Additionally, a peculiar characteristic of spatial vision in the barn owl was demonstrated in a series of psychophysical experiments. It was shown that barn owls are able to discriminate the vertical offset in a pair of abutting lines or gratings with a precision that outperforms normal visual acuity in the same subject. To my best knowledge, this was the first demonstration of a monocular hyperacuity phenomenon in an avian species, a feat that is shared with rodents, felidae and primates.

## **How does the world look like through the eyes of the barn owl?**

Finally, the question raised at the very beginning of this thesis is attempted to be answered. It goes without saying that it would be beyond the scope of this study to involve philosophical arguments, which, for that matter, might be better suited to address the question strictly verbatim. In fact, as it was already performed during the course of this thesis, the question will be addressed in a mere practicable manner, reducing the issue to its biological meaningful components. Thus, this very last section of the thesis should be regarded as an attempt to bring together the fundamental principles of barn owl vision in terms of visual neuroscience. That is, to build up educated conjecture of how the visual world is experienced in a barn owl, by special consideration of the owl's eye, and the neural components creating vision, both at earlier and later stages of information processing.

### **6.1 The eye**

A first look into the face of a barn owl reveals the animal's dedication to visual perception. Though it was already said, it is important to mention that its eyes in relation to its body size and weight are extremely large (Schaeffel and Wagner, 1996; Howland et al., 2004) – a feature that is typical for avian species. With only a few exceptions, birds generally possess large eyes. Many owls and raptors have eyes that are even larger than human eyes (Hughes, 1979; Murphy et al., 1985; Howland et al., 2004). In fact, the largest eye of a terrestrial vertebrate is that of a bird, the ostrich, with a diameter of about 50 mm, twice as long as the human eye (King and McLelland, 1984; Waldvogel, 1990). It is a given fact that large eyes result in a larger retinal image, which, in turn, could subserve to meet different ethological requirements. For a fixed number of retinal photoreceptor-cells, a larger image will increase visual acuity, because the angular distance between adjacent objects to be resolved will be increased as well. A comparison of visual acuity values in different birds is presented in the next section (6.2).

Large eyes also make way for more light to enter the eye, a prerequisite for elevated sensitivity, and, therefore, adequate for a life in dim light conditions (Warrant, 2004). Summed up in the Land sensitivity equation (Land, 1981), sensitivity is directly proportional to pupil size and inversely proportional to focal length. The same relation is expressed by the f-number, the ratio between

focal length and maximal entrance pupil diameter. As a result, a low f-number constitutes high optical sensitivity by allowing the retinal image to be brighter. In the barn owl, the f-number is quite low, 1.3 (Schaeffel and Wagner, 1996), being of equal amount as in another nocturnal owl, the tawny owl (Martin and Gordon, 1974b). Serving as a benchmark, the f-number in the dark adapted human eye is 2.1. As an extreme example, the lowest f-number ever reported is that of the deep-sea ostracod *Gigantocypris mülleri*, being as low as 0.25 (Land, 1981).

Apart from the barn owl's advantageous eye geometry – large and tubular, and thus forming a large and bright retinal image – little was known about retinal image quality, which would set the primary resolution limit to the bird's visual experience. Following an observation by Schaeffel and Wagner (1996), high optical quality was reported from photoretinoscopic images of the adult owl eye. In the course of the present thesis, this issue was addressed in a quantitative approach. I measured the ocular wavefront aberrations in eight awake barn owl eyes with a state-of-the-art Tscherning wavefront aberrometer under natural viewing conditions. The eyes' point-spread function, the modulation transfer function and theoretical retinal image quality were subsequently calculated from the measured wavefront maps (refer to section 3, page 27).

Among the whole set of ocular aberrations, it turned out that only minor astigmatism terms were present, amounting to a mean spherical equivalent of about 0.03 D. Furthermore, higher-order wave aberrations (HOA) were extremely low, with a mean RMS wavefront error of about 0.10  $\mu\text{m}$ . This is about 3-fold lower than in human eyes (Howland, 2002; Porter et al., 2001). Also, HOA in eyes of another nocturnal species, the cat, are about 3.7 times larger than those of the owl (Huxlin et al., 2004). Due to the measurement method, lacking a direct control of accommodation, no further conclusions can be drawn about the animals' normal refractive state. Nevertheless, other studies point out that accommodative range is comparably large in the barn owl, and that it has some functional properties in the assessment of distance for short ranges (Howland et al., 1991; Wagner and Schaeffel, 1991; Schaeffel and Wagner, 1992, 1996). Most of the owls' PSF resembled the diffraction limited PSF for the same pupil size, which was also presented in a set of convoluted images. Here, theoretical retinal image quality demonstrated that the barn owl's optical apparatus is sufficient to create images of exceptional sharpness. The modulation transfer function for the pooled barn owl data almost completely paralleled the human data over the whole range of spatial frequencies. Barn owl modulation transfer typically excelled at low frequencies, and fell short at

spatial frequencies higher than 25 cyc/deg. This finding might be interesting with regard to the animal's contrast sensitivity, which will be discussed in the forthcoming section. Keep in mind that modulation transfer in the owl eye is especially good at very low spatial frequencies, i.e. lower than 10 cyc/deg.

To recapitulate, the superb optical quality reported in this thesis together with earlier findings and general considerations about eye design, support the hypothesis that the eyes of a barn owl are well-adapted to meet the challenging visual requirements that are implicated by a nocturnal or crepuscular lifestyle (Martin, 1984; Schaeffel and Wagner, 1996; van der Willigen et al., 2003; Warant, 2004).

## 6.2 Visual acuity

Being stated that retinal image quality in barn owls is very good, this has no implications on how much spatial detail that is present in the image is actually perceived by the animal. Further, neural processes of vision come into play. The extent of spatial detail that is coded depends on the spatial arrangement of the receptor-cell lattice and requires the possibility that single receptors or small groups of receptors are excited independently. Furthermore, this spatial information has to be preserved up to those brain areas where the perceptual decision, i.e. vision, takes place. One way, to find out about perceptual visual acuity, is to measure the animal's resolution capabilities in a behavioral experiment. This was done in a set of psychophysical experiments, in which the barn owl's task was to discriminate the orientation of Gabor patches. Spatial frequency was altered in an adaptive procedure, and the discrimination threshold was derived from the complete psychometric function.

Grating acuity was tested at two discrete high contrasts and yielded very similar results, 3.6 and 3.5 cyc/deg, at 99 % and 78 % contrast, respectively. These results were obtained in more than 620 individual trials, and small confidence intervals at threshold level strengthen the quantitative relevance of this finding (compare figure 4.5, page 58). Moreover, the results are in very good agreement with the high-frequency cut-off of the contrast sensitivity function (3.8 cyc/deg), which will be discussed in detail in the next section.

This result, a behavioral grating acuity below 4 cyc/deg, sounds somewhat astounding, since, as was said earlier, retinal image quality is that good in this animal. It seems, there is no need to have optics that would allow visual acuities that outperform the actual acuity by an order of magnitude or more. A closer

look at the modulation transfer function – the quantitative relation of how good spatial detail is preserved in the retinal image – reveals that, especially in the barn owl, modulation transfer is raised at low spatial frequencies. Thus, the excellent optics in the owl eye affect not only maximum resolution possibilities, but also preserves contrast levels for visual detail that lies in the acuity range actually used.

There are several lines of evidence found in the literature that endorse the statement of low acuity in the barn owl. As put forward by Warrant (2004), nocturnal and crepuscular animals generally have to find a trade-off between sensitivity and acuity. The loss of information capacity of the eyes that goes along with falling light levels (Snyder et al., 1977b,a) is then counteracted by increasing sensitivity with larger, more effective channels of lower density (Laughlin, 1990; Srinivasan et al., 1982; van Hateren, 1993; Warrant, 1999), ultimately sacrificing sharp vision for higher sensitivity. It seems, that also in the barn owl this rule is utilized.

The barn owl's retina is dominated by rods (Braekevelt, 1993; Braekevelt et al., 1996) and lacks a pronounced deep fovea (Oehme, 1961), which is on the other hand typical for diurnal birds (Meyer, 1977b). The temporal area centralis of the barn owl primarily contains rods, with a rod:cone ratio of 19:1 (Oehme, 1961). Moreover, receptor-ganglion cell convergence in that area is on the order of 10:1 (Oehme, 1961). A maximum ganglion cell density of 11000–12500 per  $mm^2$  was reported for area centralis, and by application of the Shannon sampling theorem and an assumed retinal magnification factor of  $0.15\text{ mm/deg}$ , grating acuity was calculated to be 7.9–8.4 cyc/deg (Wathey and Pettigrew, 1989). This theoretical value is in good agreement with the high-frequency cut-off of the barn owl CSF (6.98 cyc/deg) that has been measured in a pattern electro-retinogram study (Ghim and Hodos, 2006). Though the grating acuity values presented throughout this study (3.6–3.8 cyc/deg) are about two-fold lower, they accompany those theoretical estimations well. Given that absolute luminance in our stimulation setup was relatively low ( $2.7\text{ cd/m}^2$ ), this fact alone could account for a reduced maximum acuity, an effect which has been demonstrated in several other studies (Patel, 1966; de Valois et al., 1974; Jacobs, 1977; Bisti and Maffei, 1974; Blake et al., 1974; Banks et al., 1987).

With a grating acuity of 3.6–8.4 cyc/deg, the barn owl is in good company with other owls. Generally, owls lie at the lower end of the acuity spectrum of birds (compare last paragraph of section 4.4.3 for a list of acuities in other birds). As discussed above, vision in the crepuscular barn owl had to find

a trade-off between absolute sensitivity and reasonable acuity, that together would engage the owl to master challenging light conditions. It does not come as a surprise that grating acuity in animals that share a similar lifestyle show similar values, e.g. in the cat (3.5–7.0 cyc/deg) (Berkley, 1976), or in the galago (2.6–4.3 cyc/deg) (Langston et al., 1986).

### 6.3 Contrast sensitivity

By measuring the perceptual limit that barn owls encounter when they are supposed to discriminate between visual objects of different spatial detail, a first step towards a description of its visual capabilities is taken. On the other hand, visual perception is not solely dedicated to detect and distinguish between objects that are close to the acuity limit. In many cases, it seems, vision deals with entities that are larger than the acuity limit. To account for those cases, the spatial contrast sensitivity functions (CSF) describes up to which minimal contrast visual detail of different spatial frequency component can be detected by the observer – a classical approach in the field of visual neuroscience.

In this study I measured the CSF of the barn owl in a psychophysical experiment. The owl had to discriminate the orientation of a Gabor patch in a typical two-alternative forced-choice discrimination paradigm. Contrast was changed adaptively according to a transformed up-down rule. From such staircases, the complete psychometric function was calculated for eleven spatial frequencies, and contrast sensitivity was expressed as the inverse of the applied contrast at threshold level. The CSF displayed the typical inversely U-shaped progression, with steep attenuation for high and low spatial frequencies. Maximum sensitivity of around 18 (equalling a contrast of 5.5 %) was found at a spatial frequency of 1 cyc/deg. Sensitivity dropped to about 2.6 (contrast: 38 %) at the lowest spatial frequency tested (0.38 cyc/deg), and also sharply declined to sensitivity values of about 3.2 (contrast: 31 %) at the highest spatial frequency (2.2 cyc/deg).

Although this was the first report of the behavioral CSF in the barn owl, an electrophysiological study on the barn owl CSF already existed (Ghim and Hodos, 2006). Here the CSF was measured with a pattern electroretinogram (PERG). Generally, the conclusions derived from the PERG are, due to the measuring principle, focussed on neural processes in the retina, and lack consideration of perceptual processes on later neural stages. To account for those as well, the necessity to measure the behavioral CSF was given. As a result,

the comparison of the behavioral and electrophysiological CSF in the barn owl was now made possible (refer to section 4.4.3). Briefly, the behavioral CSF displayed a maximum sensitivity that was about twice as high as in the PERG, and about half the cut-off frequency for high spatial frequencies. These differences can be explained by inherent features of the PERG (Peachey and Seiple, 1987; Hodos et al., 2002) and differences in the absolute luminance of visual stimulation (as was already mentioned in the last section).

Nevertheless, the results of the two CSF studies shared some principle features. The general shape of the CSF, spatial frequency at peak sensitivity, and width of the CSFs were very similar. As it is typical for avian species, bird CSFs exhibit much narrower band-pass characteristic, and, therefore, display a lower width at half amplitude than it is typical for primates and other vertebrates. This is visible in CSF measurements in all the eagle (Reymond and Wolfe, 1981), kestrel (Hirsch, 1982), pigeon (Hodos et al., 2002), quail (Lee et al., 1997), the woodpecker and the starling (Ghim and Hodos, 2006), and now the barn owl (Ghim and Hodos, 2006) (see also section 4.3.3). It is argued that this might be a consequence of different receptive field properties of ganglion cells in the different species (Irvin et al., 1993). Another striking commonality in bird CSFs, which is also present in the barn owl CSF, is the typical low maximum sensitivity. In no bird that has been tested so far, contrast sensitivity excelled 30 (corresponding to a minimum contrast detectable of around 3.3 %, measured in the kestrel) (Hirsch, 1982). Humans display, on the other hand, maximal sensitivity above 200, or, in terms of minimum contrast  $< 0.5\%$  (Georgeson and Sullivan, 1975). Several primates and even fish have maximal sensitivities of around 100 (de Valois and Morgan, 1974; de Valois et al., 1974; Merigan, 1976; Northmore and Dvorak, 1979). This observation has been studied in greater detail by Hodos et al. (1997), taking several experimental, optical and neural parameters into account, and concluded that no single parameter alone could explain low contrast sensitivity in birds (Hodos et al., 1997; Ghim and Hodos, 2006). While small band-width and low contrast sensitivity are all common among bird CSFs, the location of the CSF on the spatial frequency axis differ among species. This is easily explained by the individual maximum acuity the birds exhibit. While the eagle and kestrel, both equipped with high resolution capabilities (70–140 cyc/deg), have CSFs with maximum sensitivity at a spatial frequency of around 10 cyc/deg, the quail, pigeon and barn owl's maximum sensitivity is shifted towards lower spatial frequencies, lying somewhere around 1 cyc/deg. Consistently, these three species have maximum resolutions (pigeon: 8 cyc/deg, barn owl: 3.6 cyc/deg, quail:

2.5 cyc/deg) that are essentially lower than those of the two raptorial species.

## 6.4 Specialities of avian vision

Up to this point, some of the fundamental aspects of spatial vision in the barn owl are specified: retinal image quality in the barn owl eye is excellent, but its crepuscular lifestyle has proved to have a large impact on the barn owl's resolution capabilities, favoring sensitivity over acuity. Consistently, visual acuity was found to be comparably poor in the barn owl, yet is similar as in animals that exhibit a comparable lifestyle. Moreover, barn owls display the typical narrow-bandwidth CSF with low maximum contrast sensitivity, a feature that is common to all birds that have been tested so far.

In chapter five of this thesis, results from an additional investigation are presented (page 65). Here, light is shed upon computational mechanisms in barn owl vision. Three owls were trained to discriminate a horizontal offset in paired lines or gratings – a typical hyperacuity task, known as the vernier. Vernier discrimination thresholds were subsequently determined in an adaptive staircase procedure. It turned out that all owls were able to discriminate these stimuli with hyperacute performance. That is, the smallest offset detectable lay clearly below grating acuity values (3.6–8.4 cyc/deg, equalling 8.3–3.6 arcmin). Minimal vernier thresholds across subjects were in the range of 0.58–1.69 arcmin, being 2 to 14 fold lower (better) than grating acuity results. It should be noted, that there was only one animal which was tested both in grating and vernier acuity experiments. Thus, a direct comparison between thresholds in the two tasks is limited to those results. In this subject, however, differences between vernier and grating acuity thresholds were large. Owl SL was able to discriminate vernier targets down to 0.58 arcmin (mean: 2 arcmin), while, on the other hand, displayed a behavioral grating acuity of 8.3 arcmin. It can be concluded, that barn owls do perform the vernier task on a hyperacute level.

These data are the first behavioral report of vernier acuity thresholds in an avian visual system. They are in accordance with vernier acuity thresholds in humans, primates, rats, and cats, all reporting hyperacute performance of equal relative amount (Wülfig, 1892; Murphy and Mitchell, 1991; Kiorpes et al., 1993; Seymoure and Juraska, 1997). Given the divergent phylogenetic origins of the visual systems among those species, it can be discussed, whether hyperacute performance in positional acuity tasks could be an inherent feature of spatial vision itself. This hypothesis earns further support by the observa-



tions presented in this thesis. It was shown that binocular vernier thresholds are lower than those, that have been obtained with one eye (1.3 to 1.5 fold). Similar summation ratios are found in human subjects (Frisen and Lindblom, 1988; Lindblom and Westheimer, 1989; Banton and Levi, 1991). Furthermore, in a crowded stimulus situation, barn owls performed worse than in non-crowded trials. The same effect is visible in human observers (Levi and Klein, 1985; Barrett et al., 1999).

The earlier discovery of another hyperacuity percept in the barn owl, stereoacuity, may underpin the same argument in the binocular domain. The geometrical arrangement of the owl eyes, being oriented frontally in the head, constitutes the owl's ability for stereovision. In a series of behavioral studies, it was shown that barn owls do have global stereopsis, and indeed use horizontal disparities as a depth cue (van der Willigen et al., 1998, 2002, 2003). Interestingly, stereoacuity values were on the order of 2 arcmin, being clearly lower than behavioral grating acuity in the same animal (refer to section 4). This demonstrates that hyperacute performance in stereo tasks is not limited to human and primate observers (Sarmiento, 1975; Hadani et al., 1980). Moreover, another bird, the pigeon, exhibits hyperacute stereovision as well, although its lifestyle and binocular field differs from that in the barn owl and other typical stereo-vision animals to great amounts (McFadden, 1987). Hyperacute stereovision was also demonstrated in the cat (Mitchell et al., 1979) and the horse (Timney and Kei, 1999).

Up to now, one important feature of spatial vision has been left out of the discussion, because it was not directly addressed in the course of the present thesis. In humans, one of the most important perceptual capacities is the sense of color. Color vision adds another feature to the set of attributes natural objects are composed of, and ultimately aids object separation and identification. Because this field has never been studied in the barn owl directly, it can only be speculated whether barn owls have color vision. Generally, one has to distinguish between the mere physical capacity of wavelength discrimination and the perceptual ability of perceiving colors. Avian scientists have shown that birds possess both. The retinas of most birds contain multiple spectral classes of cones, including the typical L-, M- and S-cone classes that are found in primates (Palacios and Goldsmith, 1993; Valera et al., 1993). Additionally, birds commonly have a spectral cone-class in the ultraviolet or near ultraviolet range (Chen et al., 1984; Goldsmith, 1980). Moreover, the cones of birds contain colored oil droplets, through which light passes when striking cone photo-pigments (Valera et al., 1993). The oil acts as a filter for different wave-

lengths, and, hence, the number of functional spectral sensitivities may grow beyond the number of different cone classes.

Among nocturnal birds, color vision has been extensively studied by Martin in the tawny owl (Martin, 1974; Martin and Gordon, 1974a; Martin et al., 1975; Martin, 1977). It turned out that the tawny owl is trichromatic, with at least four different classes of oil droplets (Bowmaker and Martin, 1978). The tawny owl showed behavioral color discrimination capabilities that were independent of absolute luminance in the stimuli. Although absolute discrimination performance was comparably poor, these results suggested that the tawny owl indeed perceives color, on top of being able to discriminate different wavelengths (Martin, 1974). If the same was true for the barn owl, the decreased absolute visual acuity and low contrast sensitivity that have been presented in this thesis, could be additionally explained by the presence of different cone classes with different spectral sensitivities. Although humans are trichromatic, for example, in the very center of the human fovea, S- cones are missing, probably to preserve high acuity (Curcio et al., 1990).





## 7 Summary

Optical quality in barn owl eyes was measured with a standard Tscherning-type wavefront aberrometer. The results revealed that barn owl eyes have excellent optical quality. Higher-order aberrations were about 3-fold lower than has been reported in human eyes with similar methods and under comparable conditions.

The spatial contrast sensitivity function (CSF) of the barn owl was measured in several psychophysical experiments with an orientation discrimination task. As in humans and virtually any other animal, the CSF of the barn owl rendered the typical band-limited inverted u-shaped function, with attenuated sensitivities for high and low spatial frequencies. Maximal sensitivity of about 20 was at a spatial frequency of about 1 cyc/deg.

With a similar discrimination task, grating acuity was measured in a separate behavioral experiment. The results, 3.7 cyc/deg, are in good agreement with the high-frequency cut-off of the CSF, and put the barn owl on the very low end of the acuity spectrum compared to other owls and birds.

The barn owl displays discrimination thresholds in psychophysical vernier acuity experiments that are substantially lower than the resolution limit derived from the high-frequency cut-off of the behavioral and electrophysiological CSF. Moreover, the thresholds were also lower than the behaviorally measured grating acuity, and than theoretical values derived from an anatomical study of the bird's retina. It is concluded, that vernier acuity is a hyperacute percept in the barn owl.

Vernier acuity thresholds of the barn owl seem to be similarly influenced by the choice of stimulus configuration and viewing conditions as it is the case in human observers. Specifically, vernier thresholds were worse in a crowded stimulus situation, and better under binocular viewing conditions. The latter is referred to as binocular summation in human subjects.



# References

- Artal, P. (1990). Calculations of two-dimensional foveal retinal images in real eyes. *Journal of the Optical Society of America A*, 7(8):1374–1381.
- Banks, M. S., Geisler, W. S., and Bennett, P. J. (1987). The physical limits of grating visibility. *Vision Research*, 27(11):1915–1924.
- Banton, T. and Levi, D. M. (1991). Binocular summation in vernier acuity. *Journal of the Optical Society of America A*, 8(4):673–680.
- Barrett, B. T., Whitaker, D., and Bradley, A. (1999). Vernier acuity with compound gratings: the whole is equal to the better of its parts. *Vision Research*, 39(22):3681–3691.
- Berkley, M. A. (1976). Cat visual psychophysics: Neural correlates and comparison with man. In Sprague, J. M. and Epstein, A. N., editors, *Progress in Psychobiology*, pages 63–119. Academic Press, New York.
- Birch, D. and Jacobs, G. H. (1979). Spatial contrast sensitivity in albino and pigmented rats. *Vision Research*, 19(8):933–937.
- Bisti, S. and Maffei, L. (1974). Behavioural contrast sensitivity of the cat in various visual meridians. *Journal of Physiology*, 241(1):201–210.
- Blake, R., Cool, S. J., and Crawford, M. L. (1974). Visual resolution in the cat. *Vision Research*, 14(11):1211–1217.
- Bowmaker, J. K. and Martin, G. R. (1978). Visual pigments and colour vision in a nocturnal bird, *strix aluco* (tawny owl). *Vision Research*, 18(9):1125–1130.
- Brach, V. (1977). The functional significance of the avian pecten: a review. *Condor*, 79:321–327.

- Braekevelt, C. R. (1993). Fine structure of the retinal photoreceptors of the great horned owl (*bubo virginianus*). *Histology and Histopathology*, 8(1):25–34.
- Braekevelt, C. R., Smith, S. A., and Smith, B. J. (1996). Fine structure of the retinal photoreceptors of the barred owl (*strix varia*). *Histology and Histopathology*, 11(1):79–88.
- Campbell, F. W. and Green, D. G. (1965a). Monocular versus binocular visual acuity. *Nature*, 208(5006):191–192.
- Campbell, F. W. and Green, D. G. (1965b). Optical and retinal factors affecting visual resolution. *Journal of Physiology*, 181(3):576–593.
- Campbell, F. W. and Gubisch, R. W. (1966). Optical quality of the human eye. *Journal of Physiology*, 186(3):558–578.
- Campbell, F. W., Kulikowski, J. J., and Levinson, J. (1966). Effect of orientation on visual resolution of gratings. *Journal of Physiology*, 187(2):427–436.
- Chen, D. M., Collins, J. S., and Goldsmith, T. H. (1984). The ultraviolet receptor of bird retinas. *Science*, 225(4659):337–340.
- Coletta, N. J., Troilo, D., Moskowitz, A., Nickla, D. L., and Marcos, S. (2003). Wavefront aberrations of the marmoset eye. In *Investigative Ophthalmology & Visual Science (suppl.)*, volume 44, page U324.
- Cornsweet, T. N. (1970). *Visual Perception*. Academic Press, New York.
- Curcio, C. A., Sloan, K. R., Kalina, R. E., and Hendrickson, A. E. (1990). Human photoreceptor topography. *Journal of Comparative Neurology*, 292(4):497–523.
- Dabrowska, B. (1975). Investigations on visual acuity of some corvine species. *Folia Biologica (Krakow)*, 23(3):311–332.
- de la Cera, E. G., Rodriguez, G., Llorente, L., Schaeffel, F., and Marcos, S. (2006a). Optical aberrations in the mouse eye. *Vision Research*, 46(16):2546–2553.
- de la Cera, E. G., Rodriguez, G., and Marcos, S. (2006b). Longitudinal changes of optical aberrations in normal and form-deprived myopic chick eyes. *Vision Research*, 46(4):579–589.



- de Valois, R. L., Morgan, H., and Snodderly, D. (1974). Psychophysical studies of monkey vision. III. spatial luminance contrast sensitivity tests of macaque and human observers. *Vision Research*, 14(1):75–81.
- de Valois, R. L. and Morgan, H. C. (1974). Psychophysical studies of monkey vision. II. squirrel monkey wavelength and saturation discrimination. *Vision Research*, 14(1):69–73.
- de Weerd, P., Vandenbussche, E., and Orban, G. A. (1990). Staircase procedure and constant stimuli method in cat psychophysics. *Behavioral Brain Research*, 40(3):201–214.
- Dulac, S. and Knudsen, E. I. (1990). Neural maps of head movement vector and speed in the optic tectum of the barn owl. *Journal of Neurophysiology*, 63(1):131–146.
- Dvorak, D., Mark, R., and Reymond, L. (1983). Factors underlying falcon grating acuity. *Nature*, 303(5919):729–730.
- Edelman, S. and Weiss, Y. (1995). Vision, hyperacuity. In Arbib, M., editor, *The Handbook of Brain Theory and Neural Networks*, pages 1009–1012. MIT Press.
- Evans, H. E. and Martin, G. R. (1993). Organa sensuum. In Baumel, J., King, A., and Breazile, J. e. a., editors, *Handbook of Avian Anatomy*, pages 585–611. University of Cambridge, Cambridge, MA.
- Fite, K. V. (1973). Anatomical and behavioral correlates of visual acuity in the great horned owl. *Vision Research*, 13(2):219–230.
- Fite, K. V. and Rosenfield-Wessels, S. (1975). Comparative study of deep avian foveas. *Brain Behavior and Evolution*, 12(1-2):97–115.
- Fox, R., Lehmkuhle, S. W., and Westendorf, D. H. (1976). Falcon visual acuity. *Science*, 192(4236):263–265.
- Frisen, L. and Lindblom, B. (1988). Binocular summation in humans - evidence for a hierarchic model. *Journal of Physiology*, 402:773–782.
- Gaffney, M. F. and Hodos, W. (2003). The visual acuity and refractive state of the american kestrel (*Falco sparverius*). *Vision Research*, 43(19):2053–2059.

- Georgeson, M. A. and Sullivan, G. D. (1975). Contrast constancy: deblurring in human vision by spatial frequency channels. *Journal of Physiology*, 252(3):627–656.
- Ghim, M. M. and Hodos, W. (2006). Spatial contrast sensitivity of birds. *Journal of Comparative Physiology A*, 192(5):523–534.
- Goldsmith, T. H. (1980). Hummingbirds see near ultraviolet light. *Science*, 207(4432):786–788.
- Graham, N. (1972). Spatial frequency channels in the human visual system: effects of luminance and pattern drift rate. *Vision Research*, 12(1):53–68.
- Güntürkün, O. (2000). Sensory physiology: vision. In Whittow, G., editor, *Sturkie's Avian Physiology*, pages 1–19. Academic Press, New York.
- Hadani, I., Gur, M., Meir, A. Z., and Fender, D. H. (1980). Hyperacuity in the detection of absolute and differential displacements of random dot patterns. *Vision Research*, 20(11):947–951.
- Harris, J. P. and Fahle, M. (1995). The detection and discrimination of spatial offsets. *Vision Research*, 35(1):51–58.
- Hemmi, J. M. and Mark, R. F. (1998). Visual acuity, contrast sensitivity and retinal magnification in a marsupial, the tammar wallaby (*macropus eugenii*). *Journal of Comparative Physiology A*, 183(3):379–387.
- Hirsch, J. (1982). Falcon visual sensitivity to grating contrast. *Nature*, 300(5887):57–58.
- Hodos, W., Ghim, M., Potocki, A., Fields, J., and Storm, T. (2002). Contrast sensitivity in pigeons: a comparison of behavioral and pattern ERG methods. *Documenta Ophthalmologica*, 104(1):107–118.
- Hodos, W., Ghim, M. M., Miller, R. F., Sternheim, C. E., and Currie, D. G. (1997). Comparative analysis of contrast sensitivity. In *Investigative Ophthalmology & Visual Science (suppl.)*, volume 38, page 634.
- Hodos, W., Miller, R. F., Fite, K. V., Porciatti, V., Holden, A. L., Lee, J.-Y., and Djamgoz, M. B. A. (1991). Life-span changes in the visual acuity and retina in birds. In Bagnoli, P. and Hodos, W., editors, *The changing visual system*, pages 137–148. Plenum, New York.

- Howland, H. C. (2002). High order wave aberration of eyes. *Ophthalmic and Physiological Optics*, 22(5):434–439.
- Howland, H. C. (2005). Allometry and scaling of wave aberration of eyes. *Vision Research*, 45(9):1091–1093.
- Howland, H. C., Howland, M. J., Schmid, K., and Pettigrew, J. D. (1991). Restricted range of ocular accommodation in barn owls (aves, tytonidae). *Journal of Comparative Physiology A*, 168(3):299–303.
- Howland, H. C., Merola, S., and Basarab, J. R. (2004). The allometry and scaling of the size of vertebrate eyes. *Vision Research*, 44(17):2043–2065.
- Hubel, D. H. and Wiesel, T. N. (1962). Receptive fields, binocular interaction and functional architecture in the cat's visual cortex. *Journal of Physiology*, 160:106–154.
- Hughes, A. (1977). The topography of vision in mammals of contrasting life style: Comparative optics and retinal organisation. In Crescitelli, F., editor, *Handbook of sensory physiology*, pages 613–656. Springer-Verlag, Berlin.
- Hughes, A. (1979). A useful table of reduced schematic eyes for vertebrates which includes computed longitudinal chromatic aberrations. *Vision Research*, 19(11):1273–1275.
- Huxlin, K. R., Yoon, G., Nagy, L., Porter, J., and Williams, D. (2004). Monochromatic ocular wavefront aberrations in the awake-behaving cat. *Vision Research*, 44(18):2159–2169.
- Inzunza, O., Bravo, H., Smith, R. L., and Angel, M. (1991). Topography and morphology of retinal ganglion cells in falconiforms: a study on predatory and carrion-eating birds. *Anatomical Record*, 229(2):271–277.
- Irvin, G. E., Casagrande, V. A., and Norton, T. T. (1993). Center/surround relationships of magnocellular, parvocellular, and koniocellular relay cells in primate lateral geniculate nucleus. *Visual Neuroscience*, 10(2):363–373.
- Jacobs, G. H. (1977). Visual capacities of the owl monkey (*aotus trivirgatus*)—II. spatial contrast sensitivity. *Vision Research*, 17(7):821–825.
- Jacobs, G. H., Blakeslee, B., Mccourt, M. E., and Tootell, R. B. H. (1980). Visual sensitivity of ground-squirrels to spatial and temporal luminance variations. *Journal of Comparative Physiology A*, 136(4):291–299.

- Jahnke, M., Wirbelauer, C., and Pham, D. T. (2006). Influence of age on optical aberrations of the human eye. *Ophthalmologie*, 103(7):596–604.
- Kaemmerer, M., Mrochen, M., Mierdel, P., Krinke, H. E., and Seiler, T. (2000). Clinical experience with the tscherning aberrometer. *Journal of Refractive Surgery*, 16(5):584–587.
- Kern, T. J. (1991). Exotic animal ophthalmology. In Gelatt, K., editor, *Veterinary Ophthalmology*, pages 1273–1305. Lippincott Williams & Wilkins, Baltimore.
- Kern, T. J. (1997). Disorders of the special senses. In Altman, R., Clubb, S., and Dorrestein, G. e. a., editors, *Avian Medicine and Surgery*, pages 563–589. WB Saunders Company, Philadelphia.
- King, A. S. and McLelland, J. (1984). Special sense organs. In *Birds: Their Structure and Function*, pages 284–314. Bailliere Tindall, London.
- Kiorpes, L., Kiper, D. C., and Movshon, J. A. (1993). Contrast sensitivity and vernier acuity in amblyopic monkeys. *Vision Research*, 33(16):2301–2311.
- Knudsen, E. I. and Knudsen, P. F. (1985). Vision guides the adjustment of auditory localization in young barn owls. *Science*, 230(4725):545–548.
- Knudsen, E. I. and Konishi, M. (1979). Mechanisms of sound localization in the barn owl (*tyto-alba*). *Journal of Comparative Physiology A*, 133(1):13–21.
- Krueger, R. R., Mrochen, M., Kaemmerer, M., and Seiler, T. (2001). Understanding refraction and accommodation through 'retinal imaging' aberrometry - a case report. *Ophthalmology*, 108(4):674–678.
- Land, M. F. (1981). Optics and vision in invertebrates. In Autrum, H., editor, *Handbook of sensory physiology*, pages 471–592. Springer, Berlin Heidelberg New York.
- Langston, A., Casagrande, V. A., and Fox, R. (1986). Spatial resolution of the galago. *Vision Research*, 26(5):791–796.
- Laughlin, S. B. (1990). Invertebrate vision at low luminances. In Hess, R., Sharpe, L., and Nordby, K., editors, *Night vision*, pages 223–250. Cambridge University Press, Cambridge.

- Lee, J. Y., Holden, L. A., and Djamgoz, M. B. (1997). Effects of ageing on spatial aspects of the pattern electroretinogram in male and female quail. *Vision Research*, 37(5):505–514.
- Levi, D. and Klein, S. (1982). Differences in vernier discrimination for gratings between strabismic and anisometropic amblyopes. *Investigative Ophthalmology & Visual Science*, 23(3):398–407.
- Levi, D. M. and Klein, S. A. (1985). Vernier acuity, crowding and amblyopia. *Vision Research*, 25(7):979–991.
- Liang, J. Z. and Williams, D. R. (1997). Aberrations and retinal image quality of the normal human eye. *Journal of the Optical Society of America A*, 14(11):2873–2883.
- Lindblom, B. and Westheimer, G. (1989). Binocular summation of hyperacuity tasks. *Journal of the Optical Society of America A*, 6(4):585–589.
- Liu, G. B. and Pettigrew, J. D. (2003). Orientation mosaic in barn owl's visual wulst revealed by optical imaging: comparison with cat and monkey striate and extra-striate areas. *Brain Research*, 961(1):153–158.
- Malania, M., Herzog, M. H., and Westheimer, G. (2007). Grouping of contextual elements that affect vernier thresholds. *Journal of Vision*, 7(2):1–7.
- Mansfield, R. J. W. and Ronner, S. F. (1978). Orientation anisotropy in monkey visual-cortex. *Brain Research*, 149(1):229–234.
- Marcos, S. (2006). Aberrometry: basic science and clinical applications. *Bulletin de la Societe Belge d'Ophthalmologie*, 302(302):197–213.
- Martin, G. R. (1974). Color vision in the tawny owl (*Strix aluco*). *Journal of Comparative and Physiological Psychology*, 86(1):133–141.
- Martin, G. R. (1977). Absolute visual threshold and scotopic spectral sensitivity in the tawny owl *Strix aluco*. *Nature*, 268(5621):636–638.
- Martin, G. R. (1982). An owl's eye - schematic optics and visual performance in *Strix aluco*. *Journal of Comparative Physiology A*, 145(3):341–349.
- Martin, G. R. (1984). The visual-fields of the tawny owl, *Strix aluco*. *Vision Research*, 24(12):1739–1751.

- Martin, G. R. and Gordon, I. E. (1974a). Increment-threshold spectral sensitivity in the tawny owl (*strix aluco*). *Vision Research*, 14(8):615–621.
- Martin, G. R. and Gordon, I. E. (1974b). Visual acuity in the tawny owl (*strix aluco*). *Vision Research*, 14(12):1393–1397.
- Martin, G. R., Gordon, I. E., and Cadle, D. R. (1975). Electroretinographically determined spectral sensitivity in the tawny owl (*strix aluco*). *Journal of Comparative and Physiological Psychology*, 89(1):72–78.
- Martin, G. R. and Katzir, G. (1999). Visual fields in short-toed eagles, *circaeus gallicus* (accipitridae), and the function of binocularity in birds. *Brain Behavior and Evolution*, 53(2):55–66.
- Masino, T. and Knudsen, E. I. (1993). Orienting head movements resulting from electrical microstimulation of the brain-stem tegmentum in the barn owl. *Journal of Neuroscience*, 13(1):351–370.
- McFadden, S. A. (1987). The binocular depth stereoacuity of the pigeon and its relation to the anatomical resolving power of the eye. *Vision Research*, 27(11):1967–1980.
- McKee, S. P. (1991). The physical constraints on visual hyperacuity. In Cronly-Dillon, J., editor, *Vision and Visual Dysfunction: 5, The Limits of Vision.*, pages 221–233. Macmillan Press, London.
- Merigan, W. H. (1976). The contrast sensitivity of the squirrel monkey (*saimiri sciureus*). *Vision Research*, 16(4):375–379.
- Merigan, W. H. and Katz, L. M. (1990). Spatial resolution across the macaque retina. *Vision Research*, 30(7):985–991.
- Meyer, D. (1977a). The avian eye and its adaptations. In Crescitelli, F., editor, *Handbook of Sensory Physiology*, pages 564–566. Springer Verlag, Berlin.
- Meyer, D. (1977b). The avian eye and its adaptations. In Crescitelli, F., editor, *The Visual System in Vertebrates*, pages 611–649. Springer Verlag, New York.
- Mierdel, P., Kaemmerer, M., Mrochen, M., Krinke, H. E., and Seiler, T. (2001). Ocular optical aberrometer for clinical use. *Journal of Biomedical Optics*, 6(2):200–204.

- Mierdel, P., Krinke, H. E., Wiegand, W., Kaemmerer, M., and Seiler, T. (1997). A measuring device for the assessment of monochromatic aberrations in human eyes. *Ophthalmologe*, 94(6):441–445.
- Mitchell, D. E., Kaye, M., and Timney, B. (1979). Assessment of depth perception in cats. *Perception*, 8(4):389–396.
- Morgan, M. J. (1991). Hyperacuity. In Kulikowski, J., Murray, I., and Walsh, V., editors, *Vision and Visual Dysfunction: 5, The Limits of Vision.*, pages 87–113. Macmillan Press, London.
- Mrochen, M., Jankov, M., Bueeler, M., and Seiler, T. (2003). Correlation between corneal and total wavefront aberrations in myopic eyes. *Journal of Refractive Surgery*, 19(2):104–112.
- Mrochen, M., Kaemmerer, M., Mierdel, P., Krinke, H. E., and Seiler, T. (2000). Principles of tscherming aberrometry. *Journal of Refractive Surgery*, 16(5):570–571.
- Murphy, C. J. and Dubelzieg, R. R. (1993). The gross and microscopic structure of the golden eagle (*aquila chrysaetos*). *Progress in Veterinary & Comparative Ophthalmology*, 3:74–79.
- Murphy, C. J., Evans, H. E., and Howland, H. C. (1985). Towards a schematic eye for the great horned owl. *Fortschritte der Zoologie*, 30:703–706.
- Murphy, K. M. and Mitchell, D. E. (1991). Vernier acuity of normal and visually deprived cats. *Vision Research*, 31(2):253–266.
- Nieder, A. and Wagner, H. (1999). Perception and neuronal coding of subjective contours in the owl. *Nature Neuroscience*, 2(7):660–663.
- Nieder, A. and Wagner, H. (2000). Horizontal-disparity tuning of neurons in the visual forebrain of the behaving barn owl. *Journal of Neurophysiology*, 83(5):2967–2979.
- Northmore, D. P. and Dvorak, C. A. (1979). Contrast sensitivity and acuity of the goldfish. *Vision Research*, 19(3):255–261.
- Nye, P. W. (1968). The binocular acuity of the pigeon measured in terms of the modulation transfer function. *Vision Research*, 8(8):1041–1053.

- Oehme, H. (1961). Vergleichend-histologische Untersuchung an der Retina von Eulen. *Zoologisches Jahrbuch der Anatomie*, 79:439–478.
- Ohayon, S., Harmening, W. M., Wagner, H., and Rivlin, E. (2008). Through a barn owl's eyes: interactions between scene content and visual attention. *Biological Cybernetics*, 98(2):115–132.
- Palacios, A. G. and Goldsmith, T. H. (1993). Photocurrents in retinal rods of pigeons (*Columba livia*): kinetics and spectral sensitivity. *Journal of Physiology*, 471:817–829.
- Patel, A. S. (1966). Spatial resolution by the human visual system. the effect of mean retinal illuminance. *Journal of the Optical Society of America A*, 56(5):689–694.
- Peachey, N. S. and Seiple, W. H. (1987). Contrast sensitivity of the human pattern electroretinogram. *Investigative Ophthalmology & Visual Science*, 28(1):151–157.
- Pelli, D. G., Palomares, M., and Majaj, N. J. (2004). Crowding is unlike ordinary masking: Distinguishing feature integration from detection. *Journal of Vision*, 4(12):1136–1169.
- Petry, H. M., Fox, R., and Casagrande, V. A. (1984). Spatial contrast sensitivity of the tree shrew. *Vision Research*, 24(9):1037–1042.
- Pettigrew, J. D. (1979). Binocular visual processing in the owl's telencephalon. *Proceedings of the Royal Society*, 204(1157):435–454.
- Pettigrew, J. D. (1986). The evolution of binocular vision. In Pettigrew, J.D., S. K. L. W., editor, *Visual Neuroscience*, pages 208–222. Cambridge University Press, London.
- Pettigrew, J. D. and Konishi, M. (1976). Neurons selective for orientation and binocular disparity in the visual wulst of the barn owl (*Tyto alba*). *Science*, 193(4254):675–678.
- Pettigrew, J. D., Wallman, J., and Wildsoet, C. F. (1990). Saccadic oscillations facilitate ocular perfusion from the avian pecten. *Nature*, 343(6256):362–363.



- Porciatti, V., Fontanesi, G., and Bagnoli, P. (1989). The electroretinogram of the little owl (*athene noctua*). *Vision Research*, 29(12):1693–1698.
- Porciatti, V., Hodos, W., Signorini, G., and Bramanti, F. (1991). Electroretinographic changes in aged pigeons. *Vision Research*, 31(4):661–668.
- Porter, J., Guirao, A., Cox, I. G., and Williams, D. R. (2001). Monochromatic aberrations of the human eye in a large population. *Journal of the Optical Society of America A*, 18(8):1793–1803.
- Prieto, P. M., Vargas-Martin, F., Goelz, S., and Artal, P. (2000). Analysis of the performance of the hartmann-shack sensor in the human eye. *Journal of the Optical Society of America A*, 17(8):1388–1398.
- Ramamirtham, R., Kee, C. S., Hung, L. F., Qiao-Gridera, Y., Roordaa, A., and Smith, E. A. (2006). Monochromatic ocular wave aberrations in young monkeys. *Vision Research*, 46(21):3616–3633.
- Ramamirtham, R., Kee, C. S., Qiao-Grider, Y., Hung, L. F., Ward, M., and Smith, E. L. (2005). Corneal and internal wave aberrations in normal rhesus monkeys (*macaca mulatta*). In *Investigative Ophthalmology & Visual Science (suppl.)*, volume 46, pages E–Abstract 1972.
- Ramamirtham, R., Norton, T. T., Siegwart, J. T., and Roorda, A. (2003). Wave aberrations of tree shrew eyes. In *Investigative Ophthalmology & Visual Science (suppl.)*, pages E–Abstract U324.
- Reymond, L. (1985). Spatial visual acuity of the eagle *aquila audax*: a behavioural, optical and anatomical investigation. *Vision Research*, 25(10):1477–1491.
- Reymond, L. (1987). Spatial visual acuity of the falcon, *falco berigora*: a behavioural, optical and anatomical investigation. *Vision Research*, 27(10):1859–1874.
- Reymond, L. and Wolfe, J. (1981). Behavioural determination of the contrast sensitivity function of the eagle *aquila audax*. *Vision Research*, 21(2):263–271.
- Samuelson, D. (1991). Ophthalmic anatomy. In Gelatt, K., editor, *Veterinary Ophthalmology*, pages 31–150. Lippincott Williams & Wilkins, Baltimore, MD.

- Sarmiento, R. F. (1975). The stereoacuity of macaque monkey. *Vision Research*, 15(4):493–498.
- Schaeffel, F. and Wagner, H. (1992). Barn owls have symmetrical accommodation in both eyes, but independent pupillary responses to light. *Vision Research*, 32(6):1149–1155.
- Schaeffel, F. and Wagner, H. (1996). Emmetropization and optical development of the eye of the barn owl (*tyto alba*). *Journal of Comparative Physiology A*, 178(4):491–498.
- Schlaer, R. (1972). An eagle's eye: quality of the retinal image. *Science*, 176(4037):920–922.
- Schmid, K. L. and Wildsoet, C. F. (1998). Assessment of visual acuity and contrast sensitivity in the chick using an optokinetic nystagmus paradigm. *Vision Research*, 38(17):2629–2634.
- Seymour, P. and Juraska, J. M. (1997). Vernier and grating acuity in adult hooded rats: The influence of sex. *Behavioral Neuroscience*, 111(4):792–800.
- Snyder, A. W., Laughlin, S. B., and Stavenga, D. G. (1977a). Information capacity of eyes. *Vision Research*, 17:1163–1175.
- Snyder, A. W., Stavenga, D. G., and Laughlin, S. B. (1977b). Spatial information capacity of compound eyes. *Journal of Comparative Physiology A*, 116:183–207.
- Srinivasan, M. V., Laughlin, S. B., and Dubs, A. (1982). Predictive coding: a fresh view of inhibition in the retina. *Proceedings of the Royal Society of London B*, 216(1205):427–459.
- Steinbach, M. J. and Money, K. E. (1973). Eye-movements of the owl. *Vision Research*, 13(4):889–891.
- Sullivan, G. D., Sutherland, N. S., and Oatley, K. (1972). Vernier acuity as affected by target length and separation. *Perception & Psychophysics*, 12(5):438–444.
- Thibos, L. N. (2000). Principles of hartmann-shack aberrometry. *Journal of Refractive Surgery*, 16(5):563–565.

- Thibos, L. N., Applegate, R. A., Schwiegerling, J. T., and Webb, R. (2000). Report from the VSIA taskforce on standards for reporting optical aberrations of the eye. *Journal of Refractive Surgery*, 16(5):654–655.
- Thibos, L. N., Applegate, R. A., Schwiegerling, J. T., and Webb, R. (2002a). Standards for reporting the optical aberrations of eyes. *Journal of Refractive Surgery*, 18(5):S652–S660.
- Thibos, L. N., Cheng, X., Phillips, J. R., and Collins, A. (2002b). Optical aberrations of chick eyes. In *Investigative Ophthalmology & Visual Science suppl.*, volume 43, pages E–Abstract 180.
- Thibos, L. N., Hong, X., Bradley, A., and Cheng, X. (2002c). Statistical variation of aberration structure and image quality in a normal population of healthy eyes. *Journal of the Optical Society of America A*, 19(12):2329–2348.
- Timney, B. and Kei, K. I. (1999). Local and global stereopsis in the horse. *Vision Research*, 39(10):1861–1867.
- Treutwein, B. (1995). Adaptive psychophysical procedures. *Vision Research*, 35(17):2503–2522.
- Uhrlich, D. J., Essock, E. A., and Lehmkuhle, S. (1981). Cross-species correspondence of spatial contrast sensitivity functions. *Behavioral Brain Research*, 2(3):291–299.
- Valera, F. J., Palacios, A. G., and Goldsmith, T. H. (1993). Color vision of birds. In Ziegler, H. and Gischof, H.-J., editors, *Vision, Brain, and Behavior in Birds*, pages 77–98. MIT Press.
- van der Willigen, R. F., Frost, B. J., and Wagner, H. (1998). Stereoscopic depth perception in the owl. *Neuroreport*, 9(6):1233–1237.
- van der Willigen, R. F., Frost, B. J., and Wagner, H. (2002). Depth generalization from stereo to motion parallax in the owl. *Journal of Comparative Physiology A*, 187(12):997–1007.
- van der Willigen, R. F., Frost, B. J., and Wagner, H. (2003). How owls structure visual information. *Animal Cognition*, 6(1):39–55.

- van Hateren, J. H. (1993). Spatiotemporal contrast sensitivity of early vision. *Vision Research*, 33(2):257–267.
- Wachtler, T., Wehrhahn, C., and Lee, B. B. (1996). A simple model of human foveal ganglion cell responses to hyperacuity stimuli. *Journal of Computational Neuroscience*, 3(1):73–82.
- Wagner, H., Brill, S., Kempter, R., and Carr, C. E. (2005). Microsecond precision of phase delay in the auditory system of the barn owl. *Journal of Neurophysiology*, 94(2):1655–1658.
- Wagner, H. and Frost, B. (1993). Disparity-sensitive cells in the owl have a characteristic disparity. *Nature*, 364(6440):796–798.
- Wagner, H. and Frost, B. (1994). Binocular responses of neurons in the barn owls visual wulst. *Journal of Comparative Physiology A*, 174(6):661–670.
- Wagner, H. and Luksch, H. (1998). Effect of ecological pressures on brains: Examples from avian neuroethology and general meanings. *Zeitschrift für Naturforschung*, 53(7-8):560–581.
- Wagner, H. and Schaeffel, F. (1991). Barn owls (*tyto-alba*) use accommodation as a distance cue. *Journal of Comparative Physiology A*, 169(5):515–521.
- Waldvogel, J. A. (1990). The birds-eye-view. *American Scientist*, 78(4):342–353.
- Warrant, E. J. (1999). Seeing better at night: life style, eye design and the optimum strategy of spatial and temporal summation. *Vision Research*, 39(9):1611–1630.
- Warrant, E. J. (2004). Vision in the dimmest habitats on earth. *Journal of Comparative Physiology A*, 190(10):765–789.
- Wathey, J. C. and Pettigrew, J. D. (1989). Quantitative analysis of the retinal ganglion cell layer and optic nerve of the barn owl *tyto alba*. *Brain, Behavior and Evolution*, 33(5):279–292.
- Westheimer, G. (1972). Visual acuity and spatial modulation thresholds. In Jameson, D. and Hurvich, L., editors, *Handbook of Sensory Physiology*. Springer-Verlag, Berlin.

- Westheimer, G. (1975). Visual-acuity and hyper-acuity. *Investigative Ophthalmology*, 14(8):570–572.
- Westheimer, G. and Hauske, G. (1975). Temporal and spatial interference with vernier acuity. *Vision Research*, 15(10):1137–1141.
- Westheimer, G. and McKee, S. P. (1977). Spatial configurations for visual hyperacuity. *Vision Research*, 17(8):941–947.
- Wichmann, F. A. and Hill, N. J. (2001a). The psychometric function: I. Fitting, sampling, and goodness of fit. *Perception & Psychophysics*, 63(8):1293–1313.
- Wichmann, F. A. and Hill, N. J. (2001b). The psychometric function: II. Bootstrap-based confidence intervals and sampling. *Perception & Psychophysics*, 63(8):1314–1329.
- Williams, D. (1994). Ophthalmology. In Ritchie, B., Harrison, G., and Harrison, L., editors, *Avian Medicine: Principles and Applications*, pages 673–694. Wingers Publishing, Lake Worth, FL.
- Wilson, H. R. (1986). Responses of spatial mechanisms can explain hyperacuity. *Vision Research*, 26(3):453–469.
- Wingstrand, K. G. and Munk, O. (1965). The pecten oculi of the pigeon with particular regards to its function. *Biologiske Meddelelser : udg. af det Kgl. Danske Videnskabernes Selskab*, 14:1–64.
- Wülffing, E. A. (1892). Über den kleinsten Gesichtswinkel. *Zeitschrift für Biologie*, 29:199–202.



# Danksagung

Mein aufrichtiger Dank geht an Herrn Prof. Dr. Hermann Wagner. Seine kritische und gleichzeitig offene Art der Betreuung hat mir Raum für eine spannende wissenschaftliche Verwirklichung gegeben.

Besonders danke ich auch Herrn Prof. Dr. Frank Schaeffel für seine fein gezielten Hilfestellungen, die großen Einfluß auf den Erfolg dieser Arbeit hatten.

Für die Einführung in das spannende Feld der visuellen Psychophysik und für stets lebhaft Diskussionen bin ich meinem früheren Mentor Dr. Rob van der Willigen sehr zu Dank verpflichtet.

Den eigentlichen Startschuß für die Ernte publikationsreifer Ergebnisse gab die besonders erfolgreiche Diplomarbeit von Katrin Göbbels. Dafür und für eine schöne Zeit danke ich Dir, Katrin.

Mein herzlicher Dank geht an Petra Nikolay, die mir die täglichen Herausforderungen experimenteller Verhaltensforschung leichter machte und macht. Auch wäre diese Arbeit ohne ihre tägliche Hilfe bei der kaum überschaubaren Menge an Tiertrainings in diesem zeitlichen Rahmen wohl nicht zustande gekommen.

Ebenfalls danke ich Julius Orlowski für tatkräftige, praktische Unterstützung.

Ich danke meinen Freunden und Kollegen Peter Bremen, Shay Ohayon und Katrin Vonderschen für viele schöne Stunden im und außerhalb des Instituts.

Meinen Eltern und Geschwistern danke ich für ihre herzliche und andauernde Unterstützung in allen Belangen meiner persönlichen Entwicklung.

Meiner Liebsten, Kiki, danke ich für ein wunderbares, erfülltes Leben.





# Curriculum vitae

Name                    Wolf Maximilian Harmening  
Geburtsdatum        16. März 1978 in Köln  
Anschrift             Mariabrunnstrasse 38, 52064 Aachen

## Schulische und wissenschaftliche Ausbildung

1984 - 1990    Grundschule Swisttal-Heimerzheim  
1990 - 1997    Helmholtz-Gymnasium Bonn, Abitur  
1997 - 1998    Zivildienst in der pulmologische Ambulanz im  
                  Universitätsklinikum Bonn  
1998 - 1999    Studium der Elektrotechnik, RWTH Aachen  
1999 - 2005    Studium der Biologie, RWTH Aachen  
2004            Studentische Hilfskraft am Institut für  
                  Biologie II, Lehrstuhl für Zoologie und  
                  Tierphysiologie, RWTH Aachen  
2004 - 2005    Diplomarbeit am Institut für Biologie II  
April 2005     Abschluss zum Diplom-Biologen  
2005 - 2007    Wissenschaftlicher Angestellter am Institut für  
                  Biologie II  
2005 - 2008    Promotion am Institut für Biologie II

## Stipendien

Juli 2006        DFG-Reisestipendium: ECVP 2006,  
                  St. Petersburg, Russland  
März 2007        DZG-Stipendium für den Besuch der  
                  Göttingen Neurobiologentagung  
Juli 2007        DFG-Reisestipendium: ECVP 2007, Arezzo, Italien  
2007 - 2008     Abschlussstipendium der Graduiertenförderung  
                  der RWTH Aachen

